Technische Universität München, Fakultät für Medizin

Stability of regulatory T cells in Type 1 Diabetes - role of epigenetic modifications and miRNAs

Martin Georg Scherm

Vollständiger Abdruck der von der Fakultät für Medizin der Technischen Universität München zur Erlangung des akademischen Grades eines Doktors der Naturwissenschaften (Dr. rer. nat.) genehmigten Dissertation.

Vorsitzender: Prof. Dr. Percy A. Knolle

Prüfende/-r der Dissertation:

1. Prof. Dr. Anette-Gabriele Ziegler

2. Prof. Dr. Dr. h.c. mult. Martin Hrabĕ de Angelis

Die Dissertation wurde am 21.01.2020 bei der Technischen Universität München eingereicht und durch die Fakultät für Medizin am 16.06.2020 angenommen.

Table of content

List of figures

List of tables

List of abbreviations

AGO	Argonaute
Akt	protein kinase B
APC	antigen presenting cell
Bach2	broad complex-tramtrack-bric a brac and Cap'n'collar homology 2
Bcl6	B cell lymphoma 6
BLIMP1	B lymphocyte-induced maturation protein 1
BSA	bovine serum albumin
CD	cluster of differentiation
CNS	conserved non-coding sequence
CpG	5'-C-phosphate-G-3'
CTLA4	cytotoxic T lymphocyte antigen 4
DC	dendritic cell
FACS	fluorescence-activated cell sorting
Foxo	forkhead box protein O
Foxp3	forkhead box protein 3
GAD	glutamic acid decarboxylase
HLA	human leukocyte antigen
IA2	insulinoma antigen 2
IAA	insulin autoantibodies
IDO	indoleamine 2,3-dioxygenase
IL	interleukin
IL2R	interleukin 2 receptor
i.p.	intra peritoneal
IPEX	immunedysregulation polyendocrinopathy enteropathy X-linked syndrome
KLF2	krueppel-like factor 2
LAG3	lymphocyte-activation gene 3
MACS	magnetic-activated cell separation
MHCII	major histocompatibility complex
miRNA	microRNA
mTOR	mammalian target of rapamycin

NCOR2	nuclear receptor co-repressor 2
NFAT	nuclear factor of activated T cells
NK cell	natural killer cell
NOD	non-obese diabetic
NSG	NOD Scid IL2Rg knockout
PBMC	peripheral blood mononuclear cell
PBS	Dulbecco's phosphate-buffered saline
PHLPP2	PH domain and leucine rich repeat protein phosphatase 2
PI3K	phophatidylinositol-3-kinase
Pri-miRNA	primary miRNA
Prkdc	Protein kinase, DNA activated, catalytic polypeptide
PTEN	Phosphatase and tensin homolog
qPCR	quantitative real time polymerase chain reaction
RISC	RNA induced silencing complex
RPMI	Roswell Park Memorial Institute medium
Scid	Severe combined immunodeficiency
siRNA	silencer RNA
Smad	SMA- and MAD-related protein
Stat	signal transducers and activators of transcription
S1PR1	Sphingosin 1 phosphate receptor 1
TCR	T cell receptor
Th	T helper
TFH	cell T follicular helper cell
TGFβ	Transforming growth factor beta
Treg	regulatory T cell
T1D	Type 1 Diabetes
UTR	untranslated region
ZnT8	Zinc transporter 8

Abstract

Type 1 diabetes (T1D) is an organ-specific autoimmune disease and its high prevalence early in life and increasing incidence worldwide make it a considerable burden for the healthcare system. The disease is characterized by an immune-mediated destruction of the insulin producing beta cells in the pancreas, resulting in a loss of blood glucose control and fatal secondary complications if left untreated.

Longitudinal studies of individuals at risk for developing T1D have shown that the disease progresses through distinct identifiable stages. Specifically, the clinically overt stage of T1D is preceded by a pre-symptomatic phase in which the appearance of islet autoantibodies indicates the onset of islet autoimmunity, often many years before clinical symptoms arise. While T cells play a major role in the destruction of pancreatic beta cells, molecular underpinnings promoting aberrant T cell activation remain poorly understood. CD25$^+$Foxp3$^+$ regulatory T cells (Tregs) are key players for the maintenance of immune homeostasis and their impaired induction, stability and function can critically contribute to the loss of immune tolerance and the activation of autoimmunity. Therefore, improved Treg induction and stability are promising approaches aiming at the restoration of immune homeostasis.

Epigenetic modifications, including DNA methylation of regulatory gene elements, are well established regulators of Treg function and the demethylation of the Foxp3 CNS2 is linked to sustained Foxp3 expression and Treg stability. Furthermore, recent studies have highlighted miRNAs as critical contributors to immune function and homeostasis, by fine-tuning the expression of relevant genes. Therefore, the focus of this thesis was set on the potentially regulatory network of both miRNAs and DNA methylation contributing to aberrant immune activation, autoimmunity and the progression to symptomatic T1D.

A first set of experiments confirmed the important role of DNA methylation of the Foxp3 CNS2 for Treg identity and function and provided novel insights into the role of this regulatory region during Treg induction *in vitro*.

Using unbiased approaches including miRNA sequencing of CD4$^+$ T cells of children with and without islet autoimmunity and HITS CLIP, I identified specific miRNAs in T cells that could contribute to the onset of autoimmunity. Specifically, miR142-3p and its relevant targets and downstream pathways were further investigated. miR142-3p was upregulated during the

onset of autoimmunity which resulted in decreased expression of its direct target Tet2. The direct targeting of Tet2 was confirmed using a combination of various molecular and cellular approaches, including miRNA modulation and loss-of-function models. The downregulation of the epigenetic modifier Tet2 was directly linked to impaired DNA demethylation of the Foxp3 CNS2 during autoimmunity and correlated with reduced frequencies of Foxp3$^+$ Tregs in the pancreas of mice with ongoing islet autoimmunity. I demonstrated that the inhibition of miR142-3p restores Tet2 levels, improves Treg induction *in vitro* and reduces autoimmunity in mouse models of T1D autoimmunity *in vivo*. Furthermore, the relevance for established human T1D and therefore the translatability of the previous findings was shown in humanized mouse models.

In summary, I showed that during islet autoimmunity a miR142-3p/Tet2/Foxp3 axis in murine and human CD4$^+$ T cells leads to impaired epigenetic remodeling and consequently interferes with the efficient induction of Tregs and impaired Treg stability. These results offer a new mechanistic model where during islet-autoimmunity miR142-3p/Tet2-mediated Treg instability can contribute to autoimmune activation and progression and suggest that targeting miR142-3p and/or Tet2 could contribute to the development of novel intervention strategies, aiming at improved Treg induction and stability to interfere with islet autoimmunity.

Zusammenfassung

Typ 1 Diabetes (T1D) ist eine organspezifische Autoimmunerkrankung, die aufgrund ihrer hohen Prävalenz im Kindes- und Jugendalter und der weltweit steigenden Inzidenz eine erhebliche Belastung für das Gesundheitssystem darstellt. Die Krankheit ist durch eine immunvermittelte Zerstörung der insulinproduzierenden Beta-Zellen in der Bauchspeicheldrüse gekennzeichnet, die unbehandelt zu einem Verlust der Blutzuckerkontrolle und schwerwiegenden Folgekomplikationen führt.

Prospektive Kohortenstudien die Kinder mit einem erhöhten genetischen Risiko an T1D zu erkranken von Geburt an untersuchten, haben gezeigt, dass die Krankheit in verschiedenen, klar unterscheidbaren Stadien fortschreitet. Dem klinisch manifestierten Stadium von T1D geht eine prä-symptomatische Phase voraus. Diese sogenannte Inselautoimmunität wird durch das Auftreten von Inselautoantikörpern anzeigt, teilweise viele Jahre vor dem Auftreten von klinischen Symptomen. Zahlreiche Studien haben gezeigt, dass T-Zellen eine wichtige Rolle bei der Zerstörung der Beta-Zellen in der Bauchspeicheldrüse spielen, die molekularen Grundlagen, die zur Aktivierung von autoreaktiven T-Zellen führen, sind aber noch weitestgehend unbekannt. $CD25^+Foxp3^+$ regulatorische T-Zellen (Tregs) sind von entscheidender Wichtigkeit für die Aufrechterhaltung der Immunhomöostase und die Beeinträchtigung ihrer Induktion, Stabilität und Funktion kann entscheidend zum Verlust der Immuntoleranz und zur Aktivierung der Autoimmunreaktion beitragen. Daher sind eine verbesserte Treg-Induktion und Stabilität vielversprechende Ansätze zur Wiederherstellung der Immunhomöostase.

Epigenetische Modifikationen, wie die DNA-Methylierung von regulatorischen Genelementen, fungieren als wichtige Regulatoren der Funktion von Tregs und die Demethylierung der Foxp3 CNS2 ist mit einer dauerhaften Foxp3 Expression und der Stabilität von Tregs verbunden. Außerdem haben mehrere, kürzlich durchgeführte Studien gezeigt, dass miRNAs durch die Feinregulierung der Expression wichtiger Gene entscheidend zur Immunfunktion und -Homöostase beitragen. Daher lag der Schwerpunkt dieser Arbeit auf einem potentiell regulatorischen Netzwerk aus miRNAs und DNA-Methylierung, das zur fehlgeleiteten Immunaktivierung, zur Autoimmunität und zum Fortschreiten zum symptomatischen T1D beiträgt.

Erste Experimente bestätigten die zentrale Rolle der DNA-Methylierung der Foxp3 CNS2 für die Identität und Funktion von Tregs und lieferten darüber hinaus neue Einblicke in die Rolle dieser regulatorischen Genregion für die Treg Induktion *in vitro*.

Mit Hilfe unterschiedlicher Methoden wie miRNA Sequenzierung von CD4^{+} T-Zellen von Kindern mit und ohne Inselautoimmunität und HITS-CLIP, identifizierte ich spezifische miRNAs in T-Zellen, die zum Einsetzen der Autoimmunität beitragen könnten. In der Folge wurden miR142-3p und ihre relevanten Ziel-mRNAs, sowie nachfolgende Signalwege genauer untersucht. miR142-3p wurde während des Einsetzens der Autoimmunität hochreguliert, was zu einer verminderten Expression ihrer direkten Ziel-mRNA Tet2 führte. Unter Verwendung einer Kombination verschiedener molekularer und zellulärer Ansätze, einschließlich miRNA-Modulation und Funktionsverlustmodellen, konnte die Tet2 mRNA als direktes Ziel von miR142-3p bestätigt werden. Die verminderte Expression des epigenetischen Modulators Tet2 war direkt mit einer gestörten DNA-Demethylierung der Foxp3 CNS2 während der Autoimmunität verbunden. Dies korrelierte mit einer reduzierten Frequenz von Foxp3^{+} Tregs im Pankreas von Mäusen mit Inselautoimmunität. Die Hemmung von miR142-3p führte zu einer Normalisierung der Tet2 Abundanz, verbesserter Treg Induktion *in vitro* und verringerter Autoimmunität in T1D-Mausmodellen *in vivo*. Des Weiteren wurden mithilfe von humanisierten Mausmodellen die Relevanz der bisherigen Befunde und damit eine mögliche Anwendbarkeit für etablierten humanen T1D gezeigt.

Zusammenfassend konnte ich zeigen, dass eine miR142-3p/Tet2/Foxp3-Achse in murinen und humanen CD4^{+} T-Zellen während der Autoimmunität zu einer beeinträchtigten epigenetischen Signatur der Foxp3 CNS2 führt und folglich die effiziente Induktion von Tregs und die Stabilität von Tregs beeinträchtigt. Diese Ergebnisse bieten ein neues mechanistisches Modell, bei dem miR142-3p/Tet2-vermittelte Treg-Instabilität während der Insel-Autoimmunität zur Autoimmunaktivierung und -progression beitragen kann. Zusätzlich deuten die vorliegenden Befunde darauf hin, dass die gezielte Modulation von miR142-3p und/oder Tet2 zur Entwicklung neuartiger Interventionsstrategien beitragen könnte, die auf verbesserte Treg-Induktion und -Stabilität abzielen, um so das Einsetzen von Inselautoimmunität zu verhindern.

1 Introduction

1.1 Immunological self-tolerance and autoimmunity

The immune system detects and eliminates harmful pathogens and discriminates them from the organism's own tissues. A major contributor to appropriate function of the immune system is the discrimination between self and non-self, executed by two distinct mechanisms: recessive and dominant tolerance.

Recessive tolerance takes place during T cell development in the thymus. Lymphocytes with a high affinity for self-peptides are subjected to negative selection by deletion (apoptotic cell death) or functional inactivation (anergy). This concept was first proposed in the clonal selection theory (Burnet, 1959; Lederberg, 1959). However, autoreactive lymphocytes can escape the negative selection in the thymus and reach the periphery.

Self-tolerance in the periphery or dominant tolerance is maintained by a specific lineage of T cells that actively suppresses autoreactive T cells, called regulatory T (Treg) cells. The balance between immunity and tolerance is a complex and tightly regulated process which requires precise control of lymphocyte development and function. The dysregulation of these control mechanisms critically contributes to the development and activation of autoreactive lymphocytes which can lead to autoimmunity.

The concept of autoimmunity was first proposed by Nobel Prize Laureate Paul Ehrlich in the early twentieth century when he described the "horror autotoxicus" (Ehrlich et al., 1907). There are more than 80 diseases with an autoimmune etiology, and their high prevalence early in life and rising incidence makes them a significant burden for the healthcare system. Autoimmune diseases can be classified into systemic or organ-specific diseases, such as Multiple Sclerosis, Rheumatoid Arthritis and Type 1 Diabetes (T1D), which is the most common autoimmune disease in young children with an estimated doubling in new cases from 2005 to 2020 in children below the age of 5 years (Patterson et al., 2009).

1.2 Type 1 Diabetes

In T1D, impaired immune tolerance mechanisms result in a loss of self-tolerance to the insulin-producing islet beta cells in the pancreas, their destruction by autoreactive T cells and consequently a loss of blood glucose control (Bluestone et al., 2010). In healthy individuals,

the beta cells in the islets of Langerhans maintain physiological glucose levels in the blood within a narrow range, by sensing the level of glucose and releasing insulin as required. Thus, besides their function of producing insulin, they are sensitive glucose sensors, crucial for the maintenance of blood glucose homeostasis. In T1D immune cells infiltrate the pancreas, leading to the progressive loss of beta cell function which results in the clinically overt disease. In order to avoid fatal secondary complications resulting from hyperglycemia, livelong insulin replacement therapies are required. However, even with ongoing insulin supply secondary complications like kidney failure and heart diseases can occur (Steffes et al., 2003).

1.2.1 Role of effector T cells in T1D

As described above, T1D is mediated by an immune cell mediated destruction of the insulin producing beta cells in the pancreatic islets of Langerhans. This process is initiated by insulitis, the process of immune cell infiltration into the islets. Interestingly, the level of insulitis differs considerably between human T1D patients and mouse models like the NOD mouse, which exhibits much higher numbers of infiltrating cells (Morgan and Richardson, 2018). The infiltrating immune cells comprise of CD8^{+} T cells, CD4^{+} T cells, B cells and macrophages, with CD8+ T cells being the most abundant cell type (Leete et al., 2016). In addition to the immune cell infiltration, insulitis is characterized by an increased expression of HLA-I molecules in islet cells (Foulis et al., 1986). This hyperexpression is associated with interferon production and contributes to the explanation of the predominance of CD8^{+} T cells in the infiltrates (Richardson et al., 2016). Despite the high abundance of CD8^{+} T cells in the pancreatic infiltrates, in this thesis the focus was set on CD4^{+} T cells. Various subsets of CD4^{+} T cells have been identified as important contributors to autoimmune diseases including T1D but also multiple sclerosis (Dittel, 2008), rheumatoid arthritis (Cope et al., 2007) and Crohn's disease (Chao et al., 2014). In T1D, multiple studies have identified and further characterized infiltrating CD4^{+} T cells autoreactive against islet antigens. These identified subsets include Th1, Th2 (Szebeni et al., 2005), Th17 (Arif et al., 2011; Ferraro et al., 2011; Reinert-Hartwall et al., 2015), Th9, Th22 (Ryba-Stanisławowska et al., 2016) and TFH cells (Ferreira et al., 2015; Kenefeck et al., 2015).

1.2.2 Genetic risk and triggers of T1D

It is widely accepted that both genetic and environmental factors including diet, microbial exposure and certain viruses contribute to the risk of developing T1D. The strong genetic contribution is, besides others, indicated by an increased risk of up to ten times in children with a first-degree relative with T1D (Bonifacio et al., 2004; Hemminki et al., 2009; Winkler et al., 2019; Ziegler and Nepom, 2010). Specifically, the human leucocyte antigen (HLA) class II, with the genotype HLA-DR4, HLA-DQ8 has been identified as the most robust predictor of genetic risk to develop T1D, with a risk of around 5% even without a family history of T1D (Emery et al., 2005; Ziegler and Nepom, 2010).

1.2.3 Presymptomatic T1D: islet autoimmunity

Longitudinal studies of individuals at risk for developing T1D show that the disease progression is characterized by distinct identifiable stages prior to the onset of the clinically overt disease (Insel et al., 2015; Ziegler et al., 2013). The appearance of autoantibodies against islet autoantigens defines the pre-symptomatic phase of T1D which is therefore termed "islet autoimmunity". Islet autoantigens include insulin (Palmer et al., 1983), glutamic acid decarboxylase (GAD) (Baekkeskov et al., 1990), insulinoma-antigen 2 (IA2) (Lan et al., 2009; Rabin et al., 1994) and zinc transporter 8 (ZnT8) (Wenzlau et al., 2007), and autoantibodies can be present in the blood years or even decades before the onset of hyperglycemia (Ziegler and Nepom, 2010; Ziegler et al., 2013). Despite ongoing research efforts and although recent studies significantly contributed to our understanding of T1D pathogenesis, the molecular mechanisms underlying the heterogeneity, the onset of islet autoimmunity and the progression to symptomatic diabetes remain poorly understood.

Since at the time of onset of the symptomatic disease most of the beta cell mass is already destroyed, the pre-symptomatic phase has come into focus of research approaches aiming at the mechanistic dissection of the underlying molecular mechanisms triggering islet autoimmunity. Recently, the specific roles of different T cell subsets during the pre-symptomatic stage of T1D and their contribution to immune activation and autoimmunity have been highlighted (Heninger et al., 2017; Serr et al., 2016a, 2016b, 2018). An altered autoantigen response in CD4^{+} T cells has been shown in longitudinal samples collected starting shortly after birth from children at risk for T1D, even prior to autoantibody seroconversion (Heninger et al., 2017). Furthermore, a slow progression from pre-

symptomatic islet autoimmunity to clinical T1D in children was associated with high frequencies of insulin-specific Tregs and Treg induction from naive CD4^{+} T cells was shown to be impaired in children with recent onset of islet autoimmunity (Serr et al., 2016b). These findings suggest a crucial role for Tregs in delaying or possibly preventing the progression from pre-symptomatic islet autoimmunity to clinical T1D.

1.3 Tregs mediate immune tolerance

As above-mentioned Tregs are well established key players for the maintenance of peripheral immune tolerance by inhibiting their autoreactive counterparts in various ways, and defects in Treg induction and function are important contributors to autoimmune disorders like T1D (von Boehmer and Daniel, 2013; Josefowicz et al., 2012; Sakaguchi et al., 2008).

1.3.1 History of Treg research

This again highlights that for the maintenance of immune homeostasis, understanding both the initiation and maintenance of adequate immune responses protective to the host and the suppression of deleterious, overshooting immune responses are essential. The latter is especially important to avoid autoimmunity, allergy and immune responses to commensal microbes or to the fetus during pregnancy. The existence of cellular mediators of suppression or regulation of immune responses was already reported in 1970 when it was shown that T cells could not only boost but also reduce immune responses (Gershon and Kondo, 1970). Due to the reported function of the identified T cell population, they were termed suppressor cells. Over the following years suppressor cells were intensively studied and complex interactions with other cells, as well as soluble factors were reported to mediate their suppressive function (Green et al., 1983). However, in the 1980s successive studies questioned the interpretation of these results (Kronenberg et al., 1983) and a lack of appropriate methods to clear up this doubt resulted in a rapid decline of research interest in this field. The field of suppressor cell research regained attention in the 1990s when it was reported that a subpopulation of CD4^{+} T cells was capable of preventing autoimmunity in mice (Sakaguchi et al., 1995). In the same study, additional markers for the unambiguous identification of these cells, now called regulatory T cells (Tregs), were described.

1.3.2 Characterization of Tregs

It is now well established that Tregs are characterized by the expression of CD4, the high-affinity α chain of the interleukin 2 receptor (CD25), and most importantly the transcription factor Foxp3, which functions as a master regulator of Treg differentiation, maintenance and function (Fontenot et al., 2003; Roncador et al., 2005). The deleterious consequences of mutations in the FOXP3 gene, leading to fatal autoimmune phenotypes in both mice (scurfy mice) and humans (IPEX - immunodysregulation, polyendocrinopathy, enteropathy, X-linked syndrome) highlight the crucial role of Foxp3 in Treg development and its impact on immune homeostasis (Bennett et al., 2001; Khattri et al., 2003). Similarly, the depletion of Tregs in newborn mice results in impaired immune regulation and severe autoimmune disease (Kim et al., 2007; Lahl et al., 2007). Since its discovery the crucial role of Foxp3 for Tregs has been studied extensively. For example, multiple studies revealed regulatory regions in the Foxp3 promoter and other noncoding sequences of the Foxp3 gene. These regions control the expression of Foxp3 and are regulated by various mechanisms including epigenetic modifications (Baron et al., 2007; Floess et al., 2007; Mantel et al., 2006) and transcription factor binding (Burchill et al., 2007; Tone et al., 2008). Furthermore the structure of Foxp3 including its functional domains was identified (Bandukwala et al., 2011; Lopes et al., 2006; Walker et al., 2003) and multiple target genes (Hill et al., 2007; Marson et al., 2007; Zheng et al., 2010) and interactions partners were described (Li et al., 2007a; Ono et al., 2007; Trim et al., 2013; Wu et al., 2006; Zhang et al., 2008; Zhou et al., 2008a), forming a complex interaction network termed Foxp3 interactome (Rudra et al., 2012).

1.3.3 Suppression mechanisms of Tregs

In order to exert their regulatory function, Tregs affect a wide range of immune cells, including T cells, B cells, natural killer (NK) cells and antigen presenting cells (APCs) by suppressing their activation, proliferation and effector function, both *in vivo* and *in vitro* (Sakaguchi et al., 2008; Vignali et al., 2008). The suppression mechanisms of Tregs are highly diverse regarding their functional modes of action and include inhibitory cytokines, cytolysis, metabolic disruption and targeting of dendritic cells. The secretion of inhibitory cytokines, including IL10, IL35 and TGFβ, directly suppresses the function of effector T cells and induces cell cycle arrest (Asseman et al., 1999; Fahlén et al., 2005; Green et al., 2003). Furthermore, Tregs can function as cytotoxic cells and directly kill effector cells via granzyme A, granzyme B or perforin

dependent mechanisms, inducing apoptosis or cytolysis of the targeted effector cell (Grossman et al., 2004). Metabolic disruption of effector cells is carried out by cytokine deprivation mediated apoptosis. Tregs express high levels of CD25, the IL2 receptor α chain, which enables them to consume high amounts of IL2, leading to cytokine deprivation and subsequent apoptosis of the effector cells (Pandiyan et al., 2007). Other mechanisms are cyclic AMP mediated inhibition and CD39/CD73 generated, adenosine receptor 2A mediated immunosuppression (Deaglio et al., 2007). Last but not least, Tregs can directly target dendritic cells, inhibiting their maturation and function and thereby promoting the establishment of tolerogenic dendritic cells (Bluestone and Tang, 2005). The interaction of LAG3 with the MHC II complex mediates suppression of the maturation, while the binding of CTLA4 to CD80/CD86 induces IDO, which induces an immunosuppressive phenotype (Oderup et al., 2006). Although Tregs are highly specific for the antigen corresponding to their particular T cell receptor (TCR), their suppressive capacity does not require direct cell-cell-contact. The ability to secret and consume cytokines and other soluble mediators of immune function, enables the suppression of numerous effector cells in their proximity by a mechanism called bystander suppression (Miller et al., 1991).

1.3.4 Transcriptional regulation of Treg homeostasis

As described above Foxp3 is the master transcription factor of Tregs with an essential role for their development, maintenance and function. However, Foxp3 function depends of a highly complex network of co-factors and binding-partners. The analysis of this regulatory network revealed that Foxp3 forms numerous multiprotein complexes with more than 360 different proteins, 30% of which were related to regulation of transcription. Multiple of these proteins are directly regulated by Foxp3 while others are necessary to maintain the transcription of Foxp3. Thus, the Treg phenotype is controlled by a highly complex, self-reinforcing transcriptional network that consists of Foxp3 its multiple partners (Rudra et al., 2012). Some proteins regulating Foxp3 expression and Treg homeostasis which are of considerable importance for this thesis are described below.

Stat5 has been shown as a downstream target of IL2 and is critically involved in Treg development (Mahmud et al., 2013). CD4^{+} T cells receiving a high affinity TCR signal express IL2Rα and IL2Rβ which makes them highly responsive to IL2. In a second, TCR independent step these Treg progenitors receive IL2 signals which are transmitted via Stat5 to induce Foxp3

expression, resulting in Treg maturation. TGFβ has been shown to exhibit potent immunoregulatory properties, among others by inducing the expression of Foxp3 in Tregs (Konkel et al., 2017). TGFB binds to TGFBR which activates several transcriptions factors, including Smad proteins. These are phosphorylated and activated which results in their translocation to the nucleus where they regulate the transcription of their target genes like Foxp3. Bach2 is a transcriptional repressor which was initially described as a B cell-specific transcription factor involved in class-switch recombination and somatic hypermutation (Ichikawa et al., 2014; Muto et al., 1998). However, recent data additionally highlight a key role for Bach2 in regulating T cell differentiation and function. Bach2 belongs to a class of transcription factors that regulates transcriptional activity in T cells at super-enhancers, or regions of high transcriptional activity (Richer et al., 2016). Bach2 deficient Treg cells exhibit reduced expression of Foxp3 and an impaired suppressive function (Roychoudhuri et al., 2013). By inhibiting transcription factors involved in T cell effector function and consequently the transcriptional programs of effector T cells, Bach2 contributes to the maintenance of naive T cells as well as to the differentiation of Tregs.

1.3.5 Treg induction *in vivo*

Besides their differentiation in the thymus, Tregs can also be induced from naive T cells in the periphery upon exposure to antigen. It has been shown that the efficient *in vivo* induction of stable Tregs requires the binding of a strong-agonistic antigen to the TCR under subimmunogenic conditions (von Boehmer and Daniel, 2013; Daniel et al., 2010, 2011a; Kretschmer et al., 2005). These subimmunogenically induced Tregs are stable and can keep up their suppressive function even upon antigen exposure and stimulation. In contrast, higher doses of TCR ligands and strong co-stimulatory signals interfere with stable Treg induction by activating the PI3K/Akt/mTOR pathway, and consequently resulting in T cell activation. The costimulatory molecule CD28 activates PI3K (Garçon et al., 2008) which phosphorylates Akt, resulting in the activation of mTOR. mTOR induces the phosphorylation of Foxo proteins Foxo1 and Foxo3a, resulting in their export from the nucleus which interferes with Foxp3 induction and expression. Therefore, factors inhibiting the PI3K/Akt/mTOR pathway such as phosphatase and tensin homolog (PTEN) are crucial for Treg induction and function (Delgoffe et al., 2013; Ouyang et al., 2010).

1.3.6 Antigen-specific Treg induction

The relevance of antigen-specific Treg induction for the development of T1D and the role of insulin as an essential autoantigen have been highlighted in studies using the NOD mouse model (Jaeckel et al., 2004; Nakayama et al., 2005). The high risk of developing T1D in these mice is linked to the NOD MHCII IAg7 genotype (Hattori et al., 1986; Prochazka et al., 1987) and 90% of the pancreas infiltrating T cells recognize an IAg7-restricted insulin epitope of the B chain comprising residues 9-23 (B:9-23) (Alleva et al., 2001; Daniel et al., 1995). Here, due to a polymorphism of the IAG7 the insulin B:9-23 peptide is presented inefficiently by the MHCII, resulting in an increased escaped of autoreactive T cells from negative selection in the thymus and an inefficient Treg induction in the periphery (Stadinski et al., 2010; Wucherpfennig and Sethi, 2011). To compensate for this inefficient antigen presentation, insulin mimetopes with altered amino acid sequences were developed in order to improve antigen presentation (Crawford et al., 2011; Stadinski et al., 2010). The application of these mimetopes to young NOD mice resulted in an improved induction of antigen-specific Tregs *in vivo* as indicated by higher frequencies of insulin-specific Tregs in the pancreatic lymph nodes and the pancreas. Furthermore, the progression to T1D was delayed compared to mice treated with the natural insulin epitope (Daniel et al., 2011b).

1.3.7 Treg induction *in vitro*

Treg induction from naive CD4^{+} T cells *in vitro* is most commonly achieved by TCR stimulation in the presence of TGFβ. Even though high levels of Tregs can be induced and the resulting Tregs are functional, they do not resemble the stable phenotype and long-lasting suppressive function of their *in vivo* counterparts. However, especially in therapeutic approaches relying on Treg generation or expansion, the maintenance of Tregs is crucial for successful treatment strategies. When Tregs, induced in the presence of TGFβ, are transferred *in vivo*, they promptly lose Foxp3 expression and consequently their suppressive function (Floess et al., 2007). The TGFβ independent *in vitro* Treg induction can be achieved by limiting the activity of the PI3K/Akt/mTOR pathway, by direct inhibition of this pathway or by limited TCR stimulation (Sauer et al., 2008) . Treg development and function have been shown to be regulated by a complex network including multiple transcriptional modulators and epigenetic mechanisms, which are particularly involved in the regulation of Treg stability.

1.4 Epigenetics

The cells in a multicellular organism show and maintain different phenotypes, yet have an identical set of genetic information in their DNA. Epigenetics is commonly understood as potentially heritable mechanisms that control gene expression without directly altering the DNA sequence of the gene (Schuettengruber et al., 2011). Already in the late 1930s, before DNA was identified as the molecule carrying the genetic information, Conrad Waddington defined the term "epigenetic landscape" for mechanisms that control expression of genes and convert their information in phenotypes (Waddington, 1939). In contrast to the DNA sequence, epigenetic modifications can be easily altered in response to environmental stimuli. Furthermore, they can explain a considerable part of the phenotypic variations in humans, even more than the different genotypes alone (Turan et al., 2010).

As regulators of gene transcription, epigenetic modifications play a crucial role in various biological fields, ranging from single cell level to multicellular organisms. A multitude of fundamental cellular processes are regulated by epigenetic modifications, including regulation of gene and miRNA expression, DNA-protein interactions, suppression of transposable element mobility, cellular differentiation, embryogenesis, X-chromosome inactivation and genomic imprinting. On a single cell level epigenetic mechanisms are crucial for cell differentiation and the maintenance of these highly specialized differentiated states. Stem cells giving raise to any type of cell and fully differentiated cells dividing into two phenotypically identical cells, while both cell types contain the exact same DNA sequence illustrate well the importance of this additional layer of regulation. Cloned animals are not identical to their donor regarding their phenotype although they arise from the same genotype and similarly human monozygotic twins show differences in their epigenetic landscape while their DNA sequence is identical (Portela and Esteller, 2010).

Not all non-genetic control mechanisms are epigenetics and while it is debated whether noncoding RNAs are epigenetic, there is an agreement that epigenetic modifications should be reversible, heritable and self-perpetuating (Riddihough and Zahn, 2010). Epigenetic mechanisms can be grouped into three main categories: histone modifications, nucleosome positioning and DNA methylation, on which the focus was set in the context of this thesis.

1.4.1 DNA methylation

DNA methylation represents one of the most essential and commonly inherited epigenetic modifications in mammalian cells. It is defined as the covalent addition of a methyl group to C-5 position of the cytosine ring of DNA (Esteller, 2008) and has been shown to be crucial for genomic imprinting (Girardot et al., 2013; Reik and Walter, 2001), X-chromosome inactivation (Briggs and Reijo Pera, 2014; Robert Finestra and Gribnau, 2017) and embryonic development (Feng et al., 2010). In mammals, DNA methylation occurs almost exclusively in the context of CpG dinucleotides with 98% in somatic cells and 75% in embryonic stem cells (Lister et al., 2009). With about 1%, CpG sites are generally rare in mammalian genomes; however, they tend to form clusters called CpG islands, defined as regions longer than 200 bases, a GC content >50% and a ratio of observed to expected CpG frequencies of at least 0.6. CpG islands are localized primarily in promoter regions, with about 60% of human promoters being associated with such a region. The CpG sites in most promoter regions is unmethylated and only a low percentage (~6%) of promoters is methylated in differentiated tissues (Straussman et al., 2009).

In addition to CpG islands there are regions in close proximity but with a lower density of CpG sites which show DNA methylation. The methylation of these so-called CpG island shores is associated with inhibited gene expression and most of the differentially methylated regions involved in tissue-specific gene expression pattern contain CpG island shores (Doi et al., 2009; Irizarry et al., 2009).

In general, unmethylated CpG islands provide a chromatin structure which is favorable for transcriptional activation of genes. The CpG-binding protein Cfp1 binds selectively to non-methylated CpG sites and recruits the histone methyltransferase Setd1, creating H3K4 trimethylation (H3K4me3) histone methylation marks (Thomson et al., 2010). In contrast, DNA methylation represses transcription directly, by prevent the binding of activating DNA binding proteins like transcription factors (Esteller, 2007; Lopez-Serra and Esteller, 2008) or indirectly, by recruiting methyl-CpG-binding domain (MBD) proteins and associated repressive histone-modifying and chromatin-remodeling complexes (Kuroda et al., 2009). In addition to these direct regulatory effects in cis, DNA methylation and the associated protein complexes can also act in trans by physical interaction with distant regions, even on different chromosomes (Espada et al., 2007; Horike et al., 2005; Zhao et al., 2006).

1.4.2 Epigenetic modifications in autoimmune diseases

The fact that autoimmune diseases concordance rates in monozygotic twins range from 13-61% (Dang et al., 2013; Generali et al., 2017; Xiang et al., 2017) highlights the importance of non-genetic mechanisms and the impact of an impaired epigenetic landscape for diseases susceptibility. Epigenetic mechanisms such as altered DNA methylation patterns are a critical factor in the pathogenesis of several autoimmune diseases (Long et al., 2016; Lu, 2013; Paul et al., 2016; Strickland and Richardson, 2008). Global hypomethylation has been shown in autoimmune diseases including systemic lupus erythematosus (SLE) and rheumatoid arthritis. The mechanisms underlying these profound changes of the methylome are still poorly understood and specific hypomethylated regions are not yet sufficiently defined. However, hypomethylated genes that might be directly involved in disease pathogenesis have been reported in SLE patients (Javierre et al., 2010). In rheumatoid arthritis both hypomethylated genes and hypermethylated genes have been described (Javierre et al., 2008). In the context of T1D, several studies highlighted the potential importance of epigenetic modifications for diseases pathogenesis (Jerram et al., 2017). However, these studies did not provide sufficient insight in the underlying mechanisms to suggest novel intervention strategies based on these findings. A recent study reported multiple differentially methylated gene regulatory elements in T1D twins when compared to their healthy twins and compared to unrelated healthy controls (Paul et al., 2016). These differentially methylated regions were preferentially located in genes involved in the regulation of immune cell metabolism, cell cycle and mTOR signaling.

1.4.3 DNA methylation in Tregs

As described above, the long-term stability of Tregs, linked to constantly high levels of Foxp3 expression, is crucial for the maintenance of immune homeostasis. The expression of Foxp3 is linked to changes in DNA methylation, controlling gene activity by altering the accessibility of the DNA to transcription factors (Josefowicz et al., 2009; Kim and Leonard, 2007; Polansky et al., 2008). In particular, the hypomethylated state of four conserved non-coding sequences (CNS) within the Foxp3 locus ensures proper Foxp3 expression in Tregs. The CNS2 was identified as a critical regulator of long term stability of Foxp3 expression and consequently the Treg phenotype: it is completely demethylated in Tregs but fully methylated in conventional T cells and *in vitro*-induced Tregs (Baron et al., 2007; Feng et al., 2014; Floess et

al., 2007; Huehn and Beyer, 2015; Huehn et al., 2009; Li et al., 2014; Toker et al., 2013; Zheng et al., 2010).

1.4.4. The DNA methylation machinery

Despite ongoing research efforts, the mechanisms targeting DNA methylation to specific regions of the genome remain poorly understood. However, this presumably involves interactions between the DNA methylation machinery and chromatin-associated proteins (Robertson, 2005). The methylation of DNA is conducted by a family of proteins termed DNA methyltransferases (DNMTs) comprising DNMT1, DNMT3A and DNMT3B (Okano et al., 1998). DNMT1 is involved in reestablishing the DNA methylation pattern during DNA replication which is in line with its preference for hemimethylated DNA and its localization to the replication machinery (Probst et al., 2009). In contrast, DNMT3A and DNMT3B are involved in de novo methylation during embryonic development, explaining their preference for unmethylated CpG sites (Li, 2002; Okano et al., 1999). However, recent studies suggest that this categorization is less clear than reported before (Egger et al., 2006; Riggs and Xiong, 2004).

The removal of DNA methylation and consequently the establishment of hypomethylated regions is a multistep process, dependent on three members of the ten eleven translocation (Tet) family, Tet1, Tet2 and Tet3 (Iyer et al., 2009; Tahiliani et al., 2009). These enzymes are capable of oxidizing 5-methylcytosine (5mC) to 5-hydroxymethylcytosine (5hmC), 5-formylcytosine (5fC), and 5-carboxylcytosine (5caC), all three intermediates of DNA demethylation (He et al., 2011; Ito et al., 2011; Pastor et al., 2013; Wu and Zhang, 2014). In line with the importance of hypomethylation in regulatory regions Tet genes are critical for the differentiation of CD4^{+} T cells in mice (Ko et al., 2011; Tsagaratou et al., 2014) and humans (Nestor et al., 2016), as well as Treg homeostasis and function (Nair and Oh, 2014; Wang et al., 2013; Yang et al., 2015b; Yue et al., 2016). These findings suggest that the Tet genes might also play a pivotal role for the loss of immune homeostasis in autoimmunity.

The precise control of signaling pathways and their regulation on an epigenetic level are crucial for proper function of the immune system, including the regulation of lymphocyte development in the thymus and the prevention of autoimmune reactions in the periphery. Both, effector cell differentiation and activation as well as Treg homeostasis and function are critical for the balance of the immune system and their regulation depends on tunable

responses to minor changes in their environment. Specifically, TCR signaling can be regulated precisely by the expression of regulators of downstream signaling pathways including PI3K and NF-κB (Simpson and Ansel, 2015). Furthermore, and as described above, the establishment of differentially methylated regions in immuno-regulatory genes, as well as their precise alterations as required, are important regulators of immune function. One potential mechanism for the fine tuning of these pathways are miRNAs.

1.5 miRNAs

1.5.1 miRNAs: regulators of the immune system

miRNAs belong to the group of small non-coding RNAs (ncRNAs) which are defined by their length of 20-30 nucleotides and their Argonaute (AGO) family protein-mediated mode of action. ncRNAs have emerged as key players in the regulation of various biological processes, including immune function and homeostasis. They can be grouped in three distinct families of regulatory small ncRNAs: miRNA, siRNA (small interfering RNA) and piRNA (PIWI-interacting RNA), of which miRNAs are the most abundant class in most tissues. miRNAs are ~22 nucleotides long, single-stranded and transcribed from the genome, alone or in polycistronic clusters. They control gene expression by complementary binding of their target mRNA, recruiting AGO family proteins and inducing mRNA cleavage, translational repression and mRNA deadenylation.

The miRNA seed sequence is pivotal for its regulatory function. Spanning from nucleotide position 2 to 7, it facilitates target recognition via complementary binding to miRNA binding sites which can be located anywhere in the target mRNA but are slightly enriched for the 3' UTRs (untranslated region). While the seed sequence is crucial for the recognition of the target the miRNA to mRNA interaction is additionally supported by nucleotides 8 and 13-16 of the miRNA (Ha and Kim, 2014). miRNAs which share a highly similar seed sequence are grouped into families or clusters and their target genes overlap substantially (Bartel, 2004).

The biogenesis of miRNAs is a complex process, consisting of the transcription of a miRNA gene into primary miRNA (pri-miRNA) transcripts, processing into pre-miRNAs and finally into mature miRNAs. Pri-miRNAs are mainly transcribed by RNA polymerase II (Lee et al., 2004), and the primary transcript can contain a single miRNA or a cluster of multiple miRNAs (Berezikov, 2011). The pri-miRNA is processed by Drosha (Lee et al., 2003) and DGCR8 (Denli

et al., 2004; Gregory et al., 2004) and the resulting pre-miRNA by Dicer (Hutvágner et al., 2001) to produce the mature miRNA duplex. One strand of the mature miRNA is loaded into AGO to form the miRNA-induced silencing complex (miRISC) and guide the complex to its target mRNAs, while the other strand is discarded (Rand et al., 2005).

The miRNA database MirBase comprises more than 2,500 human miRNA sequences (Kozomara and Griffiths-Jones, 2014) although the actual number of existing miRNAs is supposed to be up to ten times higher (Rodríguez-Galán et al., 2018). Most miRNAs target a multitude of genes (Bartel, 2004) and more than 60% of human protein-coding genes contain conserved miRNA binding sites in addition to numerous non-conserved sites (Friedman et al., 2009; Ha and Kim, 2014), illustrating the complexity of miRNA-induced gene regulation. In line with their suggested contribution to the regulation of tissue homeostasis and function, miRNAs exhibit tissue-specific expression patterns, which are regulated on the level of transcription (Ha and Kim, 2014; Landgraf et al., 2007). Given the broad role of miRNAs for the regulation of various complex biological processes and the multitude of miRNA targets, dysregulated miRNA expression can contribute to various diseases, including autoimmunity, cancer (Lujambio and Lowe, 2012) and neurological diseases (Im and Kenny, 2012).

1.5.2 miRNAs as biomarkers in autoimmunity

The importance of biomarkers for studying disease and developing novel treatment strategies continues to grow in many areas of clinical practice. While most diseases symptoms are subjective, biomarkers provide an objectively quantifiable way to characterize disease to enable diagnosis and treatment as early and precise as possible, also facilitating strategies of personalized precision medicine aiming at the maximum benefit for the patient.

Levels of circulating miRNAs can be analyzed in small volumes of peripheral blood. Given this minimal invasiveness and the importance of miRNAs for immune homeostasis, several studies have investigated the impact of circulating miRNAs on diseases development and their potential suitability to predict diseases progression (Nielsen et al., 2012; Salas-Pérez et al., 2013; Sebastiani et al., 2012). miRNAs involved in the function of lymphocytes and beta cells were found to be differentially expressed in whole blood and serum obtained from newly diagnosed T1D patients compared to healthy controls. The abundance of miRNA21a and miRNA93, which are involved in NF-κB signaling and negatively regulate apoptotic and inflammatory genes, was significantly reduced in peripheral blood mononuclear cells (PBMCs)

of T1D patients (Salas-Pérez et al., 2013). In contrast, residual beta cell function and glycemic control in individuals with recent onset of T1D was associated with high levels of miRNA25 (Nielsen et al., 2012). miR146a was significantly downregulated in PBMCs of patients with newly diagnosed T1D and the decreased miRNA expression was associated with high GAD autoantibody titers in the serum (Yang et al., 2015a) while an upregulation of miR326 correlated with the presence of autoantibodies against GAD and IA2 (Sebastiani et al., 2012). A meta-analysis of studies investigating circulating miRNA profiles in T1D patients revealed eleven differentially expressed miRNAs: miR-21-5p, miR-24-3p, miR-100-5p, miR-146a-5p, miR-148a-3p, miR-150-5p, miR-181a-5p, miR-210-5p, miR-342-3p, miR-375 and miR-1275. These miRNAs were involved in immune regulation, cell proliferation and insulin processing, suggesting them as potential biomarkers for T1D (Assmann et al., 2017).

As illustrated above, the importance of the pre-symptomatic phase of T1D for the understanding of the underlying mechanisms as well as the development of intervention strategies has been increasingly recognized. Nevertheless, only few studies have investigated miRNA levels in individuals with islet autoimmunity before the onset of clinical T1D. One of these rare studies analyzed serum miRNAs in high-risk individuals positive for multiple islet autoantibodies, age-matched healthy children and recent-onset T1D patients. The authors found similar miRNA levels in the high-risk group and the healthy controls and no specific miRNA signature could be identified in the high-risk group. Furthermore, the serum miRNA levels were not able to distinguish between risk-individuals progressing to clinical disease and non-progressors. Interestingly, several miRNAs were associated with glucose homeostasis and autoantibody titers and these miRNAs correlated with glycemic status and ongoing islet autoimmunity in high-risk individuals (Åkerman et al., 2018). In a large cohort of 150 autoantibody-positive and 150 autoantibody-negative family-matched siblings revealed several miRNAs in the serum reflecting islet autoimmunity and progression to T1D with miR-21-3p, miR-29a-3p and miR-424-5p showing the strongest correlation (Snowhite et al., 2017). Nevertheless, so far it seems doubtful that circulating miRNAs are a valuable tool for T1D risk assessment.

Whole blood or serum samples of T1D patients are readily available, but their potential to give insight into the mechanisms underlying disease pathogenesis and progression seems to be rather limited: Changes in miRNA profiles of these highly diverse, mixed populations of

hematopoietic cells may result from changes in the abundance of specific cell subsets or their miRNA expression, rather than global changes in miRNA expression. In addition, in organ-specific diseases profiles from whole blood or serum might not reflect the situation in the affected organ. Therefore, the analysis of relevant miRNAs in cell types directly involved in autoimmune pathogenesis, such as Tregs, are of great interest and can provide considerable insight into the underlying mechanisms. Also, in order to validate circulating miRNAs as potential biomarkers and gain further insight into their contribution to onset and progression of autoimmunity, miRNA profiles of relevant immune cell subsets, ideally in the affected organs, are essential. However, these approaches are often impeded by the limited availability of samples of the affected organs, especially during the important presymptomatic phase. Furthermore, the affected organs generally contain only very low numbers of the relevant immune cells additionally hindering the broad applicability of these in principle promising approaches.

1.5.3 miRNA regulation of Tregs

The Treg-specific ablation of Dicer or Drosha in mouse models clearly revealed the crucial role of miRNAs for Treg homeostasis and function. While thymic Treg development was unaltered, the Treg-specific miRNA deficiency resulted in impaired Treg homeostasis resulting in reduced suppressive function and fatal systemic autoimmunity (Chong et al., 2008; Cobb et al., 2006; Liston et al., 2008; Zhou et al., 2008b). Additional studies identified individual miRNAs contributing to these defects, including effects on thymic Treg development, Treg induction, Foxp3 expression, Treg stability and suppressive function.

miR155 is highly abundant in Tregs and directly regulated by Foxp3. In mouse models miR155 deficiency resulted in impaired Treg development and homeostasis and consequently reduced levels of Tregs in the thymus and the spleen (Kohlhaas et al., 2009; Lu et al., 2009). In miR155-deficient Tregs the expression of Foxp3 is reduced and instable while *in vitro* Treg induction is unaffected. miR155 targets suppressor of cytokine signaling 1 (SOCS1), a negative regulator of STAT5 signaling which determines the responsiveness to IL2, a critical regulator of Treg homeostasis (Yao et al., 2012). However, miR155-deficient Tregs can prevent autoimmune diseases in mice, indicating that miR155 is crucial for Foxp3 expression and stability but does not directly affect Treg suppressive function (Kohlhaas et al., 2009).

miR10a is exclusively expressed in Tregs and is induced following exposure to retinoic acid. High levels of miR10a have been shown to correlate with a low susceptibility to autoimmune diseases in mice (Jeker et al., 2012; Takahashi et al., 2012). miR10a stabilizes the Treg-specific gene signature by targeting several effector T cell genes including BCL6 and NCOR2. However, the functional targets of miR10a seem to overlap with other miRNAs since miR10a deficiency does not result in impaired Treg function or autoimmunity.

The efficient *in vitro* Treg induction is also subject to regulation by miRNAs. *In vitro* Treg induction experiments using both Dicer and Drosha deficient naive CD4+ T cells resulted in a significantly reduced expression of Foxp3 in induced Tregs compared to control mice (Chong et al., 2008; Cobb et al., 2006). Interestingly, miRNAs with both positive and negative regulatory effects on *in vitro* Treg induction have been identified in a miRNA screen (Warth et al., 2015) and several miRNAs form networks to cooperatively regulate Treg induction. For example, miR150 induced reduction of mTOR occurs only in presence of miR99a and a similar cooperation has been shown for miR15a-16 and 15b-16. Another miRNA targeting the PI3K/Akt/mTOR pathway is miR126. It targets p85β, which is a regulatory subunit of PI3K, reducing PI3K/Akt/mTOR pathway activity and favoring Treg induction. By contrast, miR126 inhibition increases the activity of the PI3K/Akt/mTOR pathway, inhibiting Foxp3 expression and impairing Treg induction (Qin et al., 2013). miR155 also contributes to proper Treg induction *in vitro* by targeting SOCS1 which is in line with its role for thymic Treg generation (Murugaiyan et al., 2011). As mentioned above, the miRNA screen also revealed miRNAs with a negative effect on Treg induction *in vitro* (Warth et al., 2015). Two members of the miR17~92 cluster, miR17 and miR19, negatively regulate Treg induction while they have no impact on thymic Treg development (Jiang et al., 2011). miR17 has been shown to directly target the cAMP-responsive element binding protein 1 (CREB1) and the TGFβ-receptor II, both involved in proper Treg induction. The TGFβ signaling pathway is also a target of the miR23-miR27-miR24 cluster, and consequently a high abundance of this cluster impairs Treg generation (Cho et al., 2016).

1.5.4 T cell specific miRNAs in autoimmunity

While the studies described above provided considerable insight into the contribution of specific miRNAs to immune homeostasis and Treg function, making them of considerable importance for the field, the underlying mechanisms affecting signaling pathways in Tregs, resulting in islet autoimmunity remain poorly understood. As described above, impaired Treg function, induction and maintenance seem to be a decisive factor for an insufficient tolerance induction and the onset of islet autoimmunity. Recently, two studies have reported a direct relationship between the upregulation of two miRNAs in T cells during the onset of islet autoimmunity, contributing to an impairment of Treg induction from naive CD4$^+$ T cells.

As described above, Serr et al. provided evidence for impaired Treg induction capacity in naive CD4$^+$ T cells from children with recent onset of islet autoimmunity compared to children without islet autoantibodies or with long term islet autoimmunity without developing clinical T1D. Additionally frequencies and proliferation of Foxp3^{int}CD4$^+$ T cells were enhanced, pointing towards increased T cell activation interfering with subimmunogenic TCR stimulation and efficient Treg induction (Serr et al., 2016b, 2018). Differential expression of miRNAs during onset of islet autoimmunity, specifically high levels of miR181a which modulates signaling thresholds and sensitivity to antigenic stimulation in CD4$^+$ T cells could contribute to the observed increase in T cell activation (Li et al., 2007b). Hence, increasing the activity of miR181a using a miRNA mimic reduced murine and human Treg induction, whereas a miR181a inhibitor had the opposite effect. High levels of miR181a were accompanied by an increased abundance of nuclear factor of activated T cells 5 (NFAT5) which plays an important role in T cell activation (Vaeth et al., 2012). Additionally, PTEN which is a negative regulator of T cell activation, was identified as a direct target of miR181a and its inhibition promoted PI3K signaling and consequently activation of NFAT5. From this follows that elevated miR181a expression in CD4+ T cell during onset of islet autoimmunity are accompanied by a decrease in PTEN and an increase in NFAT5 expression, resulting in T cell activation and reduced Treg induction. The high abundance of miR181a additionally increased the expression of the costimulatory molecule CD28 which also contributed to PI3K activation (Sauer et al., 2008), NFAT5 upregulation and T cell activation.

Mouse models of T1D islet autoimmunity resembled the findings made in the human system. Specifically, Treg induction capacity was reduced in NOD mice with islet autoimmunity and

this observation was accompanied by increased levels of miR181a and NFAT5, as well as decreased PTEN expression. The *in vivo* inhibition of miR181a in IAA[+] NOD mice resulted in significantly reduced CD28 and NFAT5 expression, enhanced PTEN levels and reduced islet autoimmunity. Using an NFAT5 inhibitor or NFAT5 deficient mice enhanced Treg induction, and CD4^{+} T cells showed increased levels of PTEN and also Foxo1, which is directly involved in the positive regulation of Treg differentiation (Ouyang et al., 2010).

In a second study, the investigation of the effects of miR92a on T follicular helper (TFH) cell regulation in islet autoimmunity revealed important insights into the regulation of Treg induction by this miRNA (Serr et al., 2016a). TFH cells are a subset of CD4^{+} T cells which are an essential part of humoral immunity by providing support to B cells to produce high-affinity antibodies (Breitfeld et al., 2000). The precursors of TFH cells circulate in the blood and their function of inducing antibody responses also suggests a critical contribution to the development of autoimmune diseases (Scherm et al., 2016; Serr and Daniel, 2018). miR92a belongs to the miR17~92 cluster which is involved in the onset of autoimmunity and antibody production in mice (Xiao et al., 2008). This provided the rationale for a miRNA screen to investigate T cell-specific miRNAs in children with ongoing islet autoimmunity compared to healthy controls. miR92a was significantly upregulated in CD4^{+} T cells from children with ongoing islet autoimmunity, and the confirmation using qPCR showed that this increase was restricted to children with recent onset of islet autoimmunity whereas children with long-term autoimmunity showed miR92a levels comparable to healthy controls. Furthermore, the abundance of miR92a correlated with the frequency of TFH cell precursors in the peripheral blood. Inhibition of miR92a function resulted in decreased TFH cell induction *in vitro*, whereas a miR92a mimic increased TFH cell formation. Increased miR92a activity resulted in the downregulation of PTEN, PHLPP2, FOXO1 and CTLA4 which are negative regulators of T cell activation and known targets of miR92a. The reduced abundance of PTEN resulted in the activation of the PI3K/Akt/mTOR pathway which interferes with Treg induction. Consequently, *in vitro* Treg induction was significantly impaired in the presence of a miR92a mimic, and high miR92a levels in children with recent onset of islet autoimmunity are accompanied by reduced frequencies of insulin-specific Treg. Conversely, PI3K signaling promotes TFH cell induction, since the effect of a miR92a mimic is reduced in presence of a PI3K inhibitor and increased when PTEN signaling is inhibited. KLF2 was shown to interfere

with TFH cell differentiation by induction of S1pr1 expression and inhibition of the TFH master regulator BCL6 via upregulation of BLIMP1 (Lee et al., 2015). The study revealed KLF2 as a novel target of miR92a, thereby offering an additional mechanism of miR92a-mediated TFH cell differentiation.

These studies show that the dysregulation of an individual miRNA can critically contribute to impaired Treg induction from naive CD4^{+} T cells and consequently to the onset and progression of islet autoimmunity. Furthermore, these miRNAs and their identified downstream pathways are promising targets for strategies aiming at reestablished Treg induction *in vitro* and *in vivo*.

1.5.5 miR142-3p

miR142-3p is an evolutionary conserved miRNA of vertebrates, which is expressed in several hematopoietic cell types, including DCs, monocytes, T cells, and B cells (Sun et al., 2011; Wu et al., 2007). Its expression was first reported in murine embryonic and adult hematopoietic tissues, including bone marrow, thymus and spleen, highlighting its role for embryonic and adult hematopoiesis (Chen et al., 2004). miR142-3p can directly target the expression of tab2 and IL-6 in myeloid and dendritic cells, which makes it an important regulator of the development and function of differentiated hematopoietic cell lineages (Sun et al., 2011; Wang et al., 2012). Furthermore, miR142–3p plays critical roles in the maintenance of CD4^{+} DCs (Mildner et al., 2013) and prevents macrophage differentiation during tumor-induced myeloid differentiation (Sonda et al., 2013) and megakaryopoiesis (Chapnik et al., 2014). In the context of Treg homeostasis miR142-3p has been identified as a regulator of ATG16L1 and its role in regulating autophagy, proliferation and function in thymic-derived Tregs as well as the implication of these findings for graft-versus-host disease have been highlighted (Lu et al., 2018). Another study has shown that miR142-3p regulates GARP expression in Tregs and, as a result, their expansion in response to activation, which provides insight into mechanisms involved in Treg proliferation and expansion (Zhou et al., 2013).

2 Objectives

In T1D, islet autoantibodies, indicating the onset of islet autoimmunity, can be present in the blood often many years before clinical symptoms arise. While T cells have been shown to play a major role in the destruction of pancreatic beta cells, the molecular mechanisms triggering the onset of islet autoimmunity and promoting aberrant T cell activation and the highly variable progression to symptomatic T1D remain poorly understood. The onset of islet autoimmunity and T1D in mice or humans is accompanied by a reduced capacity of naive CD4$^+$ T cells to be differentiated into Tregs *in vitro*. Epigenetic modifications, including DNA methylation of regulatory gene elements, are well established regulators of Treg function and recent studies have highlighted miRNAs as critically contributing to immune homeostasis, by fine-tuning the expression of relevant genes. Therefore, in this thesis I aimed at gaining insights into the potentially regulatory network of both miRNAs and DNA methylation contributing to aberrant immune activation and the progression to clinically overt T1D.

The first objective of this thesis was to confirm the important role of DNA methylation of the Foxp3 CNS2 for Treg identity and function and to further dissect this regulatory mechanism by analyzing DNA methylation during Treg induction *in vitro*.

As a second objective, I aimed at the identification of specific miRNAs in T cells that contribute to the onset of autoimmunity and the identification of their relevant targets and downstream pathways. These experiments used unbiased approaches like miRNA Sequencing of CD4$^+$ T cells of children with and without islet autoimmunity and HITS CLIP to identify candidate miRNAs and their direct mRNA targets. To confirm the relevance of the identified miRNA in autoimmunity and the direct targeting of the corresponding mRNA I employed a combination of various molecular and cellular approaches, including miRNA modulation and loss-of-function models.

The third objective was the mechanistic dissection of the miRNA and its downstream pathway in order to gain insight into their involvement in impaired Treg induction and the onset and progression of autoimmunity. Specifically, I investigated the inhibition of the candidate miRNA in Treg induction experiments *in vitro* as well as in mouse models of T1D autoimmunity *in vivo* and the relevance for established human T1D and therefore the translatability of the previous findings was tested in humanized mouse models.

3 Materials and methods

3.1 Materials

Table 1. Chemicals and reagents

Chemical/reagent	Source	Identifier
Foxp3 Staining Buffer Set	eBioscience	Cat# 00-5523-00
Fixable Viability Dye eFluor450	eBioscience	Cat# 65-0863-18
Sytox Red	Thermo Fischer Scientific	Cat# S34859
Sytox Blue	Thermo Fischer Scientific	Cat# S34857
Streptavidin Microbeads	Miltenyi	Cat #130-048-101
Human CD4$^+$ microbeads	Miltenyi	Cat# 130-045-101
Streptavidin Pacific Blue	Invitrogen	Cat# S11222
Ficoll-Paque PLUS	GE Healthcare	Cat# 17-1440-03
recombinant human IL-2	ReproTech	Cat# 200-02
Tissue-Tek O.C.T. Compound	A. Hartenstein	Cat# TTEK

Table 2. Cell culture media and supplements

Medium	Manufacturer	Components
X-Vivo 15	Lonza	50ml Human serum 5ml Penicillin Streptomycin 500µl Sodium pyruvate 500µl Non-essential aminoacids 500µl GlutaMAX 500µl Fungizone 400µl
RPMI 1640	Thermo Fisher Scientific	500ml FCS 50ml Sodium pyruvate 5ml Non-essential aminoacids 5ml Penicillin Streptomycin 5ml 2-Mercaptoethanolv 500µl

Table 3. Buffers

Buffer	Manufacturer	Components
Hank's Balanced Salt Solution	Sigma-Aldrich	500ml FCS 50ml HEPES 5ml
MACS PBS	Thermo Fisher Scientific	500ml BSA 10% 25ml EDTA 2ml

Table 4. Critical commercial assays

Assay	Source	Identifier
miRNeasy Micro Kit	Qiagen	Cat# 217084
iScript Advanced cDNA Synthesis Kit	BioRad	Cat# 1725038
Eva Green SuperMix	BioRad	Cat# 1725202
Zymo Methylation Direct 200	Zymo Research	Cat# D5021
PyroMark Gold Q24 Reagents	Qiagen	Cat# 970802
SensiFAST HRM Kit	Bioline	Cat# 5001484
Universal cDNA Synthesis Kit II	Exiqon	Cat# 203301
miRCURY LNA™ microRNA PCR, ExiLENT SYBR® Green master mix	Exiqon	Cat# 203403
siRfficient™ siRNA Transfection Reagent	MBL Life Science	Cat# WU2001
NEBnext Multiplex Small RNA Library Prep Set	New England Biolabs	Cat# E7300

Table 5. Technical equipment

Device	Model	Manufacturer
Cell sorter	FACS Aria III	BD Biosciences
Centrifuge	Heraeus Multifuge X3R	Thermo Scientific
Micro centrifuge	Centrifuge 54 24 R	Eppendorf
CO_2 incubator	BBD 6220	Thermo Scientific
MACS cell separator	MACS Multistand, QuadroMACS	Miltenyi Biotec

Sterile workbench	Scanlaf Mars Class 2	LaboGene
Microplate spectrophotometer	Epoch	BioTek
Pyro-sequencer	PyroMark Q24	Qiagen
Real-time PCR system	CFX96 Touch	Bio-Rad
Thermal cycler	peqStar 2X	Peqlab
Inverted microscope	CKX41	Olympus
Microscope	Primo Star	Zeiss
Confocal microscope	LSM700	Zeiss
high-throughput sequencing system	HiSeq2000	Illumina
Luminometer	Glomax Multi Detection System	Promega
capillary electrophoresis machine	Bioanalyzer 2100	Agilent

Table 6. Biological samples

Sample	Source	Identifier
PBMCs	DiMelli study	Warncke et al., 2013
PBMCs	BABYDIAB study	Achenbach et al., 2009; Ziegler et al., 1999, 2013
PBMCs	Munich Bioresource project	approval number #5049/11, Technische Universität München, Munich, Germany

Table 7. Experimental models: organisms/strains

Experimental model	Source	Identifier
NOD/ShiLtJ	Jackson Laboratory	Stock No: 001976
Foxp3 GFP Balbc (C.Cg-Foxp3^{tm2Tch}/J)	Jackson Laboratory	Stock No: 006769
CD90.1 Balb/c (CBy.PL(B6)-$Thy1^a$/ScrJ)	Jackson Laboratory	Stock No: 005443
CD90.2 Balb/c (Balb/cByJ)	Jackson Laboratory	Stock No: 001026
miR142$^{-/-}$	Saverio Bellusci	
HLA-DQ8 transgenic NOD.Cg-Prkdcscid Il2rgtm1Wjl	Leonard D. Shultz	

Table 8. Antibodies

Antibody	Source	Identifier
anti-human CD25 APC	BD Biosciences	Cat# 340907; clone: 2A3
anti-human CD45RO APC-H7	BD Biosciences	Cat# 561137; clone: UCHL1
anti-human CD4 V500	BD Biosciences	Cat# 560768; clone: RPA-T4
anti-human HLA-DR PerCP-Cy5.5	BD Biosciences	Cat# 560652; clone: L243
anti-human CD45RA FITC	Biolegend	Cat# 304106; clone: HI100
anti-human CD3 PerCP-Cy5.5	Biolegend	Cat# 300328; clone: HIT3a
anti-human CD3 AlexaFluor700	Biolegend	Cat# 300323; clone: HIT3a
anti-human CD127 PE-Cy7	Biolegend	Cat# 351320; clone: A019D5
anti-human FOXP3 PE	eBioscience	Cat# 12-4777-42; clone: 236A/E7
Fc-Block	BioLegend	Cat# 422302
anti-mouse CD4 Biotin	BD Biosciences	Cat# 553728; clone: GK1.5
anti-mouse CD4 AlexaFluor700	eBioscience	Cat# 56-0042-82; clone: RM4-5
anti-mouse CD25 PerCP-Cy5.5	Biolegend	Cat# 102030; clone: PC61
anti-mouse CD44 PE	Biolegend	Cat# 103008; clone: IM7
anti-mouse Ki67 APC	Biolegend	Cat# 652406; clone: 16A8
anti-mouse CD62L APC	eBioscience	Cat# 17-0621-82; clone: MEL-14
anti-mouse Foxp3 FITC	eBioscience	Cat# 11-5773-82; clone: FJK-16s
anti-mouse Tet2	Abiocode	Cat# AC-M1086-4a; clone: 10F1
donkey-anti-mouse IgG APC	eBioscience	Cat# 17-4012-82; polyclonal
insulin rabbit-anti-mouse	Cell Signaling	Cat# ; clone:
donkey-anti-rabbit AlexaFluor647	Dianova	Cat# ; clone:
CD3 arm. hamster-anti-mouse	BD Biosciences	Cat# ; clone:
goat-anti-arm.hamster Dylight488	Dianova	Cat# ; clone:
Tet2	ABclonal	Cat# ; clone: A5682
horse-anti-rabbit Biotin	Vector	Cat# ; clone:
Streptavidin Dylight549	Dianova	Cat# ; clone:
anti-human CD3	Biolegend	Cat# 300432; clone: UCHT1
anti-human CD28	Biolegend	Cat# 302923; clone: CD28.2
anti-mouse CD3	BD Pharmingen	Cat# 553057; clone: 145-2C11
anti-mouse CD28	BD Pharmingen	Cat# 553294; clone: 37.51

Table 9. Primer sequences qPCR

Gene	forward	reverse	Source
Histone	ACTGGCTACAAAAGCCG	ACTTGCCTCCTGCAAAGCAC	Sigma Aldrich
Tet2 hs	TTCGCAGAAGCAGCAGTGAAGAG	AGCCAGAGACAGCGGGATTCCTT	Sigma Aldrich
Tet1 mm	ATGAGCGGCACCCTGAAGCG	GCACCGAGCCGTGAATGGGT	Sigma Aldrich
Tet2 mm	CCTTGCATTGGAGGGGTGGCT	GTGGGGTGATTCCGGTCGGG	Sigma Aldrich
Tet3 mm	CACGGCTTCGAGGCAAGCCA	CCCCGGTTCCCATCCCCCAT	Sigma Aldrich
Tgfbr1 mm	CAGCTCCTCATCGTGTTGGT	GGCAGAAACACTGTAATGCCTTC	Sigma Aldrich
ATG16L1 mm	CCGAATCTCCCCTTTTGGGA	CATGCGCATCGAAGACATACG	Sigma Aldrich
5s	N/A	N/A	Exiqon (miRCURY LNA primer set)
miR142-3p hs	N/A	N/A	Exiqon (miRCURY LNA primer set)
miR142-3p mm	N/A	N/A	Exiqon (miRCURY LNA primer set)

Table 10. Primer sequences methylation analysis

Site	forward	reverse	Pyrosequencing	Source
Foxp3 CNS2 hs	AAGTTGAATGGGGGATGTTTTTGGGATATAGATTATG	CTACCACATCCACCAACACCCATATCACC	TAGTTTTAGATTTGTTTAGATTTT	Sigma Aldrich
Foxp3 CNS2 mm	TTGGGTTTTGTTGTTATAATTTGAATTTGG	ACCTACCTAATACTCACCAAACATC	AATTTGAATTTGGTTAGATTTTT	Sigma Aldrich
Bach2 mm	TTTGTTATATTTTGGGTGAAAATGTTTTAT	ACTAAAATCCCCTTAAATAACAACTC	AATAATAGAGAATAGGGGT	Sigma Aldrich

Table 11. Sequences miRNA inhibitors and mimics

Inhibitor/mimic	Sequence	Source
miR142-3p inhibitor hs/mm	CCATAAAGTAGGAAACACT	Exiqon miRCURY LNA™ microRNA inhibitor
miR142-3p mimic hs/mm	TGTAGTGTTTCCTACTTTATGGA	Exiqon miRCURY LNA™ microRNA mimic
control inhibitor hs/mm	TAACACGTCTATACGCCCA	Exiqon miRCURY LNA™ microRNA inhibitor
control mimic hs/mm	GATGGCATTCGATCAGTTCTA	Exiqon miRCURY LNA™ microRNA mimic

Table 12. Sequences siRNAs

siRNA	Sequence	Source
Tet2 mm	N/A	Ambion (Silencer Select Pre-Designed siRNA)
Tet2 hs	N/A	Ambion (Silencer Select Pre-Designed siRNA)
Negative control	N/A	Ambion (Silencer Select Negative control no.1)

Table 13. Primer sequences for site directed mutagenesis of TET2 3'UTR

site	forward (mutation in bold type)	reverse (mutation in bold type)	source
HITS CLIP mut	ATACAAAATTG**TCGTA**CAAGTTCATTGCTC	GAGCAATGAACTTG**TACGA**CAATTTTGTAT	
predicted mut 1	GTCATATACCTCA**AACAT**AGTTTGGCAATAGG	CCTATTGCCAAACT**ATGTT**TGAGGTATATGAC	Sigma Aldrich
predicted mut 2	CTTTTGCAGTTTG**AACAT**AAGATAACTTCTGTG	CACAGAAGTTATCTT**ATGTT**CAAACTGCAAAAG	Sigma Aldrich

Table 14. Software

Software	Source	Identifier
FlowJo software (version 7.6.1)	TreeStar Inc., OR	https://www.flowjo.com/solutions/flowjo/downloads/
FACSDiva software (version 6.1.3)	Beckton Dickinson	
Prism (version 6.0.1)	GraphPad	https://www.graphpad.com/scientific-software/prism/
miRanda (v3.3a)	www.microrna.org	www.microrna.org
BTrim	Kong, 2011	http://graphics.med.yale.edu/trim/
bowtie	Langmead et al., 2009	http://bowtie-bio.sourceforge.net/index.shtml
bowtie2	Langmead and Salzberg, 2012	http://bowtie-bio.sourceforge.net/index.shtml
HTSeq-count	Anders et al., 2015	http://www-huber.embl.de/users/anders/HTSeq/doc/install.html
mirBase (release 20)	Kozomara and Griffiths-Jones, 2014	http://www.mirbase.org
DESeq2	Love et al., 2014	https://bioconductor.org/packages/release/bioc/html/DESeq2.html

Table 15. Deposited data

Data	Source	Identifier
miRNA sequencing data	This research project	NCBI GEO: GSE140064
HITS-CLIP sequencing data	This research project	NCBI GEO: GSE124264

3.2 Human studies

All human studies comply with the relevant ethical regulations for work with human participants and all study participants gave written consent prior to inclusion in the Munich Bioresource project (approval number #5049/11, Technische Universität München, Munich, Germany). Venous blood was collected using sodium heparin tubes and blood volumes were based on EU guidelines with a maximal blood volume of 2.4 ml per kg of body weight. All subjects have been already enrolled in the BABYDIAB study [3,58,59] and the DiMelli study [60] with the documented age of T1D onset. Subjects have been stratified based on the presence or absence of multiple islet autoantibodies and T1D. No islet autoimmunity and no T1D: n = 6; median age at sampling = 8 years, IQR (interquartile range) = 6-12 years; all male. Recent onset of T1D: n = 10; median age at sampling = 4 years, IQR = 3-5 years; median HbA1c = 8.9 mg/dl, IQR = 8.4-10.6 mg/dl; median time from diagnosis to sampling = 7 days, IQR = 1-11 days; all male.

3.3 Mouse experiments

CBy.PL(B6)-Thy1^a/ScrJ (CD90.1 BALB/c), Balb/cByJ (CD90.2 BALB/c), Balb/c.Cg-Foxp3tm2Tch/J (BALB/c Foxp3GFP) and NOD/ShiLtJ mice were obtained from the Jackson Laboratory and NOD/ShiLtJ mice were stratified according to their IAA status. Humanized mice, NOD.Cg-Prkdc^{scid} H2-Ab1t^{m1Gru} Il2rg^{tm1Wjl} Tg(HLA-DQA1,HLA-DQB1) 1Dv//Sz mice lack mouse MHC class II and transgenically express human HLA-DQ8. These mice were obtained from and developed by Dr. Leonard D. Shultz. To develop this stock, B10M-HLA-DQ8 mice were kindly provided by Dr. Chella David (Nabozny et al., 1996). The DQ8 transgene was backcrossed for 10 generations on the NSG strain background. The NSG-DQ8 mice were then intercrossed with NSG mice lacking mouse MHC class II (NOD.Cg-Prkdc^{scid} H2-Ab1^{tm1Gru} Il2rg^{tm1Wjl}) (Covassin et al., 2013). miR142$^{-/-}$ mice were developed by excision of the miR142 region in C57BL/6N mouse embryonic stem cells (Shrestha et al., 2015) and obtained from the mouse facility of the German Center for Lung Research, Universities of Giessen and Marburg (Mfd Diagnostics, Wendelsheim, Germany). When possible littermate controls were used, otherwise age- and sex-matched mice. Mice were maintained under specific pathogen-free conditions on 12-h/12-h light dark cycle at 25 °C with ad libitum access to water and a standard diet at the animal facility of Helmholtz Zentrum München, Munich, Germany according to guidelines established by the Institutional Animal Committees, including all relevant ethical regulations

for animal testing and research. Ethical approval for all mouse experimentations has been received by the District Government of Upper Bavaria, Munich, Germany (approval # ROB-55.2-2532.Vet_02-17-130).

3.3.1 Murine insulin autoantibody (IAA) assay

Levels of NOD insulin autoantibodies were measured with a mouse high specificity/sensitivity competitive IAA assay in an ELISA format and sera from NOD mice. In brief, high binding 96-well plates (Costar) were coated with human recombinant insulin (100 U/ml; Humulin; Lilly) overnight at 4°C. Unspecific-blocking was performed with PBS containing 2% BSA for 2 hours at room temperature. Preincubated NOD sera (diluted 1:10) with or without insulin competition were added and incubated for 2 hours at room temperature. After 4 wash steps, biotinylated anti–mouse IgG1 (Abcam), diluted 1:10,000 in PBS/BSA was added for 30 min at room temperature. After washing horseradish peroxidase–labeled streptavidin was added for 15 min. After 5 additional washing steps TMB substrate solution was added (OptEIA reagent set; BD). All samples were measured in duplicates with and without competition using human insulin.

In a second approach, to determine levels of IAA in NOD mice, a Protein A/G radiobinding assay based on 125I-labelled recombinant human insulin, was applied as previously described (Achenbach et al., 2009). Serum from C57Bl/6 mice was used as negative control.

3.3.2 Engraftment of NSG mice with human PBMCs

Murine MHCII deficient, HLA-DQ8 transgenic NOD.Cg-Prkdc[scid] Il2rg[tm1Wjl] (NSG) mice were reconstituted with PBMCs from an HLA-DQ8^{+} donor with T1D. 5×10^4 PBMCs per mouse were injected intravenously in 50 ml PBS into the retro orbital sinus without prior conditioning by irradiation or busulfan treatment. To avoid sex incompatibilities, the sex of the NSG-HLA-DQ8 mice for reconstitution was chosen in accordance with the blood donor.

3.3.3 *In vivo* miR142-3p inhibitor application

A miR142-3p inhibitor (Inhibitor Probe mmu-miR-142-3p, Exiqon) was injected i.p. into IAA^{+} NOD mice or NSG humanized mice at 10mg/kg every other day for 14 days. On day 15 Treg frequencies were analyzed in lymph nodes. CD25^{high}Foxp3^{high} Tregs were sort purified for methylation analysis. Pancreata were embedded for cryosections and analysis of pancreas pathology. For miRNA inhibitor localization experiments a FAM-labelled miR142-3p inhibitor

(mmu-miR-142-3p inhibitor 5'FAM, Qiagen) was injected i.p. into BALB/c or NSG humanized mice at 10 or 20mg/kg. The FAM-labelled miR142-3p inhibitor was detected via flow cytometry after 4 hours, 24 hours or at the end of an application period of 14 days every other day.

3.3.4 Immunofluorescence staining and histopathology of NOD pancreata

Immunofluorescence staining was carried out after aceton fixation, permeabilization and blocking with Avidin/ Protein blocking together with 5% goat serum using rabbit-anti-mouse insulin antibodies (Cell Signaling, 1:100) and donkey-anti-rabbit[AlexaFluor647] antibodies (Dianova, 1:400). For CD3 staining, arm. hamster anti-mouse antibodies (BD, 1:50) were used, followed by goat-anti-arm.hamster antibodies conjugated with Dylight[488] (Dianova, 1:100). For Tet2 staining rabbit-anti-Tet2 antibodies (ABclonal, clone A5682, 1:25) was used with biotinylated horse-anti-rabbit antibodies (Vector, 1:100) combined with SA[Dylight 549]. For Foxp3 staining, cells were incubated with rat-anti-mouse Foxp3 antibodies (eBioscience, clone FJK-16s, 1:50) and biotinylated goat anti-rabbit (BD), combined with SA[Dylight 549]. Nuclei were counterstained with DAPI (Diavona). For Tgfbr1 staining rat-anti-mouse/human Tgfbr1 antibodies (R&D, clone 141231, 1:25) was used, followed with biotinylated goat-anti-rat antibodies (1:250) combined with SA[Dylight 549] (Dianova, 1:200). Negative control slides were incubated with secondary antibodies. Cells were analyzed by confocal microscopy (Zeiss LSM700).

Pancreata of NOD mice were embedded with Tissue-Tek O.C.T. Compound and frozen on dry ice. Serial sections were stained with hematoxylin and eosin. Insulitis scoring was performed as follows: 0: intact islets/no lesions; 1: periislet infiltrates; 2: <25% islet destruction; 3: >25% islet destruction; 4: complete islet destruction. Investigators were blinded for group allocations.

3.4 Cell isolation, staining and sorting

Human peripheral blood mononuclear cells (PBMCs) were isolated from fresh venous blood by density gradient centrifugation using Ficoll-Paque PLUS (GE Healthcare). CD4$^+$ T cells were purified from PBMCs by Magnetic Activated Cell Sorting (MACS) using CD4 microbeads (Miltenyi Biotec) following the manufacturer's protocol.

Murine lymph nodes and spleens were passed through 70µm cell strainers, stained with a CD4-Biotin antibody (BD Bioscience) and MACS purified using Streptavidin Microbeads (Miltenyi Biotec) following the manufacturer's protocol.

To prevent unspecific signals the isolated cells were incubated with Fc-Block (Biolegend) and afterwards with fluorochrome-labelled antibodies for 30 minutes on ice in the dark. For FACS staining of human T cells the following monoclonal antibodies were used: From BD Biosciences (San Jose, CA): anti-CD25 APC (2A3), anti-CD45RO APC-H7 (UCHL1), anti-CD4 V500 (RPA-T4), anti-HLA-DR PerCP-Cy5.5 (L243); from Biolegend (San Diego, CA): anti-CD45RA FITC (HI100), anti-CD3 PerCP-Cy5.5 (HIT3a), anti-CD127 PE-Cy7 (A019D5), anti-CD3 AlexaFluor700 (HIT3a); from eBioscience (San Diego, CA): anti-FOXP3 PE (236A/E7). For murine FACS staining the following monoclonal antibodies were used: From BD Biosciences (San Jose, CA): anti-CD4 Biotin (GK1.5); from Biolegend (San Diego, CA): CD25 PerCP-Cy5.5 (PC61), CD44 PE (IM7) Ki67 APC (16A8); from eBioscience (San Diego, CA): CD4 AlexaFluor700 (RM4-5), CD62L APC (MEL-14), Foxp3 FITC (FJK-16s); from Abiocode: Tet2 (10F1). After surface staining, the cells were fixed and permeabilized using the Foxp3 Staining Buffer Kit (eBioscience) to enable the detection of the intracellular abundance of Foxp3, Ki67 and Tet2. Cells were acquired on the BD FACS Aria III cell sorting system using FACS Diva software with optimal compensation and gain settings determined for each experiment based on unstained and single-color stained samples. Doublets were excluded based on SSC-A vs. SSC-W plots. Live cell populations were gated on the basis of cell side and forward scatter and the exclusion of cells positive for Sytox Blue (Life Technologies) or Fixable Viability Dye eFluor450 (e-bioscience). Flow cytometry data were analyzed using FlowJo software version 7.6.1 (TreeStar Inc., OR)
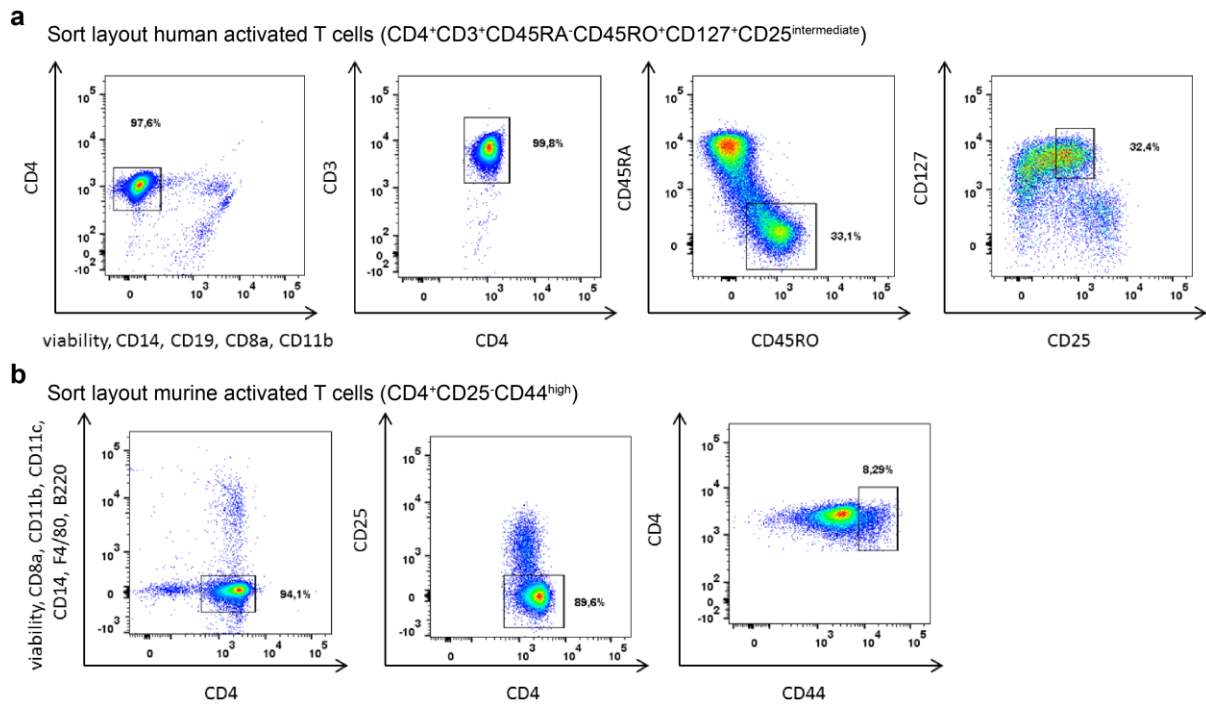
Figure 1. Gating strategy for FACS sorting of human and murine activated T cells. (a) Representative FACS plot for the sorting of human activated T cells: CD4$^+$CD3$^+$CD45RA$^-$CD45RO$^+$CD127$^+$CD25intermediate. **(b)** Representative FACS plot for the sorting of murine activated T cells: CD4$^+$CD25$^-$CD44^{high}.
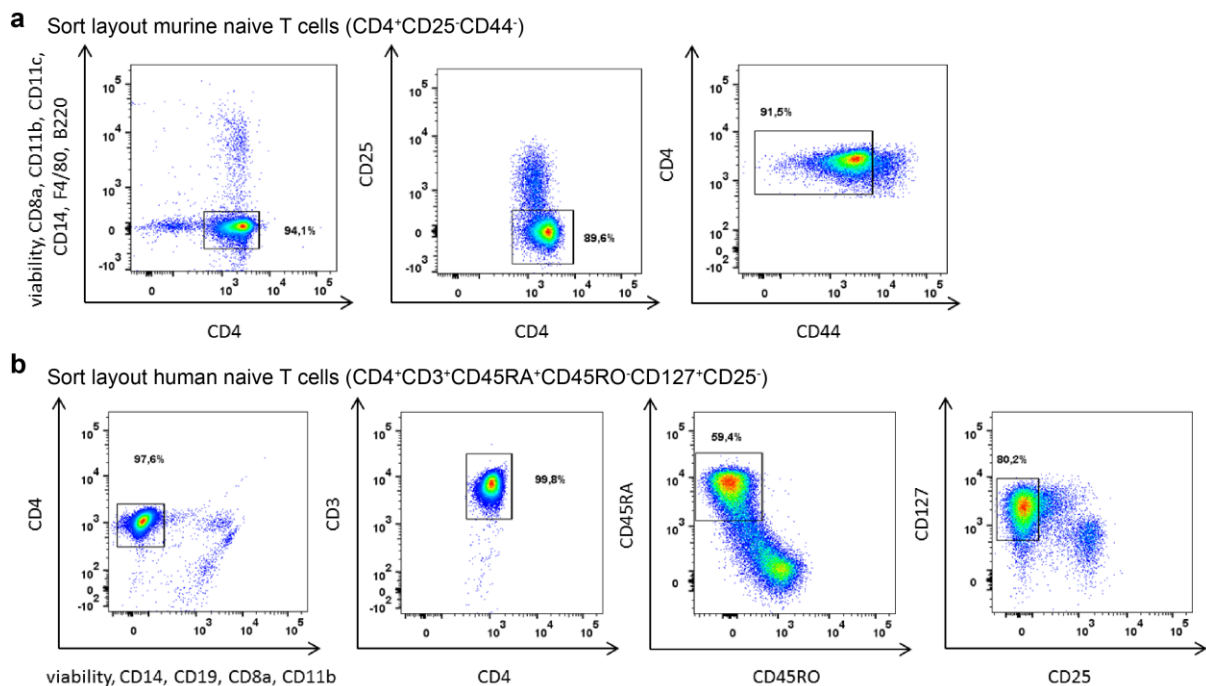
Figure 2. Gating strategy for FACS sorting of murine and human naive T cells. (a) Representative FACS plot for the sorting of murine naive T cells: CD4$^+$CD25$^-$CD44$^-$. **(b)** Representative FACS plot for the sorting of human naive T cells: CD4$^+$CD3$^+$CD45RA$^+$CD45RO$^-$CD127$^+$CD25$^-$.
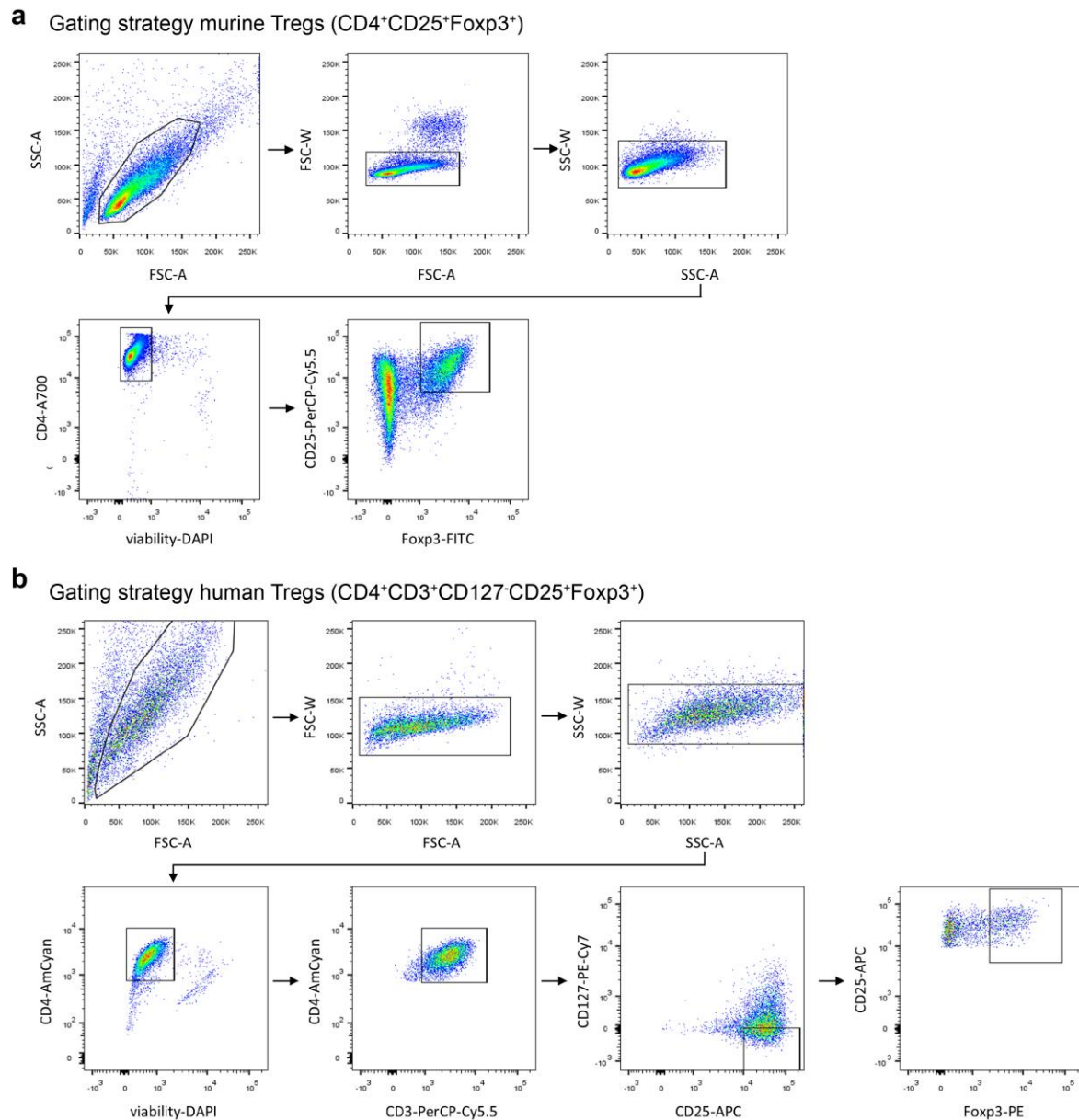
Figure 3. Gating strategy for FACS sorting of induced murine and human Treg. (a) Representative FACS plot for the sorting of induced murine Tregs: CD4$^+$CD25$^+$Foxp3$^+$. **(b)** Representative FACS plot for the sorting of induced human Tregs: CD4$^+$CD3$^+$CD127$^-$CD25$^+$Foxp3$^+$.
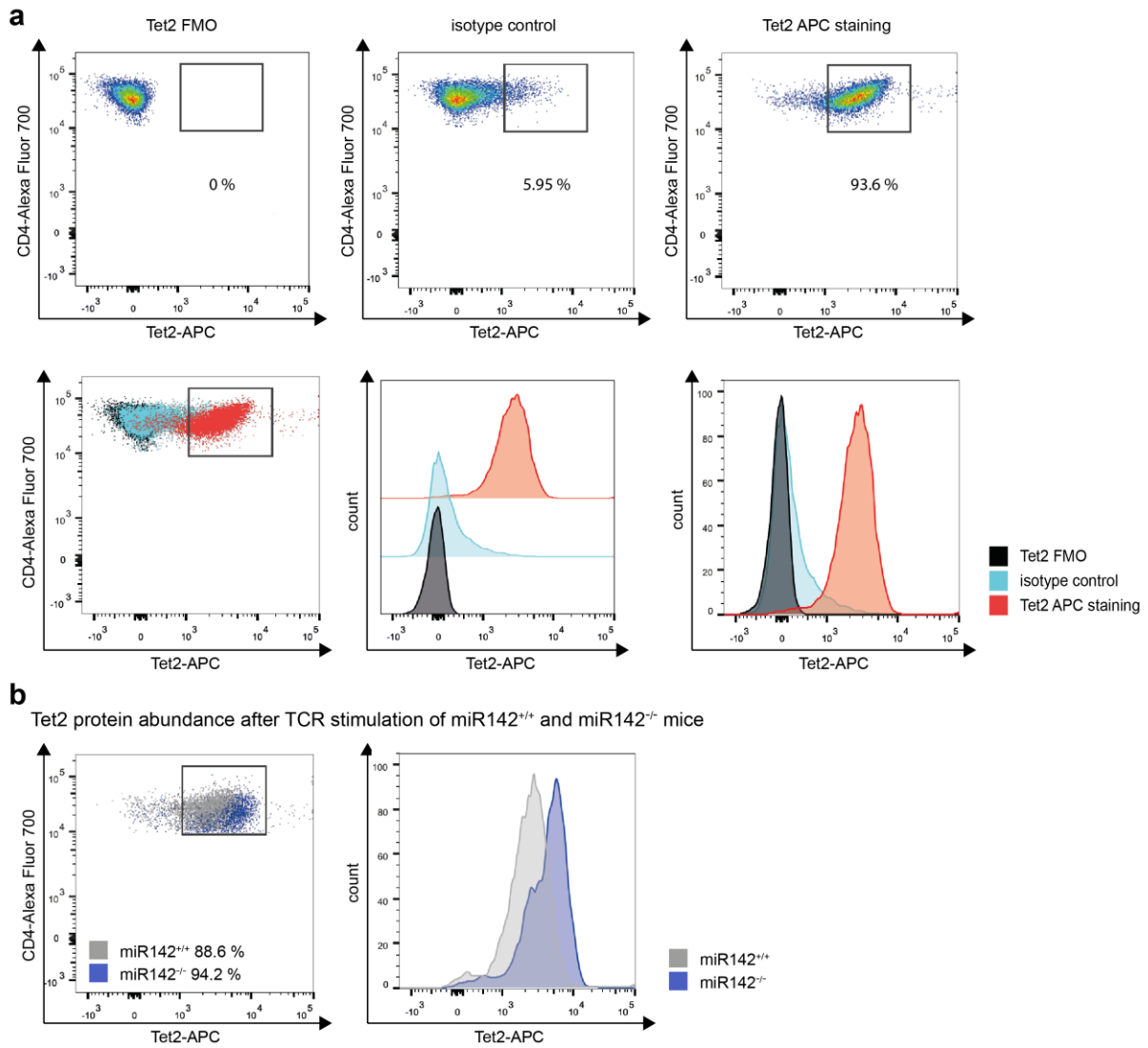
Figure 4. Tet2 flow cytometry staining of murine CD4+ T cells. (a) Upper panel: pseudocolor dot plots showing FMO, isotype control and Tet2-APC staining. Lower panel: overlay of FMO, isotype control and Tet2-APC dot plots (left) and histograms showing FMO, isotype control and Tet2-APC staining (middle and right). **(b)** Dot plots (left) and histograms (right) of a representative Tet2 flow cytometry staining of CD4$^+$ T cells isolated from lymph nodes of miR142$^{+/+}$ and miR142$^{-/-}$ mice.

3.5 *In vitro* studies with primary T cells

Freshly isolated human CD4$^+$ T cells were cultured in X-Vivo15 Medium (Lonza) supplemented with 2mM glutamine, 100 U/ml human recombinant IL-2 (ReproTech), 50 U/ml penicillin, 50 mg/ml streptomycin (Sigma Aldrich) and 5% heat-inactivated human AB serum (Invitrogen) at 37°C in an humidified CO_2 incubator. Cell culture treated 96-well U bottom plates were used (Bio-Greiner one).

Freshly isolated murine CD4$^+$ T cells were cultured in RPMI media (Gibco by life technologies) supplemented with 10% FCS, 1 mM sodium pyruvate (Sigma Aldrich), 50 mM b-mercaptoethanol (Amimed), 1X non-essential amino acids (Merck Millipore), 100 U/ml human recombinant IL-2 (ReproTech), 100 U/ml penicillin and 100 mg/ml streptomycin (Sigma Aldrich) at 37°C in an humidified CO_2 incubator. Cell culture treated 96-well U bottom plates were used (Bio-Greiner one).

3.5.1 Murine and human *in vitro* Treg induction using limited TCR stimulation

Murine naive CD4$^+$ T cells (CD4$^+$, CD25$^-$, CD44$^-$) were sorted with the BD FACS Aria III for purity and cultured (10.000 or 100.000 / well) in a 96-well plate pre-coated with 5 µg/ml anti-CD3 and 5 µg/ml anti-CD28 antibody with additional IL2 (100 U/ml). Limited TCR stimulation was achieved by pipetting the cells into uncoated wells after 18 hours, where they were cultured for additional 36 hours without further TCR-stimulation. Treg induction was measured by flow cytometry by analyzing Foxp3 expression in CD25$^+$CD4$^+$ T cells.

Human naive CD4$^+$ T cells (CD3$^+$, CD4$^+$, CD45RA$^+$, CD45RO$^-$, CD127$^+$, CD25$^-$) were sorted with the BD FACS Aria III for purity and cultured (10.000 or 100.000 / well) in a 96-well plate pre-coated with 5 µg/ml anti-CD3 and 5 µg/ml anti-CD28 antibody with additional IL2 (100U/ml). Limited TCR stimulation was achieved by pipetting the cells into uncoated wells, after 18 hours, where they were cultured for additional 36 hours without further TCR-stimulation. Treg induction efficiency was measured using flow cytometry by analyzing Foxp3 expression in CD25$^+$CD127$^-$CD4$^+$ T cells.

3.5.2 Restimulation assay

After *in vitro* Treg induction using naive CD4$^+$ T cells from BALB/c Foxp3GFP reporter mice in the presence of a miR142-3p inhibitor, Foxp3$^+$CD25$^+$CD4$^+$ Tregs were sort-purified. The Tregs were then stimulated for 30 hours with anti-CD3 and anti-CD28 antibodies in the presence of

a miR142-3p inhibitor or a control inhibitor. Maintenance of the Treg phenotype was measured by flow cytometry analysis of Foxp3 expression in CD25⁺CD4⁺ T cells.

3.6 Nanoparticles

The nanoparticles were prepared by an emulsion-diffusion-evaporation method, first described by Kumar et al. (Kumar et al., 2004) with slight modifications. The emulsion was prepared using a Harvard syringe pump for controlled dropping speed. Particles were passed through a sterile filter after preparation. The fluorescent labeled particles were prepared with a PLGA- fluoresceinamine (FA) conjugate. Preparation of FA labeled PLGA was performed according to the method described by Weiss et al. (Weiss et al. 2006). Particles were characterized with Dynamic light scattering (Zetasizer Nano ZS, Malvern). Chitosan PLGA nanoparticles and FA-labelled nanoparticles (in brackets) had a mean hydrodynamic diameter of 146.7 ± 0.8 nm (152.8 ± 1.2nm), polydispersity index 0.068 ± 0.009 (0.056 ± 0.007) and a zeta potential of $+29.6 \pm 0.3$ mV ($+29.6 \pm 0.7$mV).

3.7 Application of miR142-3p inhibitors/mimics and siRNAs

Chitosan-coated PLGA nanoparticles were loaded with the inhibitor or mimic (miRCURY LNA miRNA mimic / inhibitor, Exiqon) at a weight ratio of nanoparticles:inhibitor/mimic of 50:1 and incubated at room temperature for 30 minutes with gentle shaking. The loaded nanoparticles were added to the wells of a polyclonal Treg induction assay at a final concentration of 6 pmol/well (human) or 9 pmol/well (murine). As a control, nanoparticles loaded with miRNA mimic / inhibitor controls (Exiqon) were added to the cultures. For inhibitor/mimic sequences see Table 11.

Tet2 siRNA (Silencer Select Pre-Designed siRNA Tet2, Ambion) or control siRNA (Silencer Select Negative control no.1, Ambion) were combined with siRfficient transfection reagent (MBL Life Science) following the manufacturer's protocol. 20 pmol siRNA were added to murine and human Treg induction assays. For siRNA information see Table 12.

3.8 mRNA and miRNA expression analysis

3.8.1 qPCR analysis of mRNAs and miRNAs

mRNAs were isolated using the miRNeasy Micro Kit (Qiagen). cDNA synthesis was performed with the iScript cDNA Synthesis Kit (Biorad). For qPCR the SsoFast Evagreen Supermix (Biorad)

and self-designed gene-specific primers were used. For normalization the primers for the housekeeping gene Histone were used. For primer sequences see Table 9. The reactions were performed on a CFX96 Real Time System (Biorad).

SmallRNAs/miRNAs were isolated using the miRNeasy Micro Kit (Qiagen). RNA concentration and purity were determined by nanodrop (Epoch, Biotech). For cDNA synthesis the Universal cDNA Synthesis Kit II (Exiqon) was used according to the instructions. qPCR was performed using the ExiLENT SYBR Green PCR Master Mix (Exiqon) in combination with miRCURY LNA primers for miR142-3p. For normalization miRCURY LNA primers for the housekeeper 5s rRNA were used (Exiqon). For primer sequences see Table 9. The reaction was performed on a CFX96 real time system (Biorad).

3.8.2 miRNA NGS

For high-throughput sequencing of miRNAs total RNA of four pooled samples of activated CD4$^+$ T cells from children with or without ongoing islet autoimmunity was extracted using the miRNeasy Micro Kit (Qiagen). cDNA libraries were obtained using the NEBnext Multiplex Small RNA Library Prep Set (New England Biolabs) according to the manufacturer's protocol. Sequencing was performed on a HiSeq2000 (Illumina) with 50bp single end reads using Illumina reagents and following the manufacturer's instructions.

Unwanted adaptor sequences were trimmed from small RNA reads using BTrim (Kong, 2011) and quality of sequencing was assessed for trimmed read data with a mean phred quality score of 38, referring to a base call accuracy of 99.99%. Read data was filtered of unwanted RNA fragments by mapping on rRNA, tRNA, snRNA and snoRNA sequences obtained from the Rfam database using bowtie (Langmead et al., 2009). Remaining reads were then mapped on mature human miRNA sequences obtained from mirBase (release 20) (Kozomara and Griffiths-Jones, 2014) and summed up to read count lists using SAMTools. mRNA read data was processed comparably without unnecessary trimming and filtering. Raw read data was mapped on the human genome (build 37.2) using a gapped alignment for paired end data with bowtie2 (Langmead and Salzberg, 2012). Finally, read count lists were created by HTSeqcount 47 (Anders et al., 2015). Differential expression of miRNA was evaluated using DESeq (Love et al., 2014), handling size factor correction and normalization.

3.9 Methylation analysis

Up to 2000 CD4^{+} T cells were subjected to a combined sample lysis and bisulfite conversion using the EZ DNA Methylation-Direct Kit (Zymo Research) according to the manufacturer's instructions. For bias-controlled quantitative methylation analysis, a combination of MS-HRM and subsequent pyrosequencing was performed. Utilizing the PyroMark Assay Design Software 2.0 (Qiagen), PCR primers and the according sequencing primers were designed to cover the area of differential methylation in the first Foxp3 intron initially reported by Baron et al. 23. For primer sequences see Table 10. MS-HRM was performed using the SensiFAST HRM Kit (Bioline) and the CFX96 real time system (Biorad). Pyrosequencing was performed on the PyroMark Q24 system (Qiagen) using PyroMark Gold Q24 Reagents (Qiagen) and following the manufacturer's instructions.

3.10 HITS-CLIP
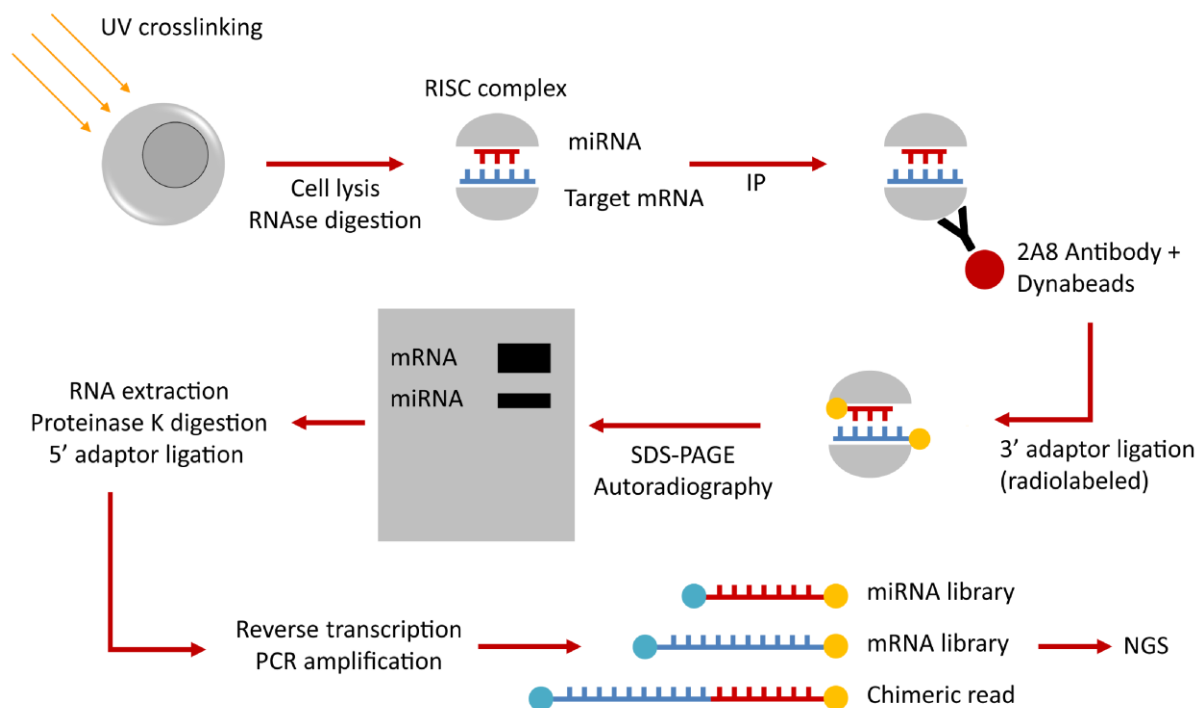
Figure 5. Schematic illustration of the HITS-CLIP technique.

Human CD4$^+$T cells were homogenized, subjected to UV-crosslinking three times at 400 mJ/cm² and extra RNA bound to the RISC complex was digested with RNase T1. The Argonaute complex was then immunoprecipitated 2-4 hours at 4°C using the monoclonal Argonaute antibody 2A8. Phosphate from the precipitated complex was removed and a 5'-32P-labelled RL3 linker was attached. The samples were separated by SDS-gel electrophoresis, transferred to a nitrocellulose membrane and visualized by autoradiography. The desired area with the complexed argonaute protein was cut and subjected to RNA extraction; afterwards the 5' RNA linker was ligated. In the following, RNAs were amplified by RT/PCR, the resulting products were separated on agarose gel and two respective populations of RNA (50-60bp for small RNAs, 80-180bp for mRNAs) extracted. After a re-PCR with Solexa Fusion Primers the desired bands on an agarose gel (miRNA – 150 bps, mRNA – smear around 200 bps) were again extracted and quality checked on an Agilent Bioanalyzer.

3.10.1 HITS-CLIP – sequencing and alignment statistics

Two libraries, mRNA- and miRNA-enriched, were sequenced to 100bp on a HiSeq 2500. Two processing pipelines were used. The first considered only the non-chimeric reads in that the alignment program, bowtie, was looking for end-to-end alignments and did not allow significant parts of the read to 'dangle'. The second, applied to just the mRNA library used STAR to align to the transcriptome and did allow dangling ends. Dangling ends were then selected for lengths consistent with mature miRNAs and aligned to miRNA hairpins.

3.10.2 HITS-CLIP – non-chimeric statistics

The non-chimeric pipeline was described previously (Schug et al., 2013). The non-chimeric pipeline trims adapter sequence using a program written in the Kaestner lab. There was some evidence of double ligation due to the enrichment for chimeric reads. We trimmed adapters from the 3' end that (partially) match GTGTCAGTCACTTCCAG or TGTCAGTCACTTCCAG. We kept sequences that were at least 16bp long. After trimming reads were aligned to the human genome, human RefSeq transcripts, and human miRNA hairpin sequences using bowtie allowing for multiple alignments. The mRNA library is enriched for long fragments, many of which will span introns or are chimeric, so the genomic alignment rate is lower than the miRNA library. RefSeq alignment for the mRNA fraction is also lower due to the chimeric fragments. The miRNA fraction of the miRNA library is relatively high. Roughly 81 million mRNA fragments and 68 million miRNA reads where used in the following steps. We identified

locations of RISC occupancy on RefSeq transcripts as described previously (Schug et al., 2013). Briefly, the alignments were processed to count the number of times each position in the transcripts occurred at the start of an alignment. Then these weighted positions were clustered (from heavy to light) into bins of 10bp to create the 5' ends of the RISC complex footprints. We identified 265,406 footprints on 28,693 transcripts. To quantify miRNA occupancy in the RISC-complex we counted the number of read that overlapped with the annotated locations (miRbase v20) on the miRNA hairpins.

Table 16. HITS CLIP sequencing libraries

Library	Raw Reads	Trimmed Reads	Genomic %	RefSeq %	RefSeq N	miRNA %	miRNA N
mRNA	236,827,218	205,594,509	45.8%	39.6%	81,389,124	15.5%	
miRNA	172,094,624	140,008,888	79.1%	74.6%		48.6%	67,980,650

3.10.3 HITS-CLIP – chimeric pipeline

The chimeric pipeline used cutadapt (Martin, 2011) to trim adapter sequence AGGGAGGACGATGCG from the 5' end and GTGTCAGTCACTTCCAGCGGTCGTATGCCGTCTTCTGCTTG from the 3' end from the mRNA reads. We allowed for up to 3 rounds of trimming. Starting with 236,827,218 raw reads as above cutadapt produced 205,052,818 trimmed reads. The trimmed reads were aligned to the RefSeq transcriptome using STAR using the following parameters, --outFilterMismatchNmax 2 and --outFilterMultimapNmax 10. We found 84,312,502 uniquely mapped reads and 1,530,815 reads that hit too many places and so were discarded. We further filtered the alignments down to 75,428,704 reads. The filtering rules were designed to select reads that were either non-chimeric well-aligned reads or chimeric reads liable to contain a miRNA fragment at the 5' end. Alignments had to be a clean end-to-end match, a match with 1 or 2 bp leading non-match, a long miRNA-like lead non-match (18bp or more), or an 8 bp trailing non-match. Alignments were considered bad if they had inserts or deletions in the alignment, or too short a match (less than 20bp). Of these reads, 3,912,266 had a potential miRNA at the 5' end. We then aligned the potential miRNA portion of the likely-chimeric reads to miRNA hairpins using bowtie. We found 728,596 (18%) reads that aligned to 290 miRNAs. We then merged the STAR and bowtie alignment information for the reads to

identify mRNA/miRNA pairs. We evaluated the quality of the chimeric pairing by measuring the distribution of chimeric reads relative to mirRanda-predicted miRNA binding sites for a few of the most frequent miRNAs. Figure 17 indicates that the chimeras generally agree well with miRanda (Betel et al., 2010) predictions.

3.11 additional *in vitro* assays

3.11.1 3'UTR luciferase reporter assay

HEK-293 cells were co-transfected with a dual-luciferase plasmid containing the wild-type or mutated full-length 3'UTR from human TET2 (RefSeq NM_001127208.2) and a miR142-3p mimic (10 pmol/well) at 10,000 cells per well in a 96-well plate using Lipofectamine 3000 (Thermo Fisher Scientific) for 24 h. Luminescence was measured with the Dual Luciferase Reporter Assay Kit (Promega) following the manufacturer's protocol. The ratio of Firefly over Renilla luminescence was determined and compared to the transfection control. The mutations were introduced in the potential binding site identified by the chimeric reads of HITS CLIP and the two predicted miR142-3p binding sites (Agarwal et al., 2015) in the TET2 3'UTR (position 4135-4141 and 5392-5398) using site directed mutagenesis by PCR. For primer sequences see Table 13.

3.11.2 miR142-3p activity assay

A miR142-3p activity sensor plasmid was constructed by inserting a double-stranded oligonucleotide containing the miR142-3p target sequences (miR142-3p reverse complement, with a central bulged mismatch) into the 3'-UTR of a dual luciferase reporter plasmid. Jurkat T cells were co-transfected with the miR142-3p activity sensor plasmid and a miR142-3p inhibitor (5 pmol/well) at 50,000 cells per well in a 96-well plate using Attractene transfection reagent (Qiagen) for 24 h. Luminescence was measured with the Dual Luciferase Reporter Assay Kit (Promega) following the manufacturer's protocol. The ratio of Firefly over Renilla luminescence was determined and compared to the transfection control.

3.11.3 3T3 fibroblasts

3T3 fibroblasts were seeded in 96-well plates at a density of 10,000 cells/well. After 24 hours the cells were transfected with 10 pmol of miR142-3p mimic or control mimic using Lipofectamine RNAiMAX Reagent, following the manufacturer's instructions. Analysis of gene expression was performed as described above.

3.12 Statistical analysis

Results are presented as mean and standard error of the mean (s.e.m) or as percentages, where appropriate. For normally distributed data, Student's t test for unpaired values was used to compare means between independent groups and the Student's t test for paired values was used to compare values for the same sample or subject tested under different conditions. For multiple testing ordinary one-way ANOVA and Tukey's multiple comparisons test were used. For all tests, a two-tailed P value of < 0.05 was considered to be significant. Statistical significance is shown as *= $P < 0.05$; **= $P < 0.01$; ***= $P < 0.001$, or not significant (NS) P > 0.05. Analyses were performed using the program GraphPad Prism 7 (La Jolla, CA).

3.13 Data availability

HITS-CLIP library sequencing data have been deposited to GEO database under the accession number GSE124264. miRNA sequencing data have been deposited to GEO database under the accession number GSE140064.

4 Results

The concept of an involvement of impaired Treg homeostasis in the activation of autoimmunity is well established, but the underlying mechanisms and how specific miRNAs and their downstream pathways contribute to this impairment and the onset of autoimmunity remain poorly understood.

4.1 Treg induction *in vitro* using limited TCR stimulation

In order to investigate a potential effect of specific miRNAs and their downstream targets on Treg induction capacity of naive CD4$^+$ T cells during the onset of islet autoimmunity, I established human and murine *in vitro* Treg induction assays using short-term TCR stimulation. The short-term TCR stimulation resembles subimmunogenic TCR stimulation which has been shown to be most efficient for murine Treg induction *in vivo* (von Boehmer and Daniel, 2013; Daniel and von Boehmer, 2011; Daniel et al., 2010; Kretschmer et al., 2005).

Short-term TCR stimulation of human naive CD4$^+$ T cells (staining examples in methods) resulted in significantly increased frequencies of induced CD127^{low}CD25^{high}Foxp3^{high}CD4$^+$ Tregs compared to continuous TCR stimulation (Figure 6). To assess their phenotypical stability, induced Treg were restimulated for 36 h. Importantly, the restimulation of CD127^{low}CD25^{high} Tregs previously induced using short-term TCR stimulation resulted in significantly higher levels of Foxp3^{high} Tregs compared to CD127^{low}CD25^{high} Tregs previously induced using continuous TCR stimulation (Figure 7).
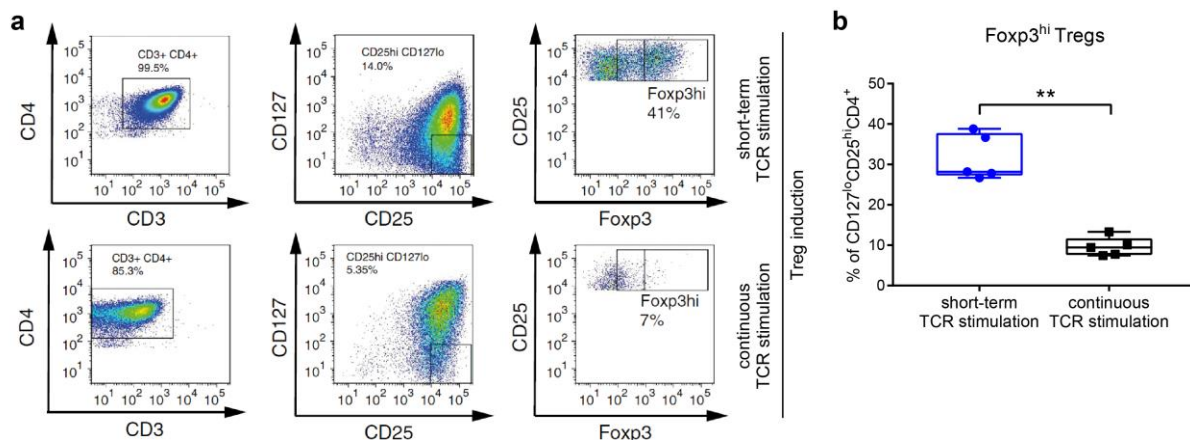
Figure 6. Short-term TCR stimulation improves Treg induction efficacy *in vitro*. (a) Representative FACS plots of *in vitro* Treg induction using limited (12 h) and continuous (54 h) TCR stimulation of naive CD4+ T cells isolated from human peripheral blood. **(b)** Frequency of Foxp3hi Tregs induced by limited or continuous TCR stimulation. *n* = 5. One data point represents one subject. Experiments were performed in three technical replicates per subject. Data are presented as box-and-whisker plots with min and max values. Student's t-test. ***P < 0.01.
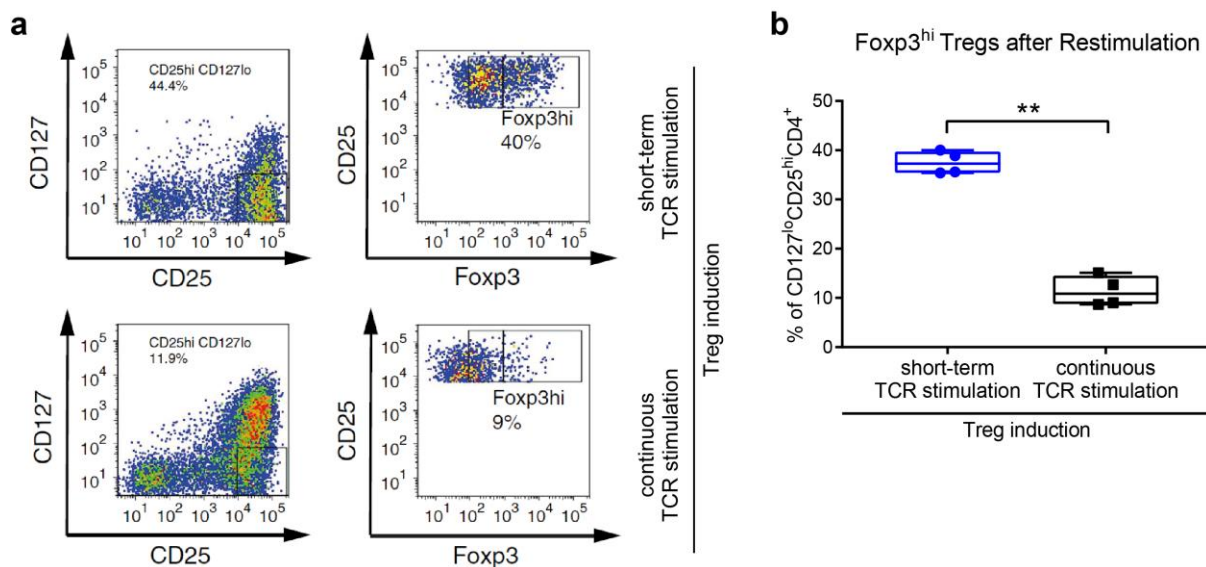
Figure 7. Short-term TCR stimulation improves stability of *in vitro* induced Tregs. (a) Representative FACS plots of restimulation experiments using Tregs previously induced using short-term or continuous stimulation of naive CD4+ T cells isolated from human peripheral blood. **(b)** Quantification of restimulation experiments as described in (a). *n = 4*. One data point represents one subject. Experiments were performed in three technical replicates per subject. Data are presented as box-and-whisker plots with min and max values. Student's t-test. ***P < 0.01.

4.2 Foxp3 CNS2 DNA methylation assay

Since the long-term stability of Tregs has been shown to be linked with the DNA methylation status of the Foxp3 CNS2, human and murine methylation assays using HRM PCR and pyrosequencing were established. The methylation assays were validated on a standard-series of unmethylated and methylated DNA for unbiased PCR amplification according to their products' uniform high-resolution melting behavior. Completely methylated, bisulfite converted and completely demethylated, bisulfite converted DNA and mixtures of both were used, corresponding to DNA mixtures with 0%, 25%, 50%, 75% and 100% methylation. All standards were amplified in the HRM PCR and showed a uniform melting behavior with a slight shift towards high methylation but clearly distinguishable melt curves for all methylation levels (Figure 8a). The obtained amplicons enabled high-quality readouts of eight successive CpG-sites in subsequent pyrosequencing reactions (exemplary file shown in Figure 8b). High correlation between methylation levels of input standards and pyrosequencing-readout of PCR products additionally verified the designed assay for even amplification (Figure 8c).

a

b

c


human Foxp3 CNS2 methylation

$r^2 = 0.995$
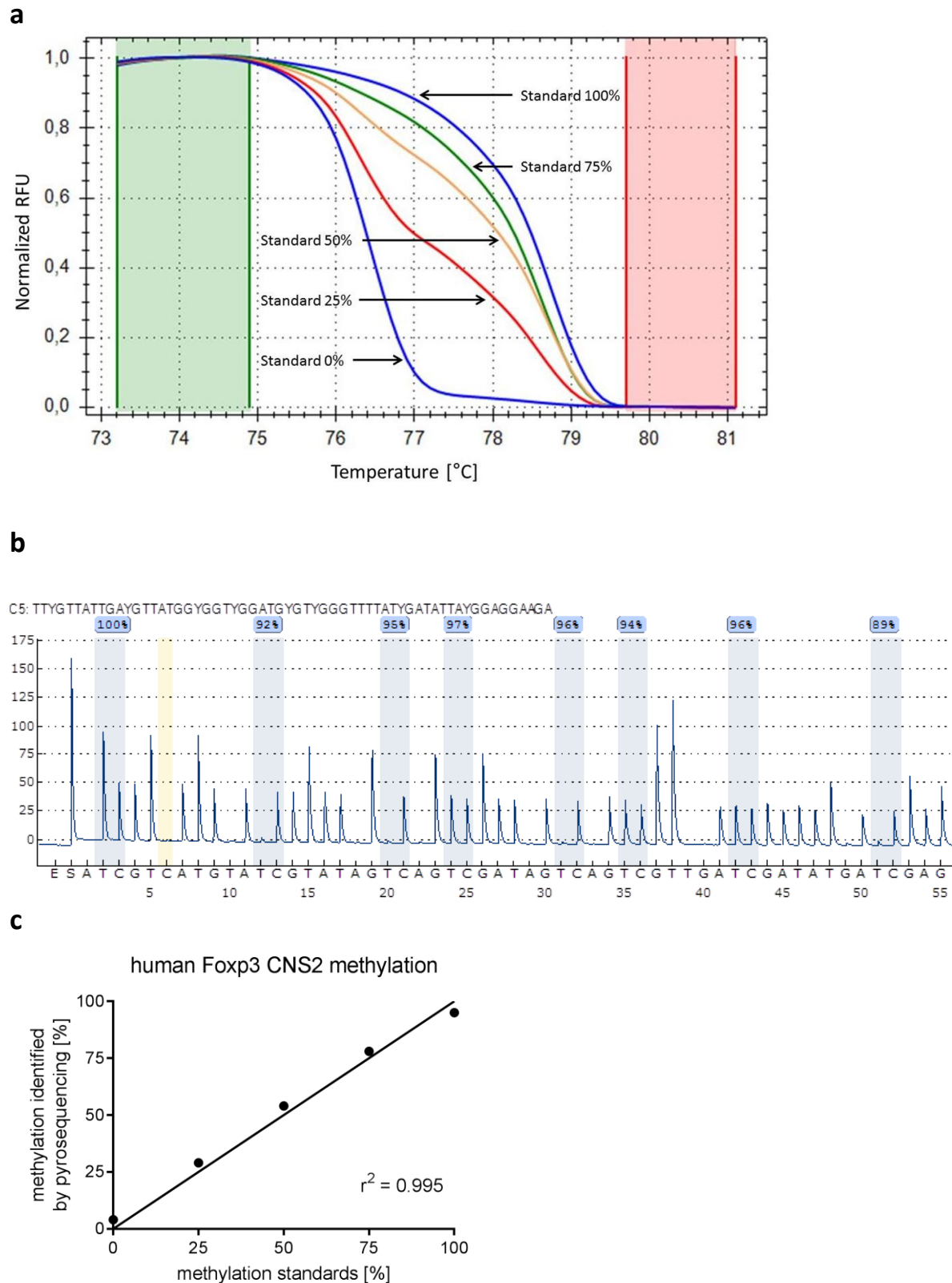
Figure 8. Human Foxp3 CNS2 DNA methylation assay. (a) Representative high resolution melting analysis of DNA methylation standards (0, 25, 50, 75, 100%). **(b)** Representative pyrosequencing analysis of the 100% DNA methylation standard. **(c)** Correlation between methylation levels of standards and pyrosequencing-readout of PCR products.

4.2.1 Foxp3 CNS2 DNA methylation in human T cell subsets

In order to analyze the DNA methylation of the Foxp3 CNS2 in different T cell subsets, CD4$^+$ T cells were FACS sorted based on surface markers and Foxp3. Considering the X-chromosomal location of the Foxp3 gene, cells from female and male donors were analyzed. As shown in Figure 9 the DNA methylation levels differed clearly between the individual CD4$^+$ T cell subsets. For both female and male donors, naive T cells and memory T cells exhibited the highest methylation level, effector Tregs the lowest and activated T cells and naive Tregs in between. Notably, except for the completely methylated cells the methylation levels of the female donors were higher than the levels of the male donors, which is in line with the X-chromosomal location of the Foxp3 gene.
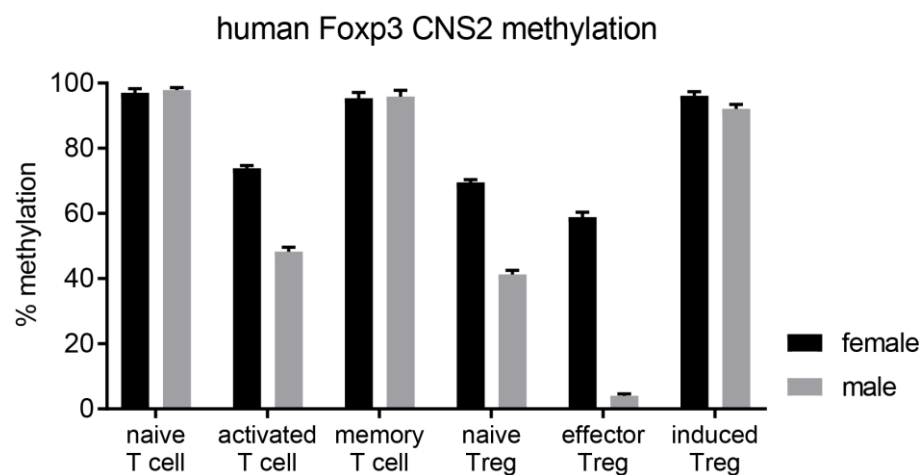
Figure 9. Methylation of the Foxp3 CNS2 in human CD4$^+$ T cells. Methylation of eight CpG sites in the human Foxp3 CNS levels in ex vivo subsets of human CD4$^+$ T cells as revealed by pyrosequencing. Female donors are shown in black and male donors are shown in grey. *n* = 4. Experiments were performed in two technical replicates per subject. Data are presented as means ± SEM.

4.2.2 Foxp3 CNS2 DNA methylation during Treg induction

To investigate if the improved Treg induction efficacy and Treg stability upon short-term TCR stimulation is accompanied by changes in Foxp3 CNS2 DNA methylation, a methylation analysis of human and murine *in vitro* induced Tregs was performed. Both short-term and continuously induced Tregs exhibit an almost completely methylated CNS2. To capture potential methylation dynamics during the early phase of murine and human Treg induction from naive CD4$^+$ T cells, I analyzed Treg markers and Foxp3 CNS2 methylation as early as 12 hours of TCR stimulation. I observed cells expressing Treg markers, especially high levels of

Foxp3, with an increase over time as shown for 12, 18 and 36 hours in Figure 10a (murine: CD4$^+$CD25^{high}Foxp3^{high}) and Figure 5c (human: CD4$^+$CD127^{low}CD25^{high}Foxp3^{high}).

The DNA methylation analysis of cells with a Foxp3hi Treg phenotype in this early phase of Treg induction showed a clear dynamic in Foxp3 CNS2 methylation which are only partially captured by the *in vitro* differentiation system. Thus, initial Treg induction from naive CD4$^+$ T cells causes rapid CNS2 demethylation (Figure 10b and d) and Foxp3 expression as expected. However, longer culture leads to methylation at the CNS2, likely a result of the culture conditions. Of note, the demethylation was restricted to cells showing a Foxp3hi Treg phenotype, while no changes in CNS2 methylation were observed in Foxp3- cells (Figure 10b and d). These results support the notion that the initial demethylation of CNS2 is linked to the expression of Foxp3 and its downstream targets, and is not solely the effect of TCR stimulation on cell proliferation.
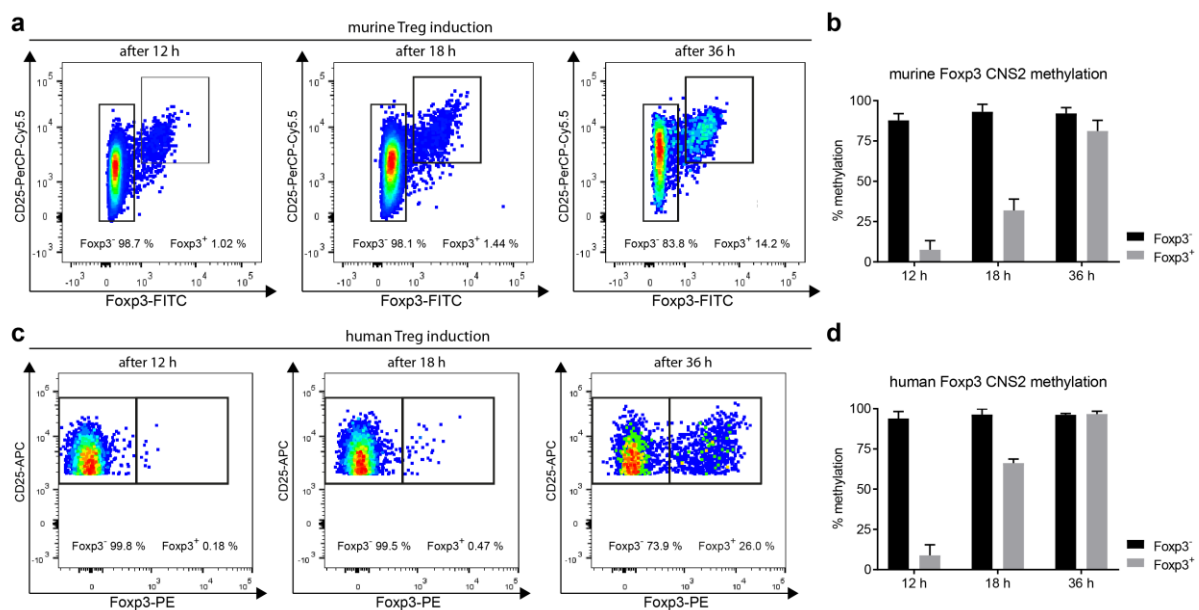
Figure 10. Early T cell activation induces rapid demethylation of the Foxp3 CNS2 in x cells. (a) Representative FACS plot indicating CD4$^+$CD25$^+$Foxp3$^+$ Tregs and CD4$^+$Foxp3$^-$ T cells after 12, 18 and 36 hours of subimmunogenic stimulation of BALB/c naive CD4$^+$ T cells. **(b)** Methylation of four CpG sites in the murine Foxp3 CNS2 of CD4$^+$CD25$^+$Foxp3$^+$ Tregs and CD4$^+$Foxp3$^-$ T cells after 12, 18 and 36 hours of subimmunogenic TCR stimulation. *n* = 6. **(c)** Representative FACS plot indicating CD4$^+$CD127$^-$CD25$^+$Foxp3$^+$ Tregs and CD4$^+$CD127$^-$CD25$^+$Foxp3$^-$ T cells after 12, 18 and 36 hours of TCR stimulation of human naive CD4$^+$ T cells. **(d)** Methylation of eight CpG sites in the human Foxp3 CNS2 of CD4$^+$CD127$^-$CD25$^+$Foxp3$^+$ Tregs and CD4$^+$CD127$^-$CD25$^+$Foxp3$^-$ T cells after 12, 18 and 36 hours of subimmunogenic TCR stimulation. *n* = 6. Experiments were performed in two technical replicates per subject. Data are presented as means ± SEM.

4.3 Onset of islet autoimmunity impairs murine and human Treg induction *in vitro*

Our group recently provided evidence for a profound impairment of Treg induction during islet autoimmunity onset (Serr et al., 2016b, 2018). In line with these findings, *in vitro* Treg induction assays using subimmunogenic stimulation of naive CD4^{+} T cells (CD4^{+}CD25^{-}CD44^{-}) from NOD mice with different stages of autoimmunity revealed impaired Treg induction capacity upon onset of islet autoimmunity. Specifically, the frequency of *in vitro* induced Foxp3^{+} Tregs was highest using naive CD4^{+} T cells from NOD mice without islet autoimmunity while naive CD4^{+} T cells from NOD mice with islet autoimmunity and even more from diabetic mice showed reduced frequencies of induced Foxp3^{+} Tregs (Figure 11a). Likewise, I used naive CD4^{+} T cells (CD4^{+}CD3^{+}CD45RA^{+}CD45RO^{-}CD127^{+}CD25^{-}) from individuals without islet autoimmunity, with recent onset of T1D, and with established T1D for *in vitro* Treg induction. The groups with recent onset or established T1D revealed an overall reduction of Treg induction efficacy compared to the healthy individuals as observed previously (Figure 11b) (Serr et al., 2016b, 2018).
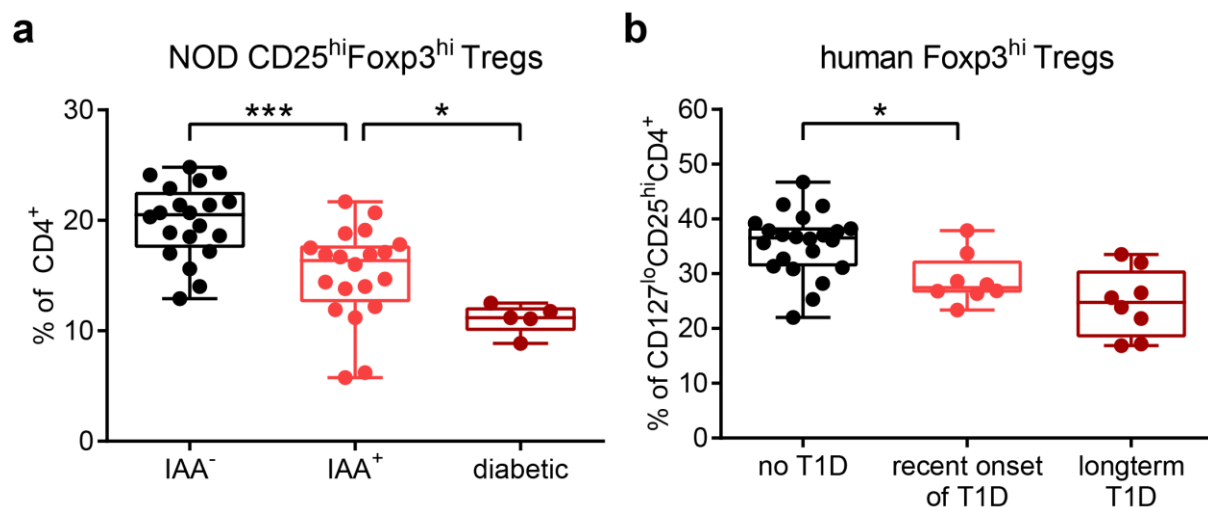
Figure 11. Onset of islet autoimmunity impairs murine and human Treg induction *in vitro*. (a) *In vitro* Treg induction assays using limited TCR stimulation of naive CD4^{+} T cells isolated from lymph nodes of NOD mice with different stages of autoimmunity. *n* = 20 for IAA^{-} and IAA^{+}; *n* = 5 for diabetic. **(b)** *In vitro* Treg induction assays using limited TCR stimulation of naive CD4^{+} T cells isolated from peripheral blood of human subjects with different stages of T1D. *n* = 22 for no T1D *n* = 8 for recent onset and longterm T1D. One data point represents one subject. Experiments were performed in three technical replicates per subject. Data are presented as box-and-whisker plots with min and max values. Ordinary one-way ANOVA, Tukey's multiple comparisons test. *$P < 0.05$, ***$P < 0.001$.

A critical question is whether the impaired expression of individual miRNAs is linked to the mechanisms underlying diseases, such as the activation of islet autoimmunity in T1D. Although recent studies provided considerable insight into the role of miRNAs in immune homeostasis, the specific contribution of individual miRNAs, their direct targets and affected signaling pathways remain poorly understood, especially in T cells.

4.4 Increased miR142-3p expression in activated CD4$^+$ T cells during islet autoimmunity and T1D

In order to reveal potential links between differential miRNA expression and the onset of islet autoimmunity, I isolated the miRNA fraction from activated CD4$^+$ T cells (CD4$^+$CD3$^+$CD45RA$^-$CD45RO$^+$CD127$^+$CD25^{intermediate}) of children with and without islet autoimmunity to screen for differentially expressed miRNAs by high throughput sequencing. This analysis identified multiple differentially expressed miRNAs, with both down- and upregulation of up to tenfold. One of the miRNAs specifically upregulated in activated CD4$^+$ T cells from children with ongoing islet autoimmunity was miR142-3p, with a fold change of about 2 (Figure 12a).

The differential expression of miR142-3p was validated by qPCR analysis of activated CD4$^+$ T cells isolated from peripheral blood of individuals without T1D and with recent onset of T1D (Figure 12b).

In order to expand these findings to the murine system, offering valuable research tools not available in the human system, non-obese diabetic (NOD) mice, a well-established model of T1D, were used. Here, in line with the human data, activated CD4$^+$ T cells (CD4$^+$CD25$^-$CD44^{high}) isolated from lymph nodes of NOD mice with recent development of insulin autoantibodies (IAA) also showed elevated levels of miR142-3p expression compared to IAA$^-$ littermates (Figure 12c). These results suggest a potential involvement of miR142-3p in activation of islet autoimmunity in humans and mice.
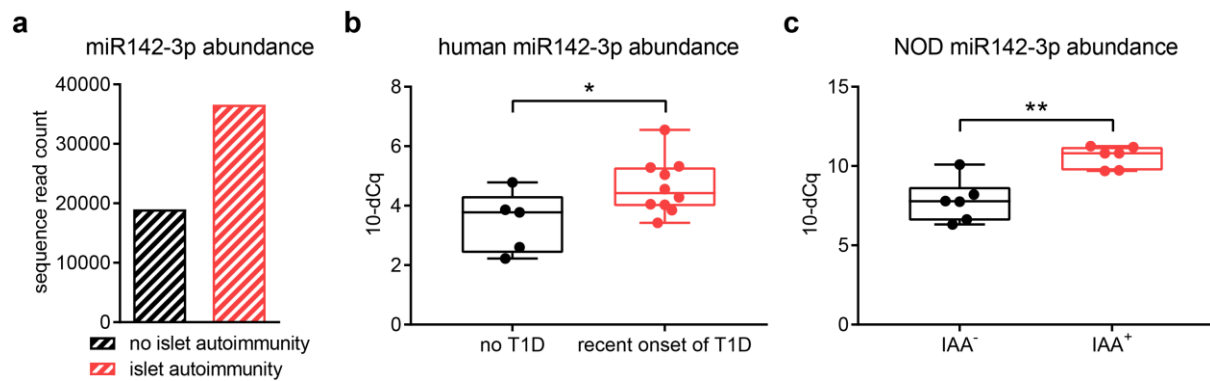
Figure 12. miR142-3p is upregulated upon onset of islet autoimmunity. (a) miR142-3p expression in activated CD4^{+} T cells isolated from peripheral blood of children with and without islet autoimmunity by miRNA sequencing of 4 pooled samples per group. **(b)** miR142-3p abundance in activated CD4^{+} T cells isolated from peripheral blood of children without T1D and with recent onset of T1D. $n \geq 5$. **(c)** miR142-3p abundance in CD4^{+} T cells with an activated phenotype isolated from lymph nodes of NOD mice with and without islet autoimmunity. $n = 6$. One data point represents one subject. Experiments were performed in three technical replicates per subject. Data are presented as box-and-whisker plots with min and max values. Student's t-test. *$P < 0.05$, **$P < 0.01$.

Furthermore, I analyzed an existing mRNA sequencing dataset of individuals with ongoing islet autoimmunity and healthy controls for differential expression of predicted miR142-3p targets. The majority of the predicted miR142-3p targets was downregulated in CD4^{+}T cells of individuals with ongoing islet autoimmunity (Figure 13), supporting the important role of this miRNA for the activation of T cell specific islet autoimmunity.
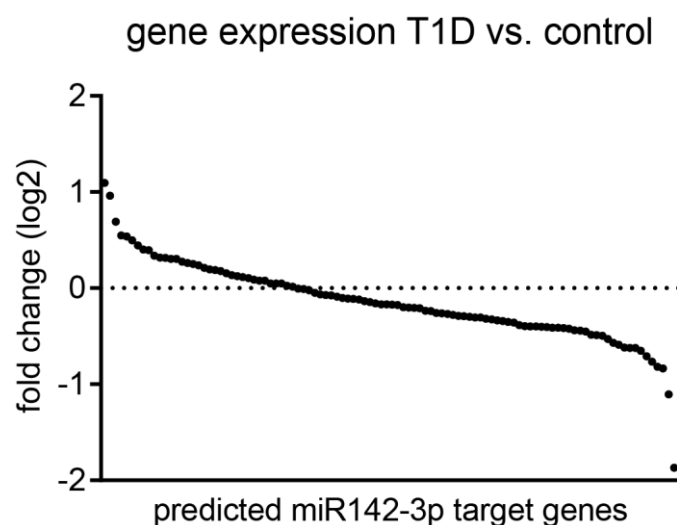

Figure 13. Predicted miR142-3p targets are downregulated in CD4^{+} T cells from individuals with ongoing islet autoimmunity. Fold expression change of 104 predicted miR142-3p target genes in CD4^{+} T cells from individuals with ongoing islet autoimmunity compared to healthy controls.

4.5. HITS CLIP analysis of human CD4⁺ T cells

Multiple previous studies analyzed miRNA profiles in different diseases contexts and various cell types. However, the specific contribution of individual miRNAs to mRNA regulation as well as the miRNA-mRNA target relationships remain largely unclear. By analyzing miRNA and mRNA fragments present in the RNA-induced silencing complex (RISC) following immunoprecipitation with an antibody against Argonaute 2, HITS-CLIP (high-throughput sequencing of RNA isolated by crosslinking immunoprecipitation) offers a valuable tool to overcome this knowledge gap (Figure 14a). The HITS-CLIP analysis of human CD4⁺ T cells and mapping of the sequencing reads to the human genome identified 271 unique RISC-associated miRNAs and 7,829 corresponding mRNA targets. The analysis of the obtained sequencing libraries revealed that the miRNA binding sites are located at comparable levels in the 3' UTR and the coding sequence of the mRNA targets (Figure 14b), with a slight preference for the 3' UTR when the size of the respective region was taken into account (Figure 14c). These findings are in contrast to previous findings which suggested that miRNA binding occurs preferentially in the 3' UTR (Friedman et al., 2009).
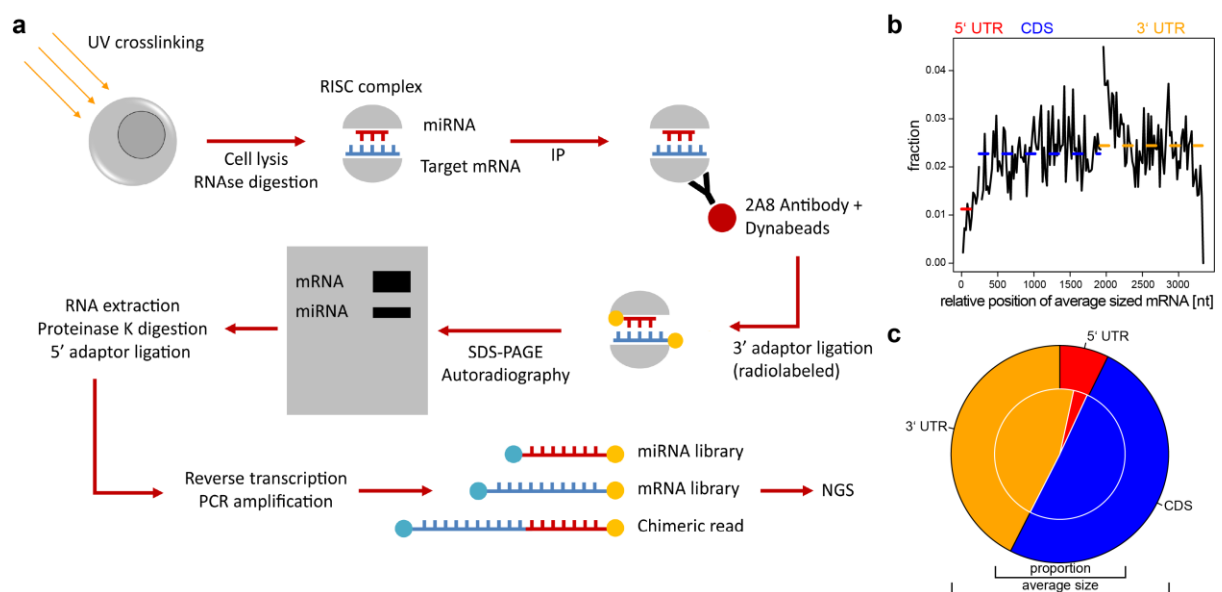
**Figure 14. HITS-CLIP analysis of human CD4⁺ T cells. (a)** Schematic illustration of the HITS-CLIP technique. **(b)** Average read coverage of RISC associated mRNA fragments over a standardized mRNA. Dashed lines show the average levels. (CDS = coding sequence). **(c)** The outer pie shows the average size of the regions. The inner pie indicates the proportion of RISC associated mRNA fragments found in each section.

The abundance of the 271 miRNAs present in the RISC of human CD4$^+$ T cells varied notably and miR142-3p was the most abundant miRNA (Figure 15a), suggesting a critical role of this miRNA in the regulation of CD4$^+$ T cells. Gene ontology analysis of the 500 most targeted mRNAs showed a significant enrichment of biological processes associated with immune activation and regulation such as "T cell signaling" and "T cell activation" (Figure 15b). These findings support the notion that miRNAs function as critical regulators of immune activation vs. tolerance induction in CD4$^+$ T cells.
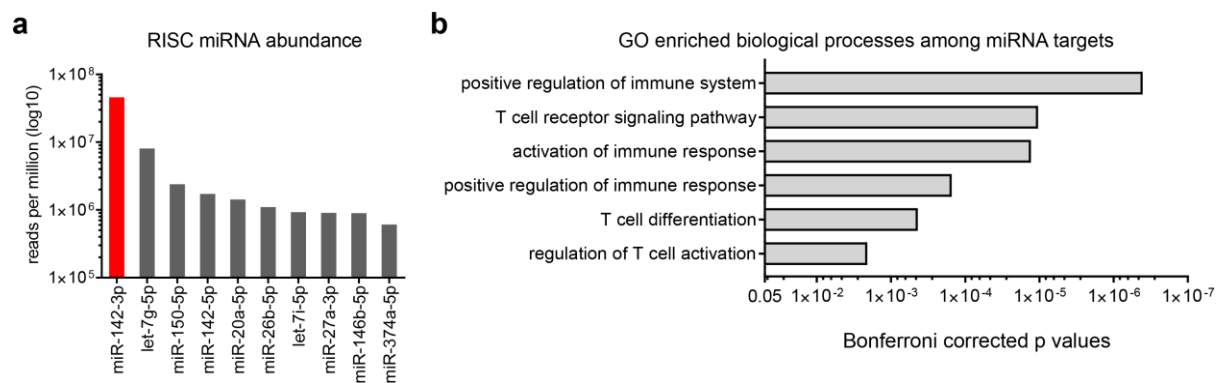
Figure 15. miR142-3p is highly abundant in the RISC complex of CD4$^+$ T cells. (a) The ten most abundant RISC associated miRNAs in human CD4$^+$ T cells as identified by HITS-CLIP. **(b)** Significantly enriched gene ontology (GO) biological processes in target genes of RISC associated miRNAs in human CD4$^+$ T cells.

4.6 miR142-3p targets the methylcytosine dioxygenase Tet2, a modulator of DNA methylation

Since the DNA methylation status of the Foxp3 CNS2 is a crucial mediator of Treg stability, I analyzed the HITS-CLIP dataset in order to identify genes potentially involved in the modulation of DNA methylation. One mRNA target associated with the RISC in human CD4$^+$ T cells was the methylcytosine dioxygenase Tet2, which is a mediator of DNA demethylation. Multiple RISC associated mRNA fragments aligned to the Tet2 transcript (Figure 16). These findings indicate that Tet2 is subject to regulation by miRNAs, however, they do not reveal which miRNA might be involved in this regulation.

Besides mRNAs and miRNAs, the HITS-CLIP analysis also captures rare chimeric reads which result from the ligation of miRNAs and their mRNA targets while they're in close proximity in the RISC. These chimeric reads have been previously reported for other cell types

(Kameswaran et al., 2014; Schug et al., 2013) and they provide direct evidence for the specific target relationship between miRNAs and mRNAs. The quality of the chimeric reads pairing was evaluated by measuring the distribution of chimeric reads relative to miRanda-predicted (Betel et al., 2010) miRNA binding sites for a set of the most frequent miRNAs indicating that the chimeric reads strongly correlate with *in silico* predictions (Figure 17).

Remarkably, the chimeric read sequencing library contained several chimeric reads for the miR142-3p – Tet2 pair. The mRNA fragments of the chimeric reads aligned to a specific region in the 3' UTR of Tet2 transcript NM_001127208 between bases 7,600 and 7,800 of the Tet2 transcript, which also showed RISC footprints (Figure 16). Furthermore, the Tet2 transcript contains two predicted miR142-3p binding sites in the 3'UTR (Agarwal et al., 2015) pointing to an involvement of this miR142-3p in Tet2 regulation.
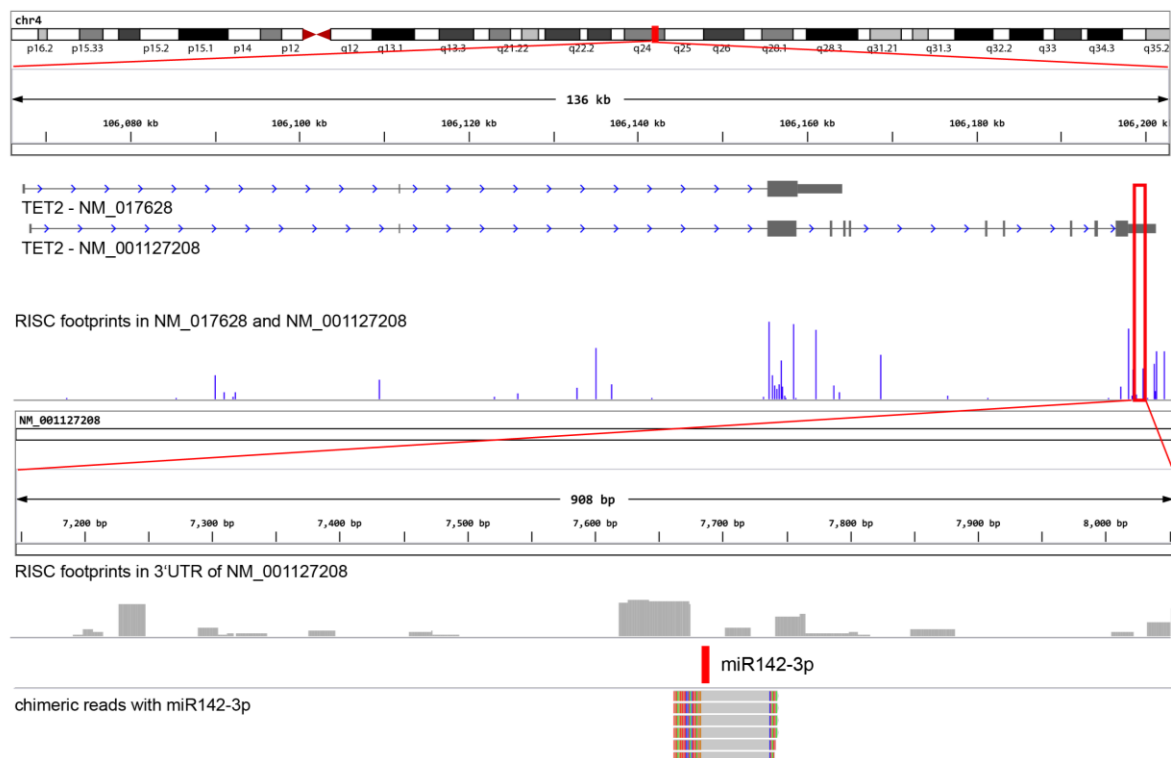
Figure 16. **Analysis of miR142-3p – Tet2 chimeric reads in human CD4^{+} T cells.** From top to bottom: Location of the human TET2 gene on chromosome 4. The human TET2 transcripts NM_017628 and NM_001127208 and RISC footprints (purple bars) on these transcripts. Transcript NM_001127208 zoomed in on a region of the 3'UTR between 7150 and 8050, showing RISC footprints (grey bars) and miR142-3p – Tet2 – chimeric reads (colored portion indicates the miR142-3p part of the chimeric reads).
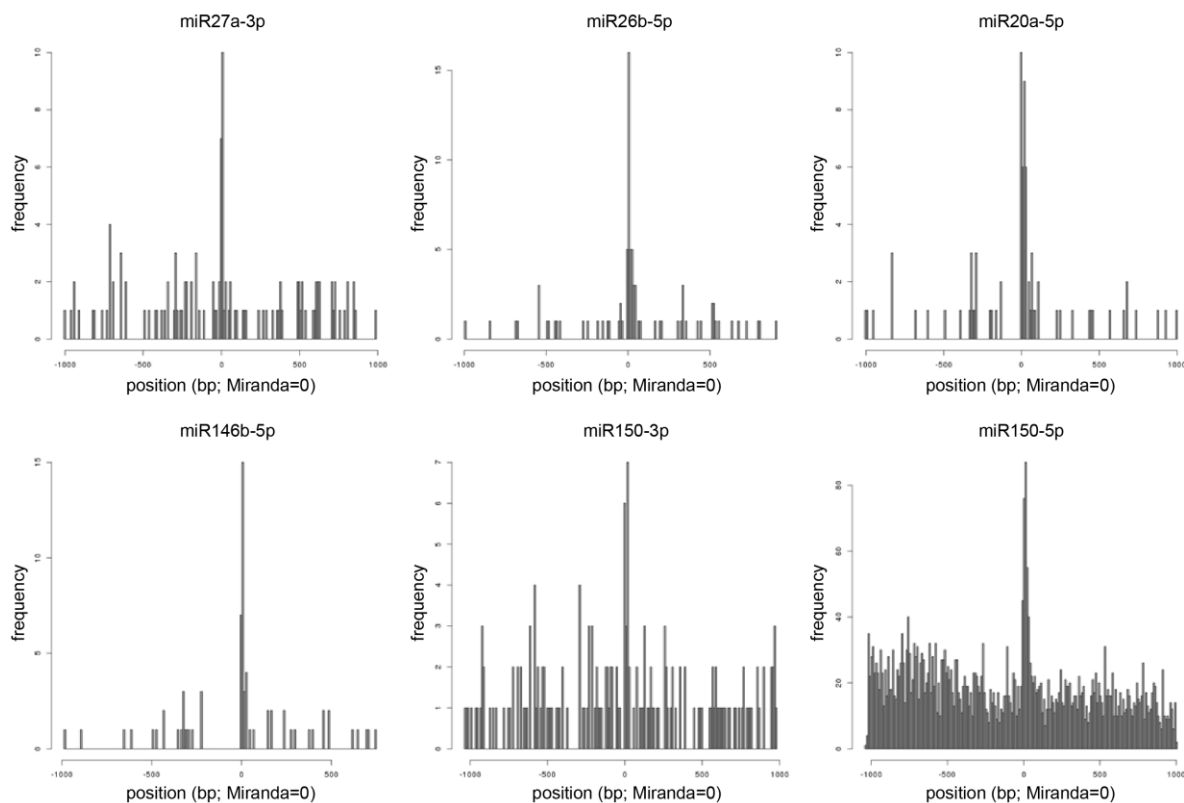
Figure 17. Chimeric reads correlate with miRanda-predicted miRNA binding sites. X-axis indicates the position of the chimeric reads relative to the predicted binding sites (position 0); Y-axis indicates the frequency of the chimeric reads.

4.7 Reduced Tet2 abundance upon onset of islet autoimmunity

To integrate these findings into the context of islet autoimmunity I analyzed if altered miR142-3p levels in CD4^{+} T cells directly modulate Tet2 abundance upon onset of islet autoimmunity. The increased miR142-3p levels during the onset of islet autoimmunity were reflected by a reduced abundance of the potential miR142-3p target Tet2 in CD4^{+} T cells from IAA^{+} mice as shown by flow cytometry analysis (Figure 18a). This reduction in Tet2 abundance was also shown directly in the pancreas by immunofluorescence microscopy of pancreatic cryosections from NOD mice with or without islet autoimmunity. Specifically, the analysis revealed significantly reduced numbers of pancreas-infiltrating CD3^{+}Tet2^{+} T cells in IAA^{+} NOD mice (Figure 18b and c), despite an increase in the total number of pancreas-infiltrating CD3^{+} T cells (Figure 18d). Moreover, the abundance of human CD4^{+}CD3^{+}Tet2^{+} T cells was reduced in peripheral blood from subjects with recent onset of T1D compared to subjects without T1D (Figure 18e and f).
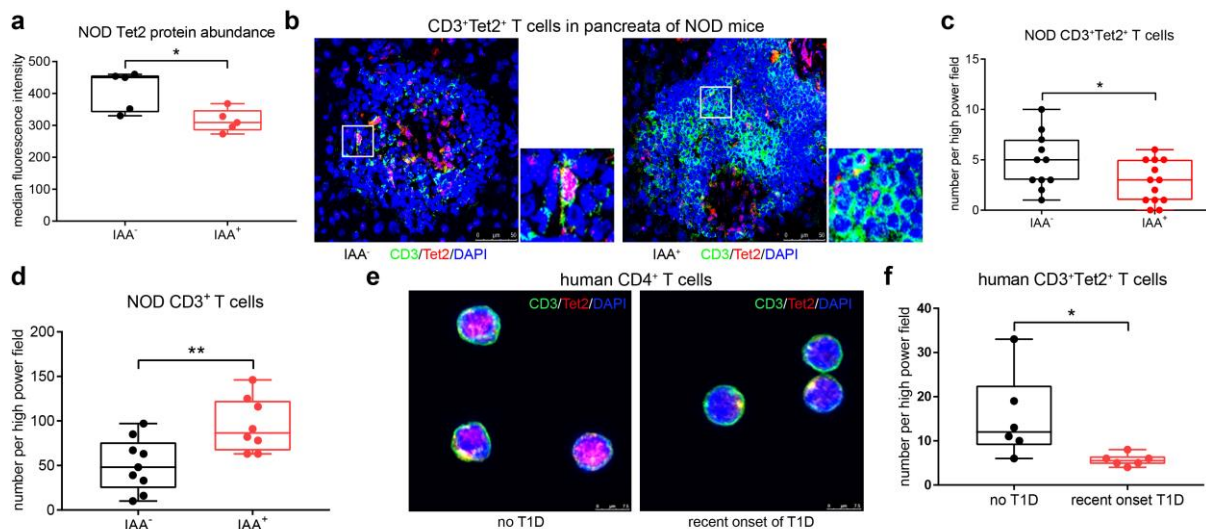
Figure 18. Tet2 abundance is changed upon onset of islet autoimmunity and T1D. (a) Ex vivo Tet2 protein abundance (median fluorescence intensity) in CD4$^+$ T cells isolated from pancreatic lymph nodes of NOD mice with and without islet autoantibodies. $n = 5$. **(b)** Immunofluorescence staining for CD3 (green), Tet2 (red) and DAPI (blue) in pancreas cryosections of NOD mice with and without islet autoimmunity. Scale bars: 50 μm. **(c)** Quantification of CD3$^+$Tet2$^+$ T cells per high power field in samples from (b). $n = 12$. **(d)** CD3$^+$ T cells per high power field in samples from (b). $n \geq 8$. **(e)** Immunofluorescence staining for CD3 (green), Tet2 (red) and DAPI (blue) in cytospins of human CD4$^+$ T cells isolated from peripheral blood of individuals with and without recent onset of T1D. Scale bars: 75 μm. **(f)** Quantification of CD3$^+$Tet2$^+$ T cells per high power field in samples from (d). $n = 6$. Experiments were performed in three technical replicates per subject. Data are presented as box-and-whisker plots with min and max values. Student's t-test. $*P < 0.05$, $**P < 0.01$.

4.8 Foxp3 CNS2 methylation changes upon onset of islet autoimmunity

The stability of Tregs is directly linked to the methylation status of the CNS2 within the Foxp3 gene: it is demethylated in Tregs which is associated with stable Foxp3 expression and a stable Treg phenotype. The identification of Tet2, an enzyme involved in DNA demethylation, as a direct target suggested a potential link between increased miR142-3p levels, reduced Tet2 abundance and Treg stability. The comparison of Foxp3 CNS2 methylation of Tregs from NOD mice with recent development of IAAs, and also from children with recent onset of T1D to controls without IAA/T1D indeed revealed changes in DNA methylation within the Foxp3 locus. In both mice and humans, all individual CpG sites within the CNS2 of Tregs from individuals with islet autoimmunity/T1D showed higher DNA methylation levels, reaching statistical significance at several sites and when analyzing the entire Foxp3 CNS2 region (Figure 19a and c). These results suggest a direct link between miR142-3p levels, Tet2 expression and Foxp3 CNS2 DNA methylation during ongoing islet autoimmunity.

To dissect the question if the impaired demethylation of the Foxp3 CNS2 contributes to autoimmune activation or if it is a consequence thereof, CNS2 DNA methylation was assessed in NOD mice below 30 days of age with a very early onset of IAA$^+$ positivity and compared to non-autoimmune prone BALB/c mice (Figure 19b). The increased Foxp3 CNS2 DNA methylation in these very young IAA$^+$ NOD mice supports the concept that early changes in Foxp3 CNS2 methylation can contribute to promoting autoimmune activation and progression.

To exclude differences in the composition of the Treg pool with regard to thymic-derived and peripheral Tregs as a contributing factor on differential Foxp3 CNS2 DNA methylation, I analyzed Tregs isolated from peripheral blood of human subjects without T1D and with recent onset of T1D. The expression of Helios, which is a marker of thymic-derived Tregs (Thornton et al., 2010), did not differ between the two groups (Figure 19d), suggesting that the observed differences in Foxp3 CNS2 DNA methylation are not affected by the composition of the Treg pool.
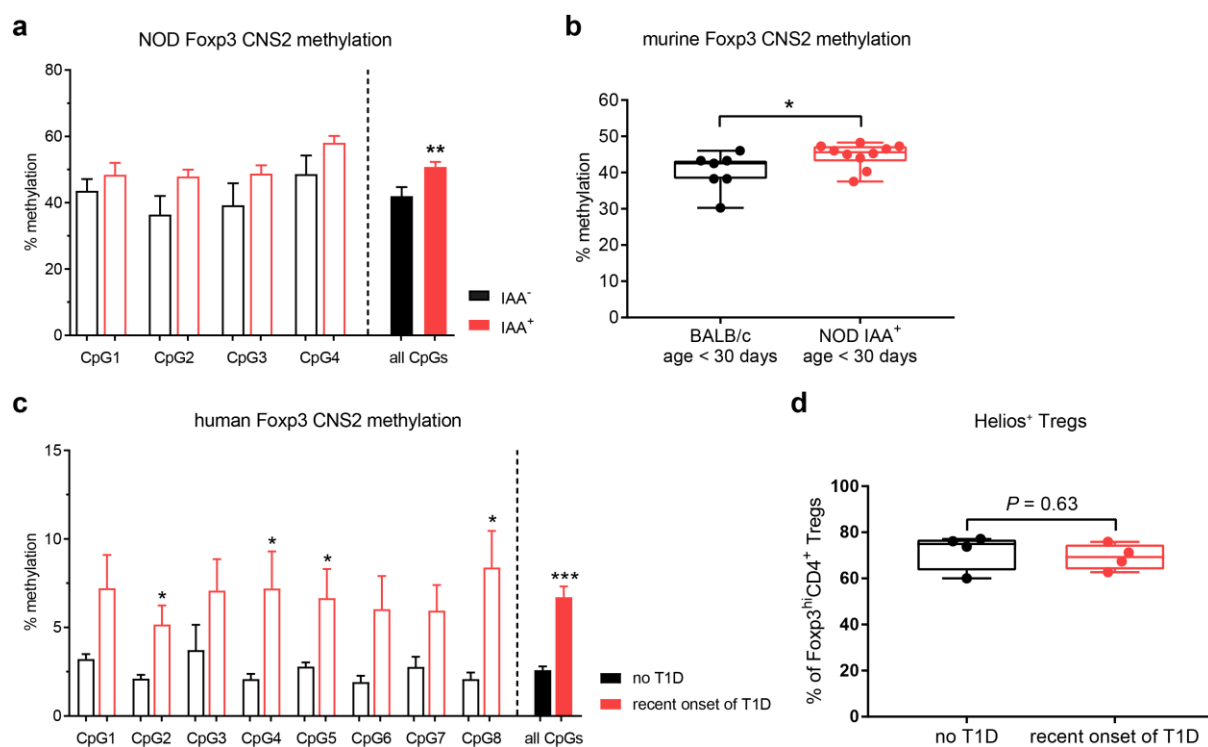
Figure 19. Foxp3 CNS2 methylation is changed upon onset of islet autoimmunity and T1D. (a) Methylation of the Foxp3 CNS2 (four CpG sites and combination of all sites) in Tregs isolated from pancreatic lymph nodes of female NOD mice with and without autoimmunity. n = 6. **(b)** Methylation of the Foxp3 CNS2 (mean of all sites) in Tregs isolated from lymph nodes of young female BALB/c mice or IAA$^+$ NOD mice, age < 30 days. $n \geq$ 7. **(c)** Methylation of the Foxp3 CNS2 (eight CpG sites and

combination of all sites) in Tregs isolated from peripheral blood of male human subjects with recent onset of T1D and healthy controls. $n = 8$. **(d)** Helios^{+} Tregs (% of CD4^{+}Foxp3^{hi} Tregs) isolated from peripheral blood of human subjects with recent onset of T1D and healthy controls. $n = 4$. One data point represents one subject. Experiments were performed in two (a-c) or three (d) technical replicates per subject. Data are presented as box-and-whisker plots with min and max values or as means ± SEM. (a and c) Ordinary one-way ANOVA, Tukey's multiple comparisons test. (b and d) Student's t-test. *$P < 0.05$, **$P < 0.01$, ***$P < 0.001$.

4.9 Tet2 plays an important role for Treg induction *in vitro*

In order to provide evidence for the potentially important role of Tet2 for Treg induction, Tet2 abundance was analyzed during the early phase of *in vitro* Treg induction from BALB/c naive CD4^{+} T cells. I observed a strong increase in Tet2 mRNA levels after 3 hours of TCR stimulation, followed by a decrease to baseline levels or below after 6 hours (Figure 20a). This activation of Tet2 upon TCR stimulation was also reflected on the protein levels with increased Tet2 abundance after 6 hours and an additional increase after 12 hours (Figure 20b).
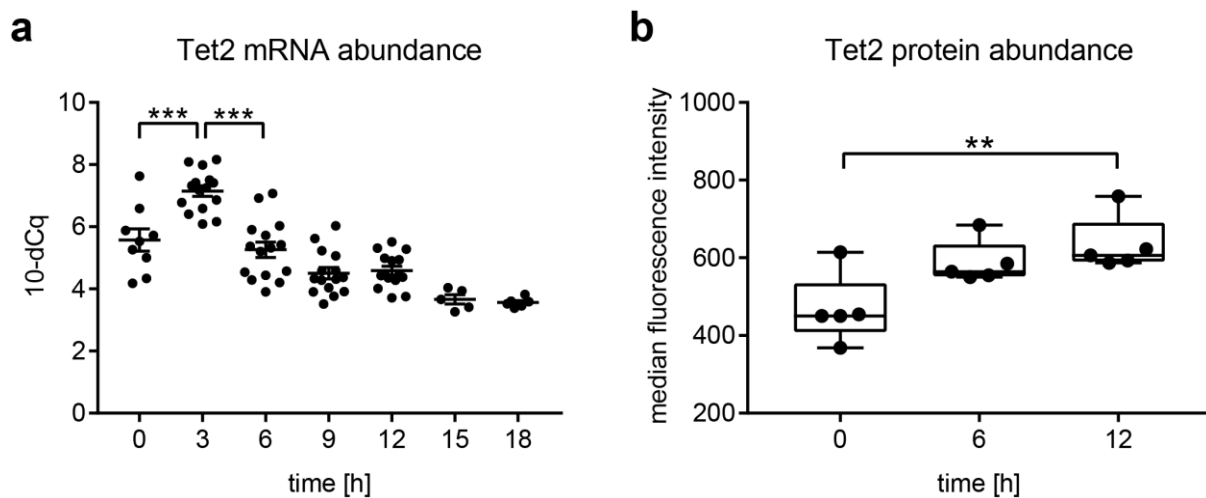
Figure 20. Early T cell activation induces Tet2 expression *in vitro*. (a) Tet2 mRNA abundance at various time points (0 – 18 hours) of TCR stimulation of CD4^{+} T cells isolated from lymph nodes of BALB/c mice. $n \geq 8$. **(b)** Tet2 protein abundance (median fluorescence intensity) after 0, 6 and 12 hours of TCR stimulation of CD4^{+} T cells isolated from lymph nodes of BALB/c mice. $n = 5$. One data point represents one subject. Experiments were performed in three technical replicates per subject. Data are presented as box-and-whisker plots with min and max values (b) or as means ± SEM. (a) Ordinary one-way ANOVA, Tukey's multiple comparisons test. *$P < 0.05$, **$P < 0.01$, ***$P < 0.001$.

To further highlight the importance of Tet2 during the early phase of Treg induction, I performed Tet2 knockdown Treg induction experiments using naive CD4^{+} T cells from BALB/c mice and healthy human subjects in presence of a Tet2 siRNA. The reduced Tet2 abundance resulted in significantly attenuated Treg induction efficacy in both the murine (Figure 21a)

and the human system (Figure 21b), suggesting a critical role of Tet2 for T cell activation and Treg induction.
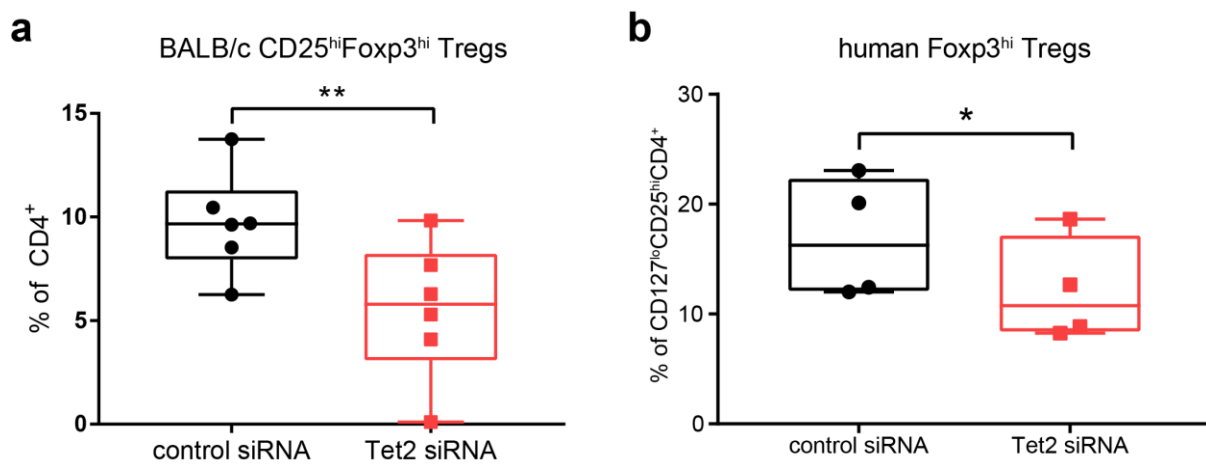
Figure 21. Tet2 is essential for efficient Treg induction *in vitro*. (a) *In vitro* Treg induction in presence of a control siRNA or a Tet2 siRNA, using limited TCR stimulation of naive CD4$^+$ T cells isolated from lymph nodes of BALB/c mice. *n* = 6. **(b)** *In vitro* Treg induction in presence of a control siRNA or a Tet2 siRNA, using limited TCR stimulation of naive CD4$^+$ T cells isolated from human peripheral blood. *n* = 4. One data point represents one subject. Experiments were performed in three technical replicates per subject. Data are presented as box-and-whisker plots with min and max values Student's t-test. *$P < 0.05$, **$P < 0.01$.

4.10 Analysis of miR142-3p inhibition *in vitro*

To better understand the potential role of miR142-3p and Tet2 for Treg induction and stability I analyzed miR142-3p inhibition during Treg induction *in vitro*.

4.11 Delivery of functional miR142-3p inhibitors *in vitro*

The uptake as well as the high efficacy and specificity of the miRNA inhibitor were demonstrated in several independent experimental settings. First, the chitosan-coated PLGA nanoparticle-mediated miRNA uptake in CD4$^+$ T cells including intracellular co-localization of the nanoparticles and the miRNA was shown using a fluorescently-labeled miRNA (Serr et al., 2018). Specifically, naive CD4$^+$ T cells were stimulated in the presence of FA-labeled nanoparticles and/or a fluorescently-labeled miRNA. As shown in Figure 22a and b, FA-labeled nanoparticles and the miRNA were efficiently taken up by the cells and confocal microscopy images in Figure 22a show the intracellular co-localization of nanoparticles and miRNA.
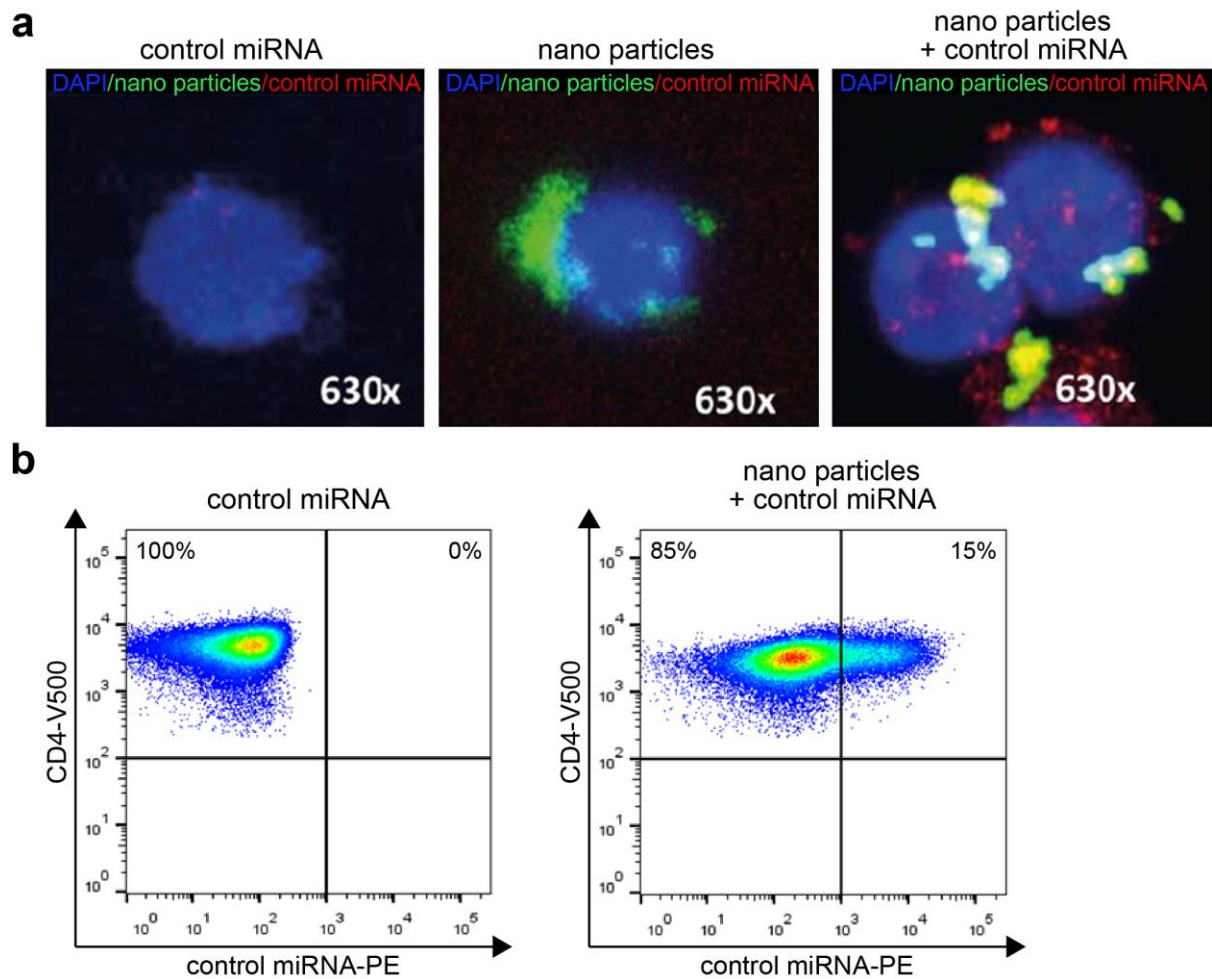
Figure 22. Nanoparticle-mediated miRNA uptake in CD4+ T cells. (a) Confocal microscopic images showing the intracellular co-localization of FA-labeled nanoparticles (green) and Dy457-labeled transfected control miRNAs (red) in CD4+T cells stimulated with anti-CD3/anti-CD28 for 18 hours. **(b)** Uptake of PE-labeled miRNAs in Treg induction assays, *in vitro*, as assessed by FACS analyses, pre-gated on live CD4+ T cells.

Second, to demonstrate the efficacy of the miR142-3p inhibitor in T cells *in vitro*, the stimulation of CD4+ T cells in presence of the miR142-3p inhibitor reduced miR142-3p abundance by more than 99% after three hours of incubation (Figure 23a). Third, the co-transfection of Jurkat T cells with a miR142-3p sensor plasmid, constructed by inserting a double-stranded oligonucleotide containing the miR142-3p target sequences into the 3'-UTR of a dual luciferase reporter plasmid, and the miR142-3p inhibitor significantly de-repressed luciferase expression (Figure 23b). Fourth, the functional blockade of miR142-3p activity in CD4+ T cells was demonstrated by showing increased expression of Tgfbr1 and ATG16L1, two established target genes of miR142-3p (Lu et al., 2018; Talebi et al., 2017), in T cells stimulated in presence of a miR142-3p inhibitor compared to a control inhibitor (Figure 23c and d).
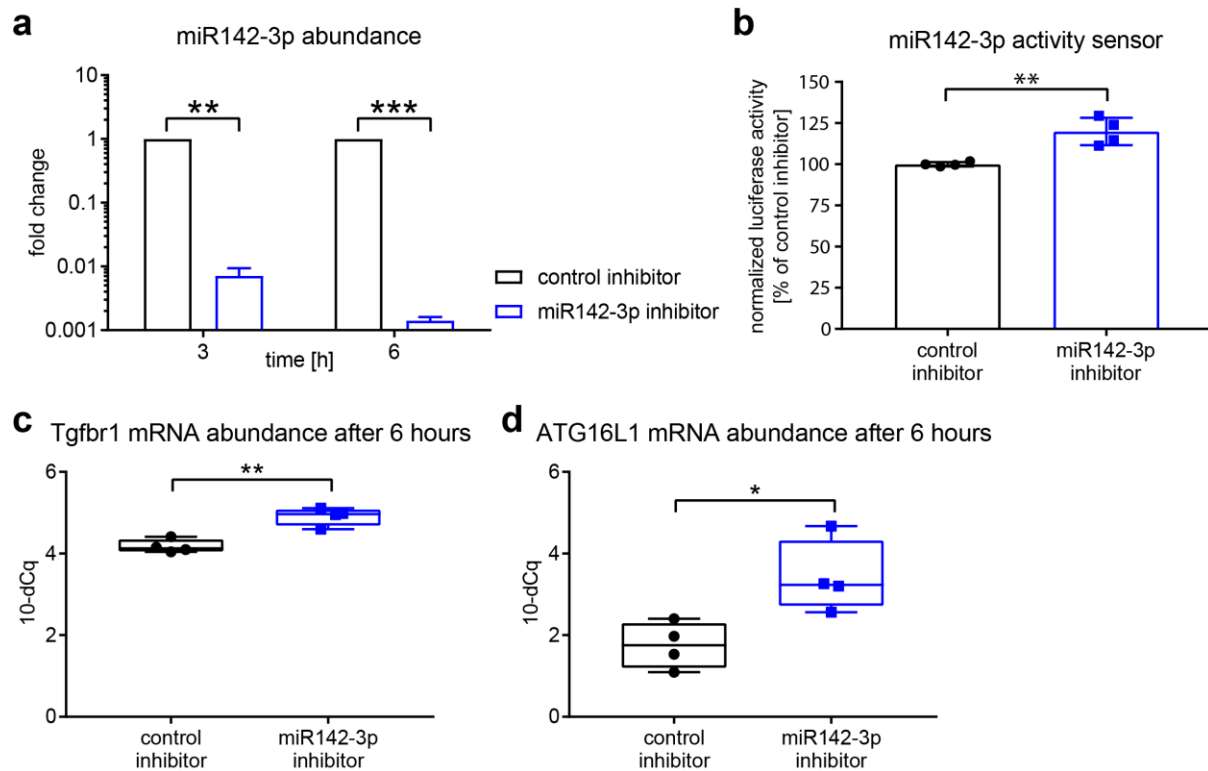
Figure 23. A miR142-3p inhibitor efficiently blocks its target miRNA *in vitro*. (a) Effect of a miR142-3p inhibitor on miR142-3p mRNA abundance upon TCR stimulation of naive CD4^{+} T cells isolated from lymph nodes of BALB/c mice. Data are shown as fold change compared to a control inhibitor. *n* = 4. **(b)** Normalized luciferase activity of Jurkat T cells co-transfected with a miR142-3p inhibitor and a miR142-3p activity sensor plasmid containing the miR142-3p target sequences in the 3'-UTR. *n* = 4. **(c)** mRNA abundance of Tgfbr1, an established target of miR142-3p, after 6 hours of TCR stimulation of CD4^{+} T cells isolated from lymph nodes of BALB/c mice, in presence of a miR142-3p inhibitor and a control inhibitor respectively. *n* = 4. **(d)** mRNA abundance of ATG16L1, an established target of miR142-3p, after 6 hours of TCR stimulation of CD4^{+} T cells isolated from lymph nodes of BALB/c mice, in presence of a miR142-3p inhibitor and a control inhibitor respectively. *n* = 4. One data point represents one subject. Experiments were performed in three technical replicates per subject. Data are presented as box-and-whisker plots with min and max values or as means ± SEM. (a) Ordinary one-way ANOVA, Tukey's multiple comparisons test. (b, c and d) Student's t-test. *$P < 0.05$, **$P < 0.01$, ***$P < 0.001$.

4.12 miR142-3p inhibition increases Tet2 abundance

To underline Tet2 as a direct target of miR142-3p, Treg induction experiments using naive CD4^{+} T cells from BALB/c mice in presence of the miR142-3p inhibitor were performed and the levels of Tet2 mRNA and protein were analyzed. Of note, the inhibition of miR142-3p resulted in significantly higher Tet2 mRNA levels after 6 hours of TCR stimulation (Figure 24a) and increased Tet2 protein abundance after 12 hours (Figure 24b).
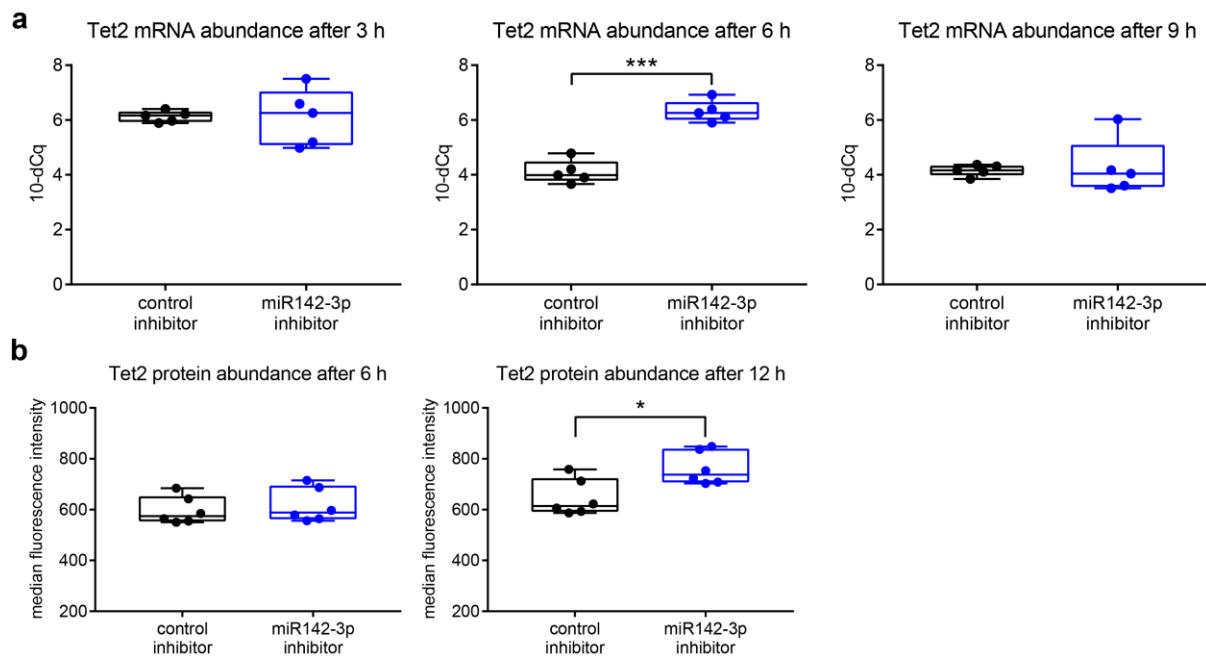
Figure 24. Inhibition of miR142-3p increases Tet2 levels during early T cell activation. (a) Tet2 mRNA abundance after 3, 6 and 9 hours of TCR stimulation of CD4^{+} T cells isolated from lymph nodes of BALB/c mice, in presence of a miR142-3p inhibitor and a control inhibitor respectively. *n* = 5. **(b)** Tet2 protein abundance (median fluorescence intensity) after 6 and 12 hours of TCR stimulation of CD4^{+} T cells isolated from lymph nodes of BALB/c mice, in presence of a miR142-3p inhibitor and a control inhibitor respectively. *n* = 6. One data point represents one subject. Experiments were performed in three technical replicates per subject. Data are presented as box-and-whisker plots with min and max values. Student's t-test. *$P < 0.05$, **$P < 0.01$, ***$P < 0.001$.

While the levels of the two other members of the Tet enzyme family, Tet1 and Tet3, were also dynamic upon TCR stimulation there was no effect of miR142-3p inhibition (Figure 25a and b), providing further evidence that miR142-3p specifically targets Tet2.
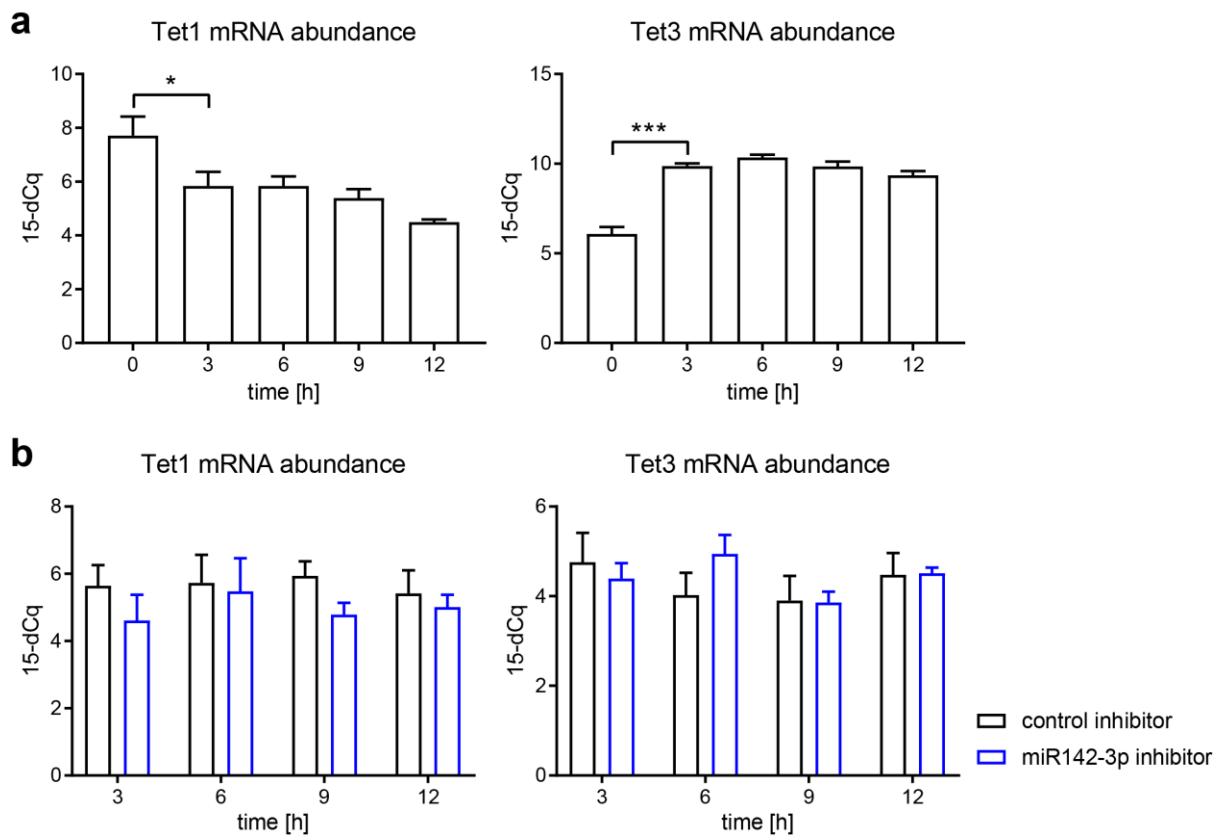
Figure 25. Tet1 and Tet3 expression upon TCR stimulation and miR142-3p inhibition. (a) Tet1 and Tet3 mRNA abundance at various time points (0 – 12 hours) of TCR stimulation of CD4+ T cells isolated from lymph nodes of BALB/c mice. n = 6. **(b)** Tet1 and Tet3 mRNA abundance after 3, 6, 9 and 12 hours of TCR stimulation of CD4+ T cells isolated from lymph nodes of BALB/c mice, in presence of a miR142-3p inhibitor and a control inhibitor respectively. n = 4. One data point represents one subject. Experiments were performed in three technical replicates per subject. Data are presented as means ± SEM. Ordinary one-way ANOVA, Tukey's multiple comparisons test. *P < 0.05, ***P < 0.001.

4.13 Tet2 3'UTR luciferase reporter assay confirms Tet2 as a direct miR142-3p target

In order to provide further mechanistic evidence for the direct miR142-3p – Tet2 target relationship a Tet2 3'UTR luciferase reporter assay was performed. The co-transfection of HEK-293 cells with a TET2 3'UTR reporter construct and a miR142-3p mimic resulted in a significantly lower luciferase activity compared to the control mimic (Figure 26a). To further support these findings, I used site directed mutagenesis by PCR to mutate the potential miR142-3p binding sites in the Tet2 3'UTR. I first mutated the potential binding site identified by the chimeric reads from HITS-CLIP data (HITS CLIP mut) and second two other binding sites in the Tet2 3'UTR (position 4135-4141 and 5392-5398; predicted mut), which were predicted using Targetscan (Agarwal et al., 2015). As before, HEK-293 cells were co-transfected with the respective luciferase reporter construct and a miR142-3p mimic. In the HITS CLIP mut the mimic showed an effect comparable to the wildtype construct (Figure 26b). Importantly, the effect of the miR142-3p mimic was fully abrogated using the predicted mut (Figure 26c), indicating that the binding sites in the Tet2 3´UTR at positions 4135-4141 and 5392-5398 are the ones targeted by miR142-3p. These findings therefore provide further evidence for the direct targeting of Tet2 by miR142-3p.
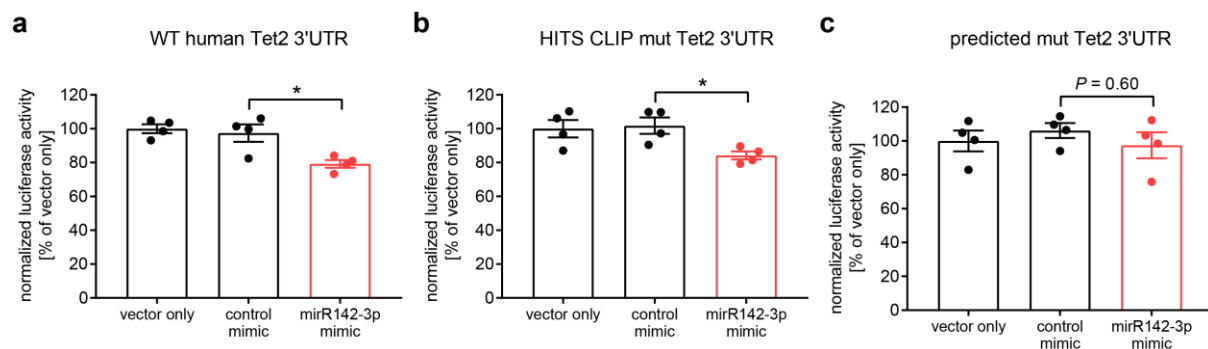
Figure 26. miR142-3p targets the methylcytosine dioxygenase Tet2 3' UTR. (a) Normalized luciferase activity of HEK-293 cells co-transfected with a miR142-3p mimic and a wildtype TET2 3'UTR reporter construct. *n* = 4. **(b)** Normalized luciferase activity of HEK-293 cells co-transfected with a miR142-3p mimic and a TET2 3'UTR reporter construct, with a mutation in the potential miR142-3p binding site, identified by HITS-CLIP chimeric reads. *n* = 4. **(c)** Normalized luciferase activity of HEK-293 cells co-transfected with a miR142-3p mimic and a TET2 3'UTR reporter construct, with a mutation in the predicted miR142-3p binding sites. *n* = 4. One data point represents one subject. Experiments were performed in three technical replicates per subject. Data are presented as means ± SEM. Student's t-test. *$P < 0.05$.

4.14 miR142 loss-of function models confirm Tet2 as a direct target of miR142-3p *in vitro*

Furthermore, I employed two loss-of-function models, 3T3 fibroblasts and miR142 knockout (miR142$^{-/-}$) mice, to support the direct miR142-3p – Tet2 target relationship. As virtually all non-hematopoietic cells the 3T3 fibroblast cell line lacks miR142-3p expression almost completely (Figure 27a), providing a suitable experimental system to study the effect of miR142-3p in absence of endogenous miR142-3p expression. The introduction of miR142-3p in these cells via transfection with a miR142-3pc mimic resulted in significantly decreased Tet2 mRNA levels (Figure 27b).
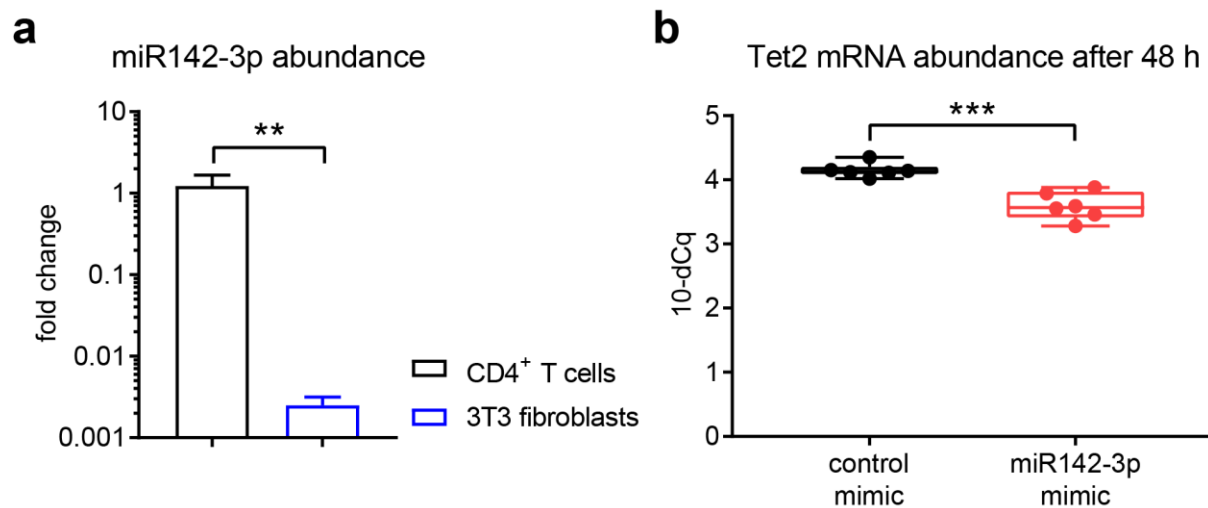
Figure 27. miR142-3p targets Tet2 in 3T3 fibroblasts. (a) miR142-3p abundance in CD4+ T cells isolated from lymph nodes of BALB/c mice and 3T3 fibroblasts. *n* = 4. Data are presented as fold change compared to CD4+ T cells. **(b)** Tet2 mRNA abundance in 3T3 fibroblasts, 48 hours after transfection with a miR142-3p mimic and a control mimic respectively. *n* = 6. One data point represents one individual experiment. Experiments were performed in three technical replicates per subject. Data are presented as box-and-whisker plots with min and max values or as means ± SEM. Student's t-test. **P < 0.01, ***P < 0.001.

Next, I used T cells from miR142 deficient animals (Figure 28a) to validate the direct targeting of Tet2 by miR142-3p directly in a mouse model. The stimulation of CD4^{+} T cells from miR142^{-/-} mice resulted in significantly increased Tet2 mRNA levels when compared to T cells from miR142^{+/+} mice (Figure 28b). In line with the increased expression of Tet2 mRNA, Tet2 protein levels were likewise elevated in T cells from miR142 deficient mice following TCR stimulation when compared to T cells from mice expressing miR142 (Figure 28c).
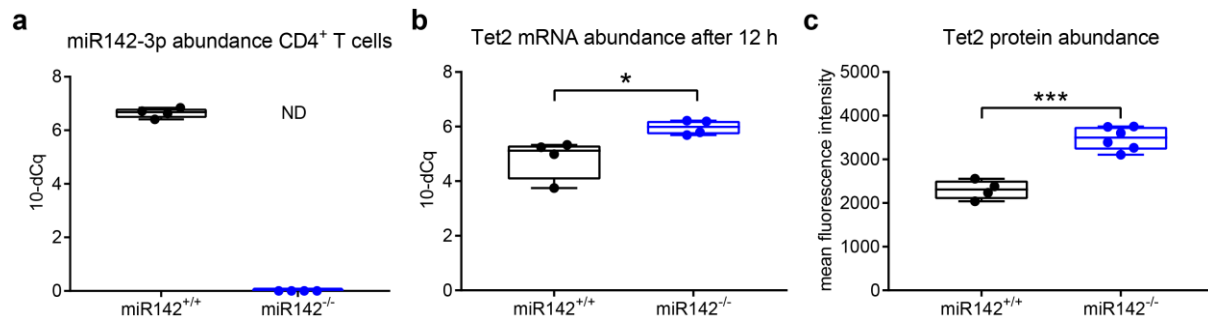
Figure 28. Increased Tet2 abundance in miR142^{-/-} mice. (a) miR142-3p abundance in CD4^{+} T cells isolated from lymph nodes of miR142 knockout (miR142^{-/-}) and control (miR142^{+/+}) mice. n = 4. ND = not detectable. **(b)** Tet2 mRNA abundance after 12 hours of TCR stimulation of CD4^{+} T cells isolated from lymph nodes of miR142^{+/+} and miR142^{-/-} mice. n = 4. **(c)** Tet2 protein abundance (median fluorescence intensity) after limited TCR stimulation (18 hours stimulation, 36 hours no stimulation) of CD4^{+} T cells isolated from lymph nodes of miR142^{+/+} and miR142^{-/-} mice. n = 6. One data point represents one subject. Experiments were performed in three technical replicates per subject. Data are presented as box-and-whisker plots with min and max values. Student's t-test. *P < 0.05, ***P < 0.001.

As described above, stimulation of BALB/c T cells in presence of a miR142-3p inhibitor resulted in increased expression of Tet2 (Figure 24a and b) and two well-established miR142-3p targets, Tgfbr1 and ATG16L1 (Figure 23c and d), when compared to a control inhibitor. To confirm that these changes are due to a direct effect of miR142-3p inhibition, I performed corresponding experiments with T cells from miR142^{-/-} mice which indicated the absence of any difference between T cells stimulated in presence of a miR142-3p inhibitor and a control inhibitor (Figure 29). The findings in both loss-of-function models again underline the direct effect of the miR142-3p inhibitor and provide compelling evidence that Tet2 is a direct target of miR142-3p.
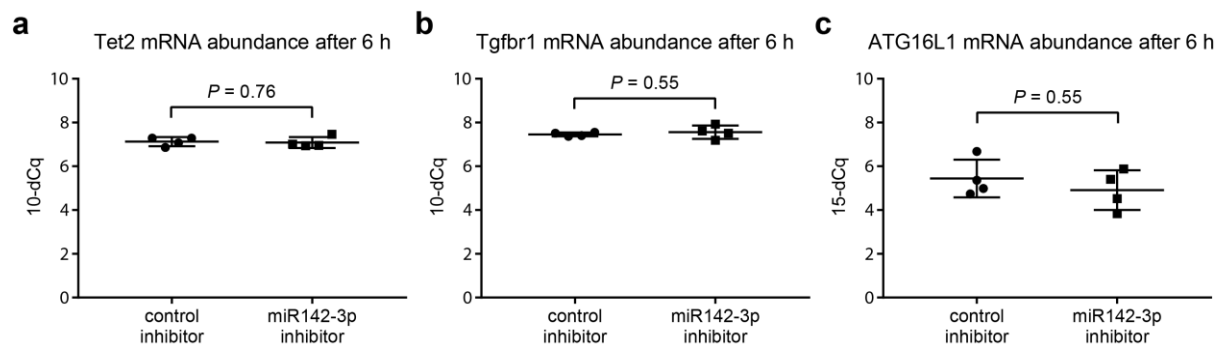
Figure 29. Inhibition of miR142-3p has no effect in miR142 deficient CD4+ T cells *in vitro*. (a) Tet2 mRNA abundance after 6 hours of TCR stimulation of CD4+ T cells isolated from lymph nodes of miR142^{-/-} mice, in presence of a miR142-3p inhibitor and a control inhibitor respectively. *n* = 4. **(b)** Tgfbr1 mRNA abundance after 6 hours of TCR stimulation of CD4+ T cells isolated from lymph nodes of miR142^{-/-} mice, in presence of a miR142-3p inhibitor and a control inhibitor respectively. *n* = 4. **(c)** ATG16L1 mRNA abundance after 6 hours of TCR stimulation of CD4+ T cells isolated from lymph nodes of miR142^{-/-} mice, in presence of a miR142-3p inhibitor and a control inhibitor respectively. *n* = 4. One data point represents one subject. Experiments were performed in three technical replicates per subject. Data are presented as means ± SEM. Student's t-test.

4.15 Inhibition of miR142-3p improves Treg induction from naive CD4+ T cells *in vitro*

Having established impaired Treg induction from naive CD4+ T cells and upregulation of miR142-3p in CD4+ T cells during onset of islet autoimmunity, I next investigated the potential specific contribution of this miRNA to diminished Treg induction during autoimmune activation. I wondered if the differentially expressed miR142-3p might interfere with Treg induction from naive T cells, thereby promoting autoimmune activation and progression. To integrate the role of miR142-3p activity with Treg induction and islet autoimmunity, murine and human *in vitro* Treg induction experiments were performed in presence of a miR142-3p mimic or inhibitor respectively. Increasing miR142-3p activity using a mimic significantly reduced Treg induction efficacy using naive CD4+ T cells from non-autoimmune prone in BALB/c mice, resembling the previously reported impaired Treg induction efficacy upon onset of islet autoimmunity in NOD mice (Figure 30). Concordantly, inhibiting miR142-3p resulted in a significant improvement of Treg induction (Figure 30). The mimic- or inhibitor-mediated modulation of miR142-3p activity likewise decreased or enhanced Treg induction efficacy using naive CD4+ T cells from NOD mice with and without islet autoimmunity, while no

significant changes were observed using naive CD4$^+$ T cells from NOD mice with established T1D (Figure 31).

Next, to assess the relevance of miR142-3p activity for human Treg induction, I used naive CD4$^+$ T cells from individuals without islet autoimmunity, with recent onset of T1D, and with established T1D. In naive CD4$^+$ T cells from subjects without islet autoimmunity, the miR142-3p mimic significantly reduced the frequency of induced Tregs, while the inhibition of miR142-3p improved Treg induction efficacy (Figure 32), just as observed in the mouse model.

Increasing miR142-3p activity did not further reduce Treg induction efficacy in naive CD4$^+$ T cells from children with recent onset of T1D (Figure 33a) or individuals with established T1D (Figure 33b), presumably because miR142-3p levels were already saturated in these cells. However, in both groups the inhibition of miR142-3p resulted in significantly higher frequencies of induced Tregs (Figure 33). These findings suggest that high levels of miR142-3p limit *in vitro* Treg induction efficacy during islet autoimmunity and T1D in humans and mice, while miR142-3p inhibition was able to restore this impairment.

Of note, there were no significant differences in cell viability and Ki67 expression after Treg induction with the miR142-3p inhibitor and the control inhibitor, excluding altered cell survival or proliferation as a contributing factor to the improved Treg induction (Figure 34).
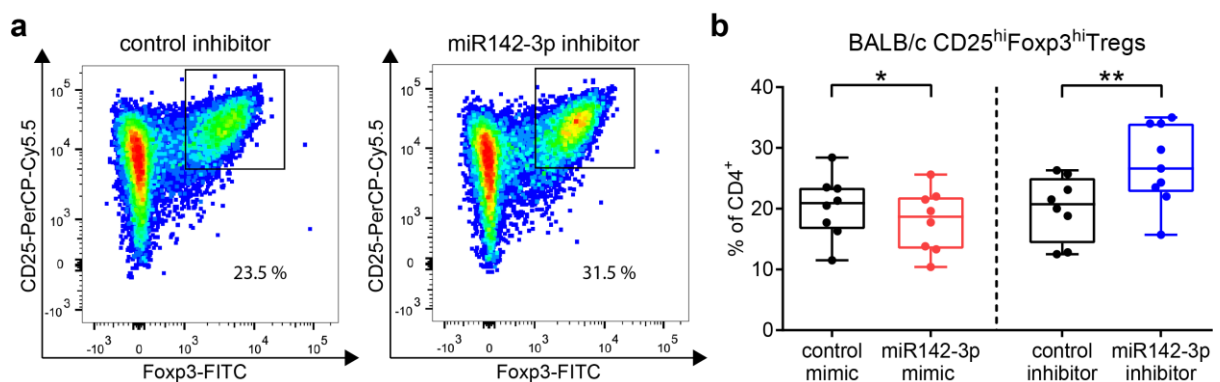
Figure 30. Inhibition of miR142-3p improves murine Treg induction *in vitro*. (a) Representative FACS plots for *in vitro* Treg induction assays in presence of a miR142-3p inhibitor and a control inhibitor respectively, using naive CD4$^+$ T cells isolated from lymph nodes of BALB/c mice. **(b)** *In vitro* Treg induction assays in presence of a miR142-3p mimic and a miR142-3p inhibitor respectively, using naive CD4$^+$ T cells isolated from lymph nodes of BALB/c mice. *n* = 8. One data point represents one subject. Experiments were performed in three technical replicates per subject. Data are presented as box-and-whisker plots with min and max values. Student's t-test. *$P < 0.05$, **$P < 0.01$.
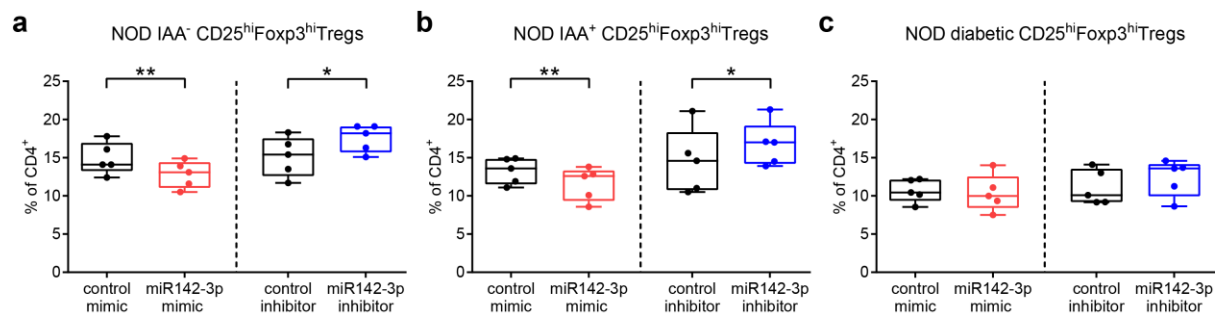
Figure 31. Inhibition of miR142-3p improves NOD Treg induction *in vitro*. (a-c) *In vitro* Treg induction assays in presence of a miR142-3p mimic and a miR142-3p inhibitor respectively, using naive CD4$^+$ T cells isolated from lymph nodes of NOD mice with different stages of autoimmunity. (a) IAA$^-$ (b) IAA$^+$ (c) diabetic. *n* = 5. One data point represents one subject. Experiments were performed in three technical replicates per subject. Data are presented as box-and-whisker plots with min and max values. Student's t-test. *$P < 0.05$, **$P < 0.01$.
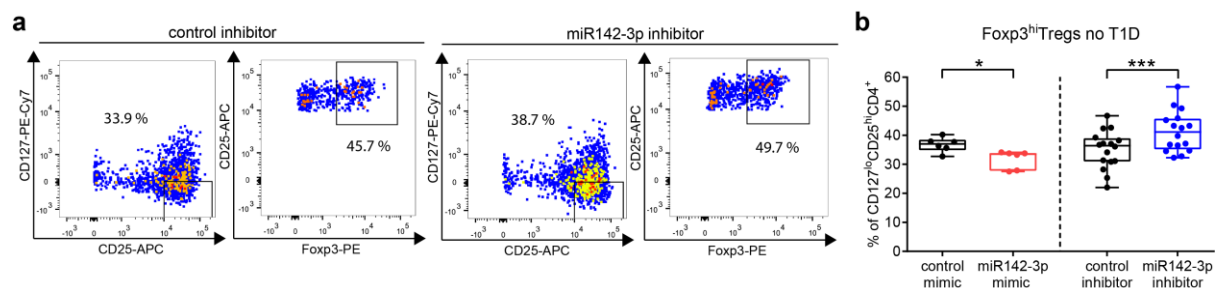

Figure 32. Inhibition of miR142-3p improves human Treg induction *in vitro*. (a) Representative FACS plots for *in vitro* Treg induction assays in presence of a miR142-3p inhibitor and a control inhibitor respectively, using naive CD4$^+$ T cells isolated from human peripheral blood. **(b)** *In vitro* Treg induction assays in presence of a miR142-3p mimic and a miR142-3p inhibitor respectively, using naive CD4$^+$ T cells isolated from peripheral blood of human subjects without autoimmunity. *n* = 6 for mimic *n* = 16 for inhibitor. One data point represents one subject. Experiments were performed in three technical replicates per subject. Data are presented as box-and-whisker plots with min and max values. Student's t-test. *$P < 0.05$, ***$P < 0.001$.
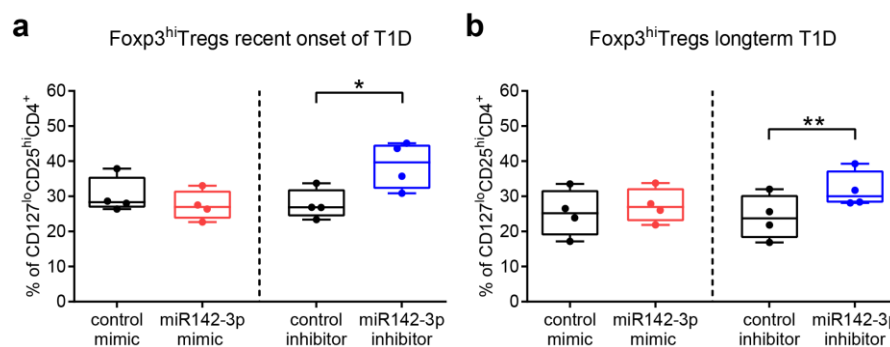
Figure 33. Inhibition of miR142-3p improves human Treg induction *in vitro* during onset of T1D. (a, b) *In vitro* Treg induction assays in presence of a miR142-3p mimic and a miR142-3p inhibitor respectively, using naive CD4$^+$ T cells isolated from peripheral blood of human subjects with recent onset of T1D (a) and longterm T1D (b). *n* = 5. One data point represents one subject. Experiments were performed in three technical replicates per subject. Data are presented as box-and-whisker plots with min and max values. Student's t-test. *$P < 0.05$, **$P < 0.01$.
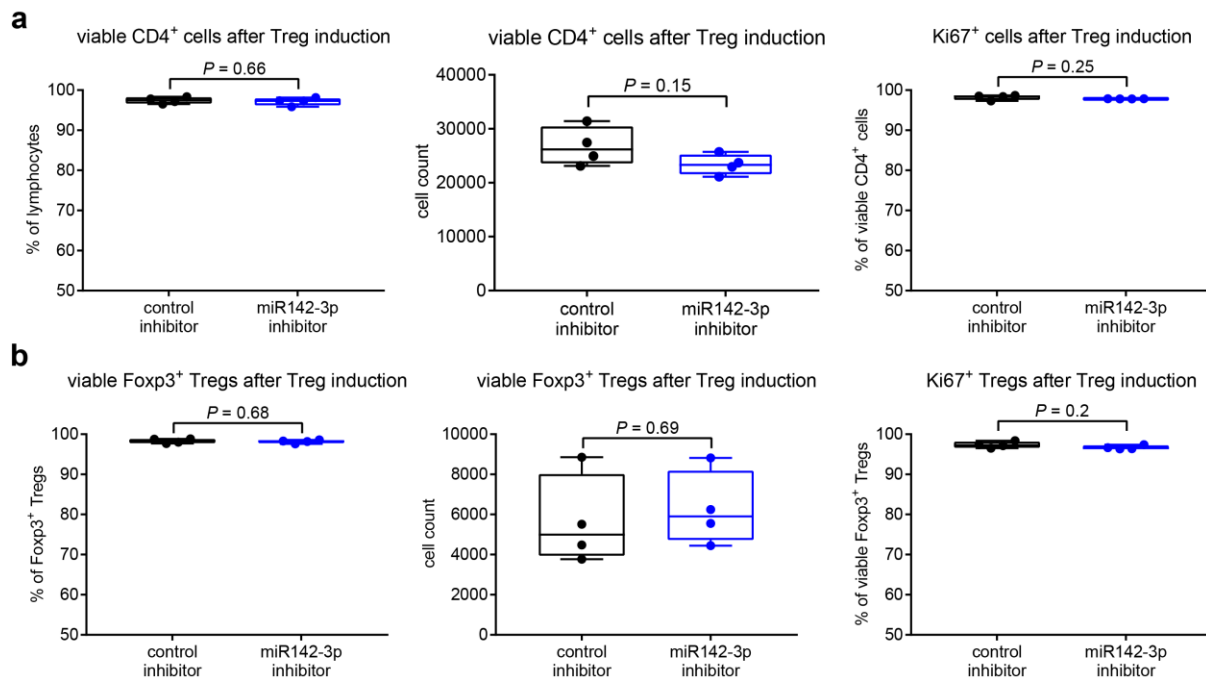
Figure 34. miR142-3p inhibition does not affect cell viability or proliferation during Treg induction *in vitro*. **(a)** Cell viability (% and cell count) and Ki67$^+$ cells of CD4$^+$ T cells after Treg induction using subimmunogenic stimulation of naive CD4$^+$ T cells isolated from lymph nodes of BALB/c mice. *n* = 4. **(b)** Cell viability (% and cell count) and Ki67$^+$ cells of Foxp3$^+$ Tregs after induction *in vitro* using subimmunogenic stimulation of naive CD4$^+$ T cells isolated from lymph nodes of BALB/c mice. *n* = 4. One data point represents one subject. Experiments were performed in three technical replicates per subject. Data are presented as box-and-whisker plots with min and max values. Student's t-test.

4.16 Inhibition of miR142-3p improves stability of *in vitro* induced Tregs

Based on the beneficial effect of miR142-3p inhibition on murine and human Treg induction efficacy *in vitro*, I wanted to investigate if this improvement was accompanied by increased Treg stability. To analyze the phenotypic stability, I re-stimulated *in vitro* induced Tregs for 30 hours, which leads to a considerable loss of the Treg phenotype, in presence of the miR142-3p inhibitor or a control inhibitor. Remarkably, the inhibition of miR142-3p during re-stimulation of *in vitro* induced Tregs resulted in a significantly higher maintenance of the Treg phenotype, as evidenced by high levels of Foxp3 and CD25 (Figure 35). Thus, the miR142-3p inhibition improves both *in vitro* Treg induction efficacy and stability of induced Tregs.
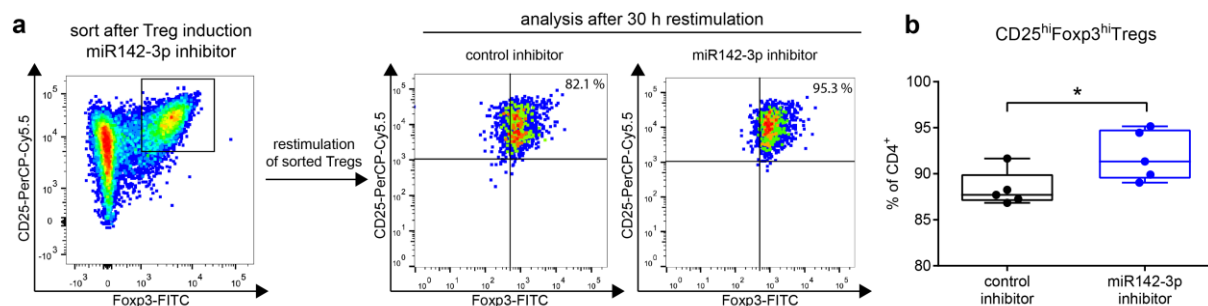
Figure 35. miR142-3p inhibition improves stability of *in vitro* induced Tregs. (a) Procedure and representative FACS plots of restimulation experiments in presence of a miR142-3p inhibitor and a control inhibitor respectively, using Tregs previously induced from naive CD4+ T cells isolated from lymph nodes of BALB/c Foxp3GFP reporter mice. **(b)** Quantification of restimulation experiments as described in (a). *n = 5*. One data point represents one subject. Experiments were performed in three technical replicates per subject. Data are presented as box-and-whisker plots with min and max values. Student's t-test. *$P < 0.05$.

There were no significant differences in cell viability and Ki67 expression after Treg induction or restimulation, excluding altered cell survival or proliferation as a contributing factor (Figure 36).
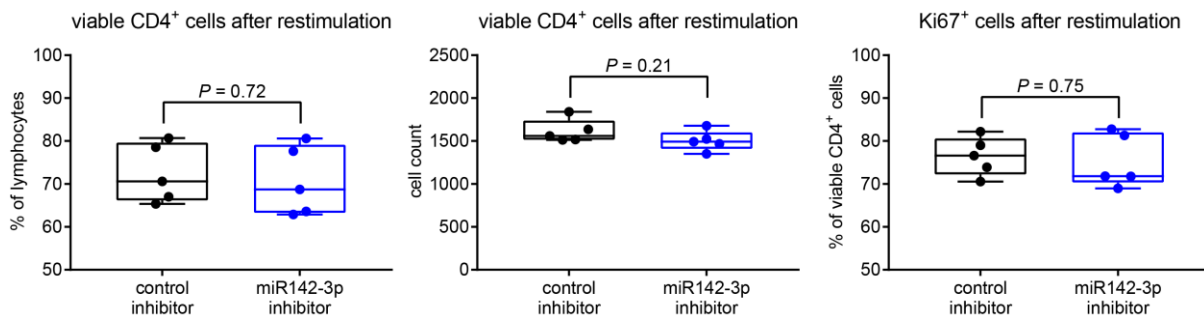
Figure 36. miR142-3p inhibition does not affect cell viability or proliferation during restimulation *in vitro*. Cell viability (% and cell count) and Ki67$^+$ cells of CD4$^+$ T cells after restimulation of *in vitro* induced Tregs for 30 hours. *n* = 5. One data point represents one subject. Experiments were performed in three technical replicates per subject. Data are presented as box-and-whisker plots with min and max values. Student's t-test.

4.17 Inhibition of miR142-3p *in vivo*

In order to expand these findings to the *in vivo* system and to address the potential pathological relevance, I next analyzed the effect of miR142-3p inhibition *in vivo*.

4.18 Delivery of functional miR142-3p inhibitors *in vivo*

For the inhibition of miR142-3p *in vivo* I used an LNA *in vivo* miRNA inhibitor which has been shown to accumulate in a broad range of tissues and to efficiently inhibit its targets in several independent studies. When delivered systemically, a series of studies have documented that LNA miRNA inhibitors distribute broadly into most tissues, including hematopoietic tissues such as lymph nodes, spleen and bone marrow (Cantafio et al., 2016; Straarup et al., 2010). In order to provide experimental evidence for the delivery of functional miR142-3p inhibitors specifically to CD4$^+$ T cells *in vivo* I used a fluorescently-labeled miR142-3p inhibitor. Importantly, the successful delivery of the inhibitor to CD4$^+$ T cells in relevant draining lymph nodes including liver-draining lymph nodes, mesenteric lymph nodes as well as pancreatic lymph nodes and directly in pancreas-residing CD4$^+$ T cells was shown after 4 hours (Figure 37a) and 24 hours (Figure 37b). Previous miRNA inhibition experiments *in vivo* worked best with a miRNA inhibitor application for 14 days every other day. Therefore, the successful delivery of the inhibitor to CD4$^+$ T cells in lymph nodes was likewise assessed at the end of the 14-days application period (Figure 37c and d).
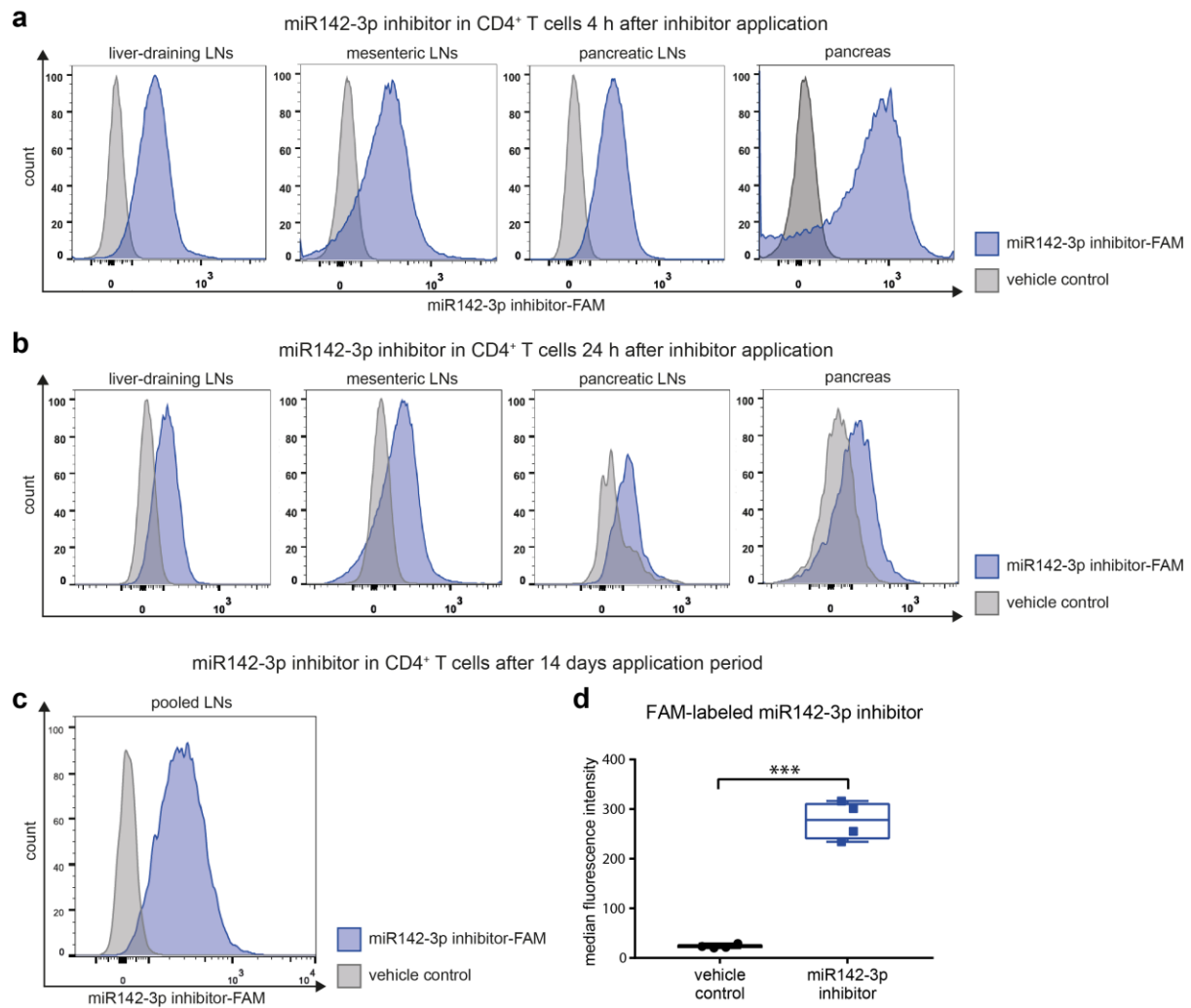
Figure 37. miR142-3p inhibitor accumulates in CD4⁺ T cells *in vivo*. (a) Representative histograms showing the accumulation of the FAM-labelled miR142-3p inhibitor in CD4⁺ T cells isolated from relevant lymph nodes and the pancreas 4 hours after inhibitor application. **(b)** Representative histograms showing the accumulation of the FAM-labelled miR142-3p inhibitor in CD4⁺ T cells isolated from relevant lymph nodes and the pancreas 24 hours after inhibitor application. **(c)** Representative histograms showing the accumulation of the FAM-labelled miR142-3p inhibitor in CD4⁺ T cells isolated from lymph nodes of mice treated with a miR142-3p inhibitor or control inhibitor for 14 days with 10 mg/kg i.p. every other day. **(d)** miR142-3p inhibitor abundance (median fluorescence intensity) in CD4⁺ T cells isolated from lymph nodes of mice treated as described in (c). *n* = 4. One data point represents one mouse. Data are presented as box-and-whisker plots with min and max values. Student's t-test. ***$P < 0.001$.

In addition, the efficacy of the successfully delivered inhibitors was demonstrated by showing increased expression of Tgfbr1, a well-established target of miR142-3p, in pancreatic T cells (Figure 38).
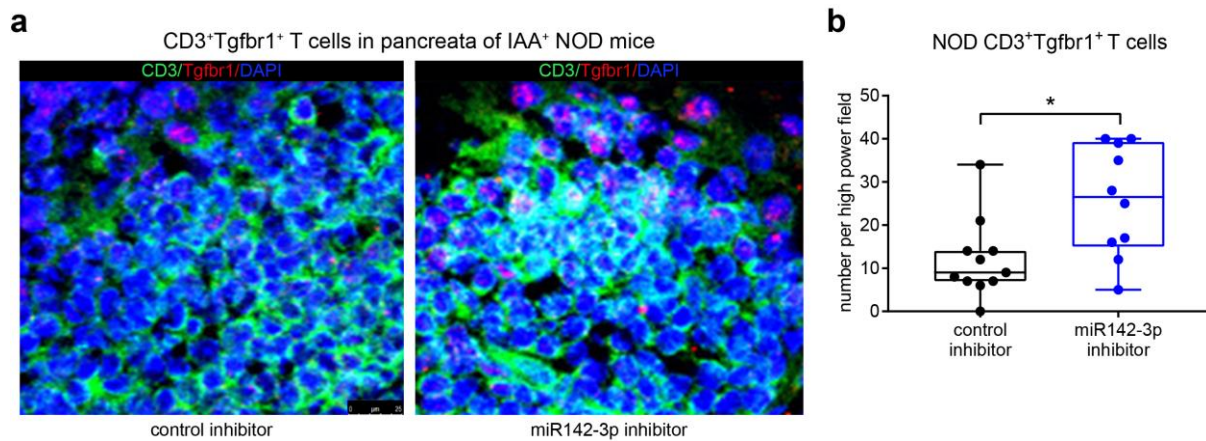
Figure 38. **miR142-3p inhibitor efficiently blocks its target miRNA *in vivo*. (a)** Immunofluorescent staining for CD3 (green), Tgfbr1 (red) and DAPI (blue) in pancreas cryosections of IAA+ NOD mice after treatment with a miR142-3p inhibitor or control inhibitor for 14 days with 10 mg/kg i.p. every other day. Scale bar: 25 μm **(b)** Quantification of CD3+Tgfbr1+ T cells per high power field in samples from (a). *n* ≥ 10. One data point represents one high power field. Data are presented as box-and-whisker plots with min and max values. Student's t-test. *$P < 0.05$.

4.19 Inhibition of miR142-3p improves murine islet autoimmunity *in vivo*

To address the potential pathological relevance of the proposed miR142-3p/Tet2 axis *in vivo*, I investigated the effect of miR142-3p inhibition in NOD mice with ongoing islet autoimmunity. The miR142-3p inhibitor was applied at 10 mg/kg bodyweight, intraperitoneally (i.p.) every other day for 14 days.

In line with a direct targeting of Tet2 by miR142-3p its inhibition *in vivo* resulted in significantly elevated Tet2 levels in pancreatic T cells of IAA+ NOD mice (Figure 39a and b). In addition, this effect was accompanied by an increased Tet2 expression (Figure 39c) and a lower Ki67 expression (Figure 39d), indicating reduced proliferation, in peripheral T cells of miR142-3p inhibitor treated IAA+ NOD mice.
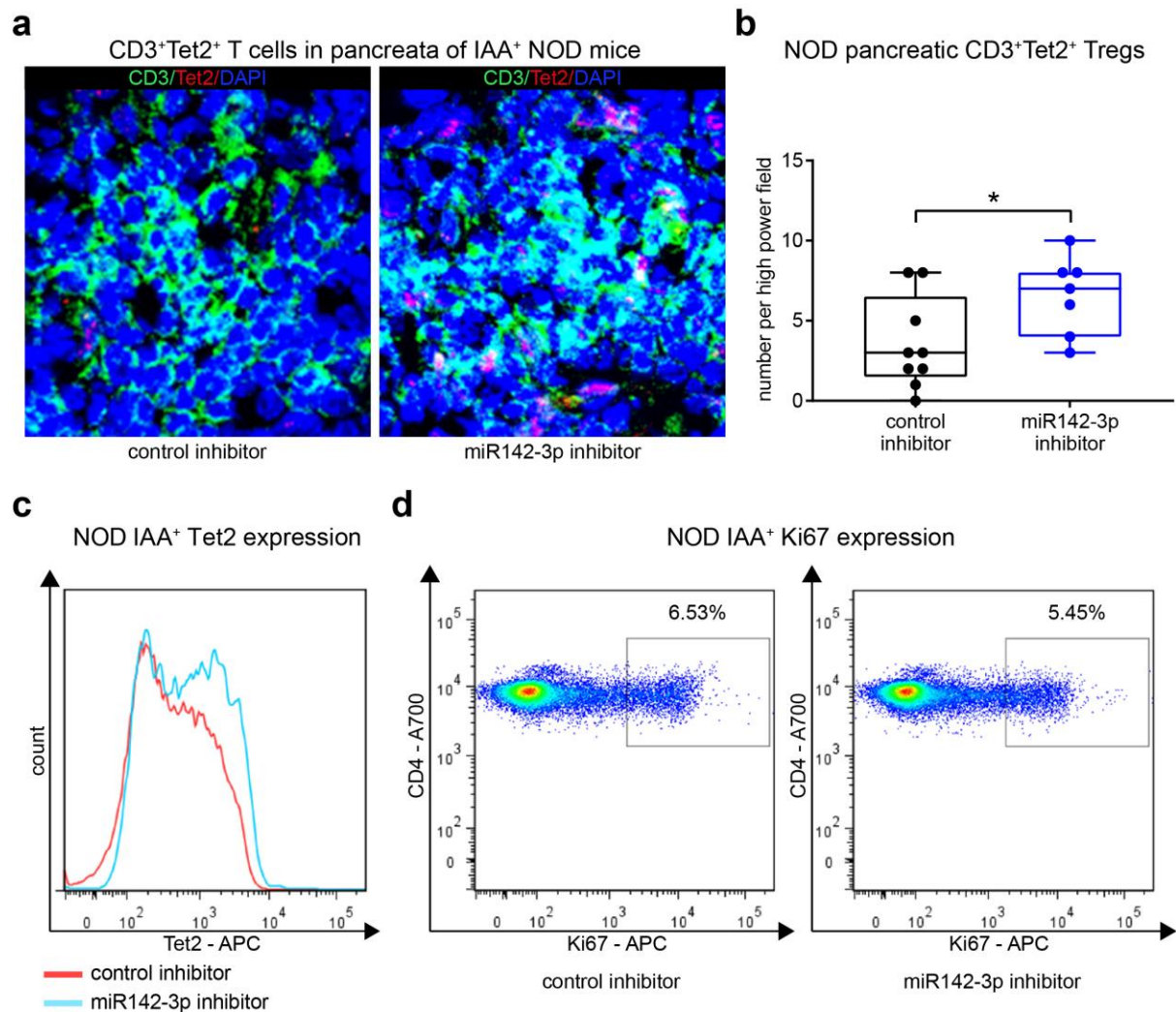
Figure 39. miR142-3p inhibition increases frequency of Tet2$^+$ T cells in murine islet autoimmunity *in vivo*. (a) Immunofluorescent staining for CD3 (green), Tet2 (red) and DAPI (blue) in pancreas cryosections of IAA$^+$ NOD mice treated with a miR142-3p inhibitor or control inhibitor for 14 days with 10 mg/kg i.p. every other day. **(b)** Quantification of CD3$^+$Tet2$^+$ T cells per high power field in samples from (a). *n* ≥ 7. **(c)** Representative histogram of Tet2 staining in CD4$^+$ T cells isolated from peripheral blood of IAA$^+$ NOD mice treated with a miR142-3p inhibitor or control inhibitor as described in (a). **(d)** Representative FACS plots indicating CD4$^+$Ki67$^+$ T cells in peripheral blood of IAA$^+$ NOD mice treated as described in (a). One data point represents one high power field. Data are presented as box-and-whisker plots with min and max values. Student's t-test. *$P < 0.05$.

In order to link the increased Tet2 expression upon miR142-3p inhibition *in vivo* to Tet2 mediated demethylation in Tregs, the DNA methylation status of the Foxp3 CNS2 was assessed in Tregs isolated from pancreatic lymph nodes of inhibitor-treated IAA⁺ NOD mice. DNA methylation was decreased at all individual CpG sites within the Foxp3 CNS2 of miR142-3p inhibitor-treated mice when compared to mice treated with a control inhibitor, and this reduction reached statistical significance when the entire CNS2 region was considered (Figure 40).
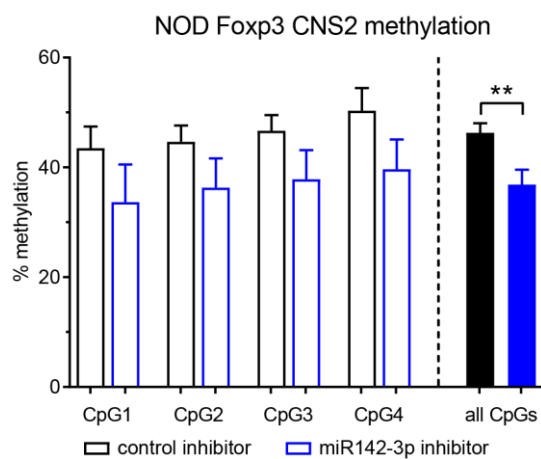
Figure 40. miR142-3p inhibition decreases Foxp3 CNS2 methylation in murine islet autoimmunity *in vivo*. Methylation of the Foxp3 CNS2 (four CpG sites and combination of all sites) in Tregs isolated from pancreatic lymph nodes of IAA⁺ NOD mice treated with a miR142-3p inhibitor or control inhibitor for 14 days with 10 mg/kg i.p. every other day. Experiments were performed in two technical replicates per subject. Data are presented as means ± SEM. Ordinary one-way ANOVA, Tukey's multiple comparisons test. **$P < 0.01$.

Importantly, immunofluorescence analyses revealed significantly enhanced frequencies of Foxp3+ Tregs within the pancreas following inhibition of miR142-3p *in vivo*, linking a miR142-3p inhibition-mediated increase in Tet2 expression to epigenetic remodeling and a higher Treg stability directly in the pancreas of NOD mice with islet autoimmunity (Figure 41).
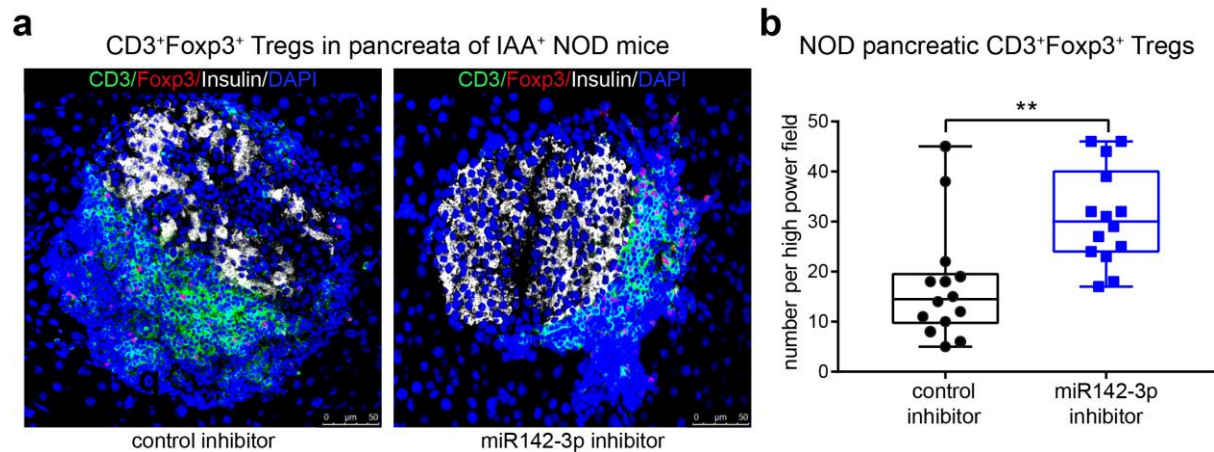
Figure 41. miR142-3p inhibition increases frequency of Foxp3+ Tregs in murine islet autoimmunity *in vivo*. (a) Immunofluorescent staining for CD3 (green), Foxp3 (red), Insulin (white) and DAPI (blue) in pancreas cryosections of IAA+ NOD mice treated with a miR142-3p inhibitor or control inhibitor for 14 days with 10 mg/kg i.p. every other day. Scale bars: 50 μm. **(b)** Quantification of CD3+Foxp3+ T cells per high power field in samples from (a). *n* = 14. One data point represents one high power field. Data are presented as box-and-whisker plots with min and max values. Student's t-test. **$P < 0.01$.

In addition, miR142-3p signaling could be directly linked to the state of islet autoimmunity *in vivo.* The inhibition of miR142-3p in IAA$^+$ NOD mice reduced pancreatic T cell infiltration as shown by histopathological analyses of pancreatic cryosections (Figure 42a) and the corresponding insulitis scoring (Figure 42b). These effects were accompanied by reduced IAA levels (Figure 42c) while the inhibition of miR142-3p did not result in changes of blood glucose or body mass (Figure 42d and e).
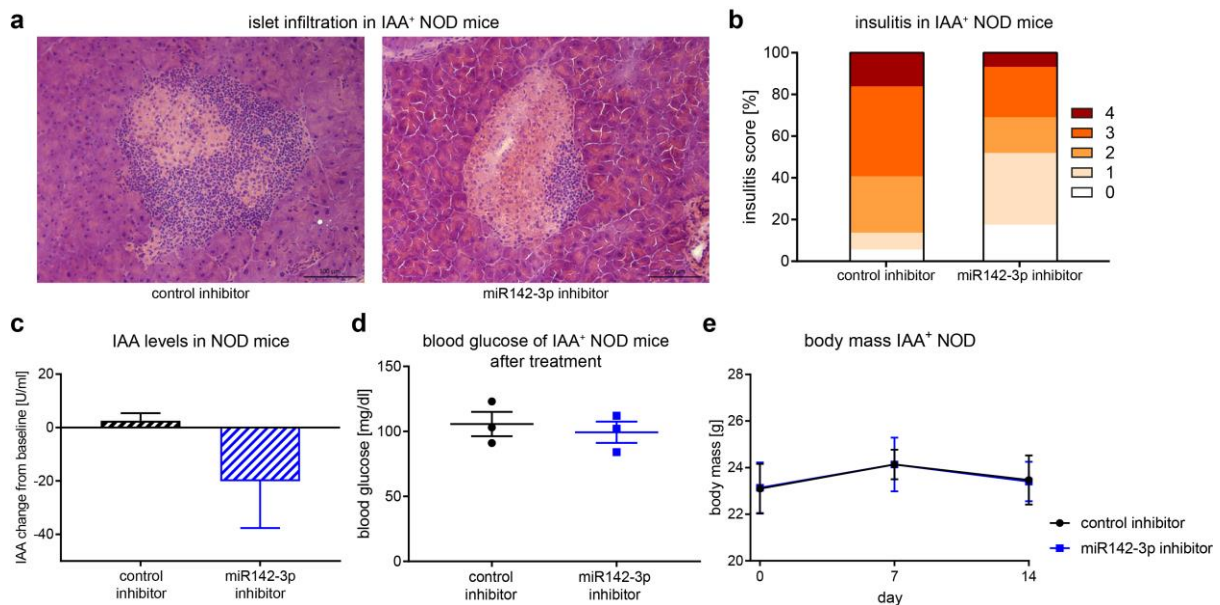
Figure 42. miR142-3p inhibition improves murine islet autoimmunity *in vivo*. (a) Representative hematoxylin and eosin stained pancreas cryosections from IAA$^+$ NOD mice treated with a miR142-3p inhibitor or control inhibitor for 14 days with 10 mg/kg i.p. every other day. Scale bars: 100 μm. **(b)** Grading of insulitis from mice treated as described in (a). *n* = 3 per group. **(c)** IAA levels in serum of IAA$^+$ NOD mice after treatment with a control inhibitor or a miR142-3p inhibitor as described in (a). Data are shown as change from baseline. *n* = 3. **(d)** Blood glucose levels in IAA$^+$ NOD mice treated as described in (a). *n* = 3. **(e)** Body mass development in IAA$^+$ NOD mice treated as described in (a). *n* = 3. One data point represents one individual (d) or mean of three individuals (e). Data are presented as means ± SEM. Student's t-test.

In order to confirm that the observed effects on Tet2 expression, Foxp3 CNS2 methylation and Foxp3+ Tregs *in vivo* were directly mediated by inhibition of miR142-3p, the inhibitor was applied to miR142 deficient mice. Expectedly, the application of the miR142-3p inhibitor to miR142 deficient mice had no effect on Treg frequency (Figure 43a), Tet2 protein abundance (Figure 43b) or Foxp3 CNS2 methylation (Figure 43c).
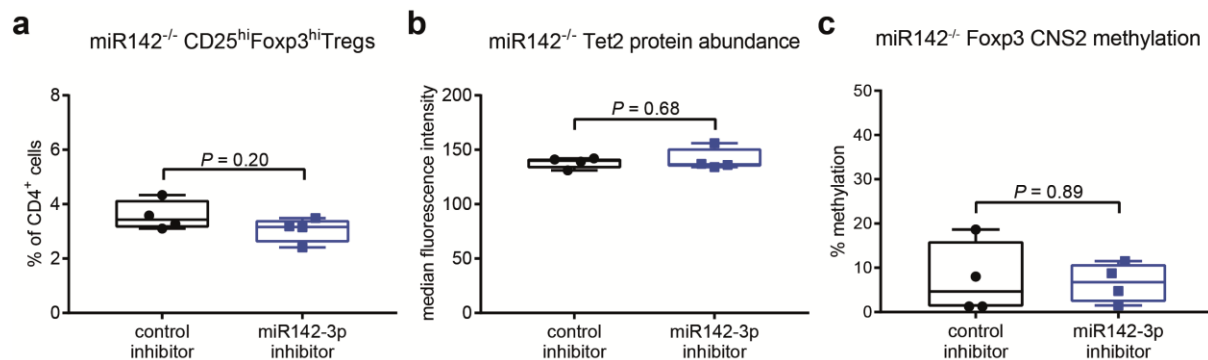
Figure 43. miR142-3p inhibitor has no effect in miR142-/- mice *in vivo*. (a) Ex vivo CD25hiFoxp3+ Tregs isolated from lymph nodes of miR142-/- mice treated with a miR142-3p inhibitor or control inhibitor for 14 days with 10 mg/kg i.p. every other day. *n* = 4. **(b)** Ex vivo Tet2 protein abundance (median fluorescence intensity) in CD4+ T cells isolated from lymph nodes of miR142-/- mice treated with a miR142-3p inhibitor or control inhibitor as described in (a). *n* = 4. **(c)** Methylation of the Foxp3 CNS2 (mean of all sites) in Tregs isolated from lymph nodes of miR142-/- mice treated with a miR142-3p inhibitor or control inhibitor as described in (a). *n* = 4. One data point represents one mouse. Data are presented as box-and-whisker plots with min and max values. Student's t-test.

Finally, to expand these *in vivo* findings to a model of human T1D, MHCII deficient HLA-DQ8 transgenic NOD.Cg-Prkdcscid Il2rgtm1Wjl (NSG) mice were reconstituted with PBMCs from individuals with T1D for a pilot experiment. The inhibition of miR142-3p in these humanized mice revealed significantly increased levels of Tet2 in pancreatic T cells and a trend towards elevated frequencies of CD127^{low}CD25^{high} Tregs (Figure 44).
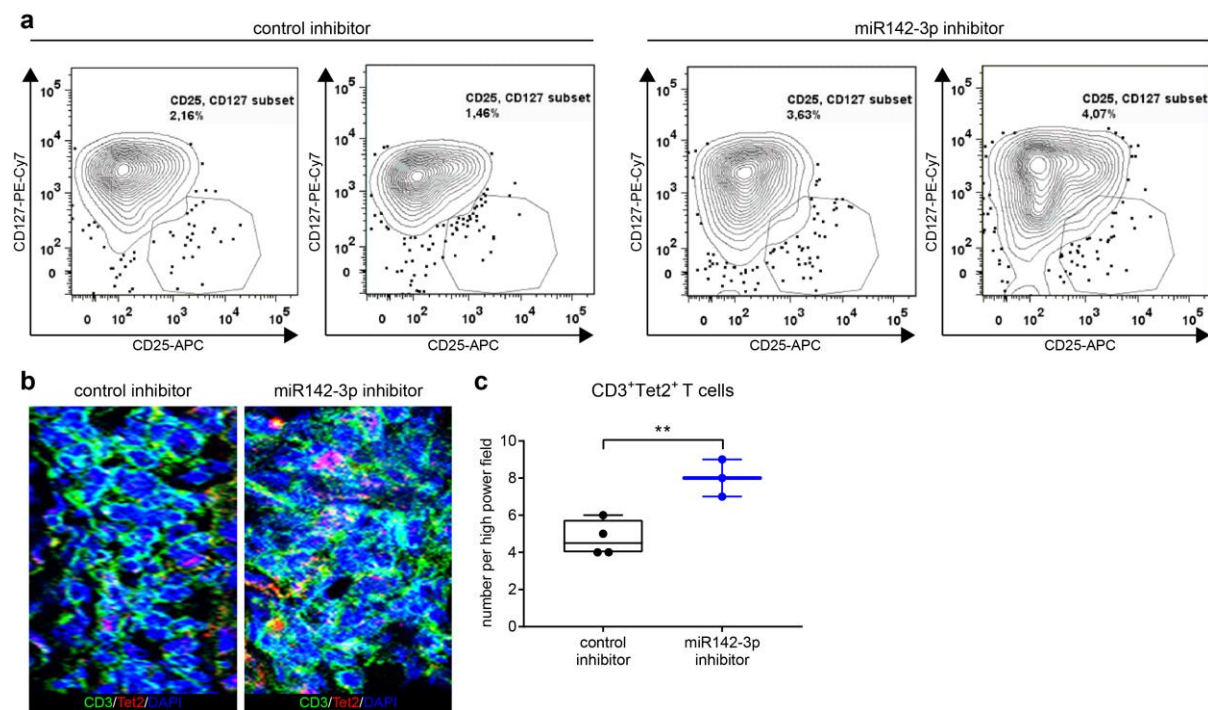
Figure 44. Effects of miR142-3p inhibition in humanized NSG mice. (a) Representative set of FACS plots indicating CD25^{hi}CD127^{lo} Tregs in lymph nodes and spleen of humanized NSG mice treated with a miR142-3p inhibitor or control inhibitor for 14 days with 10 mg/kg i.p. every other day. **(b)** Immunofluorescent staining for CD3 (green), Tet2 (red) and DAPI (blue) in pancreas cryosections of humanized NSG mice treated with a miR142-3p inhibitor or control inhibitor as described in (a). **(c)** Quantification of CD3$^+$Tet2$^+$ T cells per high power field in samples from (b). *n* ≥ 3. One data point represents one high power field. Data are presented as box-and-whisker plots with min and max values Student's t-test. **$P < 0.01$

4.20 Additional targets of miR142-3p

miRNAs target a multitude of genes, regulating their expression and downstream pathways. Therefore, I analyzed the HITS CLIP dataset and made use of in silico target prediction tools to identify additional target genes of miR142-3p that might be involved in Treg development and function. Specifically, Stat5, Smad3 and TGFB receptors (TGFBR1, TGFBR2 and TGFBR3) were identified and as for Tet2, the direct targeting of these genes by miR142-3p was validated by showing elevated mRNA expression levels after 6 hours of TCR stimulation in presence of a miR142-3p inhibitor compared to a control inhibitor (Figure 45).
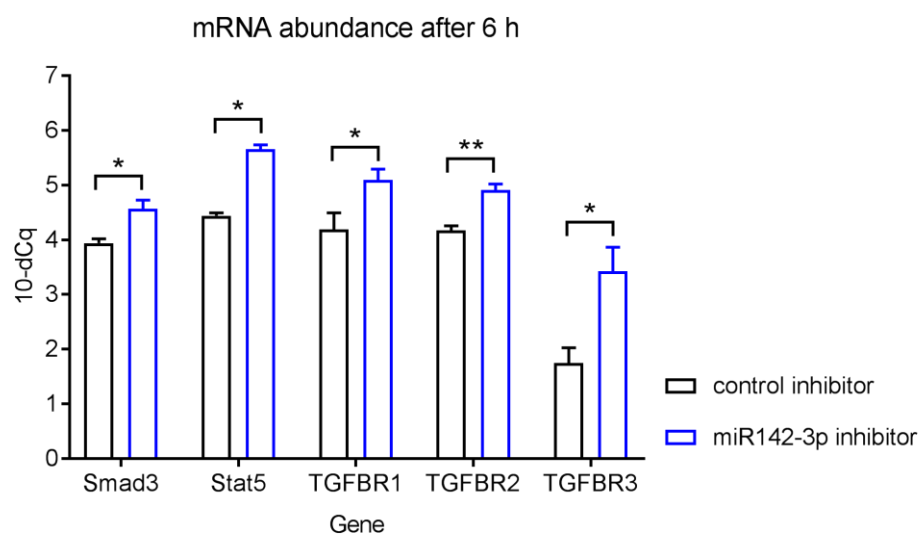
Figure 45. Inhibition of miR142-3p increases levels of genes important for Treg function. Abundance of Smad3, Stat5, TGFBR1, TGFBR2 and TGFBR3 mRNA after 6 hours of TCR stimulation of CD4$^+$ T cells isolated from lymph nodes of BALB/c mice, in presence of a miR142-3p inhibitor and a control inhibitor respectively. n = 5. One data point represents one subject. Experiments were performed in three technical replicates per subject. Data are presented as means ± SEM. Student's t-test. *$P < 0.05$, **$P < 0.01$.

4.21 Tet2 mediated regulation of Bach2

Given the broad role of Tet2 in various cell types, including T cells, I performed Tet2 ChIP sequencing of CD4$^+$ T cells in order to identify additional genes that are regulated by Tet2 and could potentially contribute to Treg homeostasis. The analysis revealed Tet2 binding peaks in numerous genes and the results for one interesting candidate gene, Bach2, is shown in Figure 46. Four Tet2 binding sites were identified upstream of the Bach2 transcription start site and three of them correlated with DNase I hypersensitive sites indicating open chromatin and therefore putative regulatory regions. To investigate if these regions are involved in regulation of the Bach2 gene by Tet2 mediated DNA demethylation I established an HRM and Pyrosequencing based methylation assay for one of the four potential binding sites, covering eight CpG sites. The methylation analysis revealed differential methylation of the putative Bach2 regulatory region with very low levels of methylation in naive T cells and Tregs and considerably increased levels in activated T cells (Figure 47).
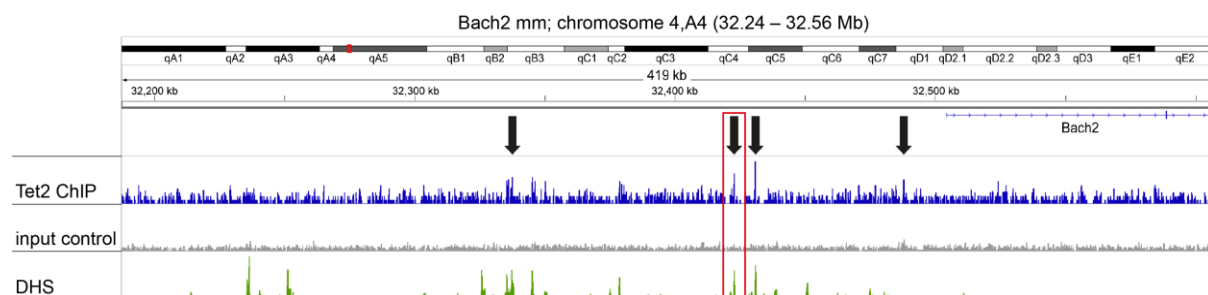
Figure 46. ChIP-Seq of CD4$^+$ T cells identifies four Tet2 binding sites upstream of the Bach2 transcription start site. Tet 2 ChIP-Seq analysis of a putative regulatory region upstream of Bach2 showing Tet2 binding peaks, the input control and DNase I hypersensitive sites (DHS). Methylation analysis was performed in the region marked with a red box (32,422,750 – 32,422,924).
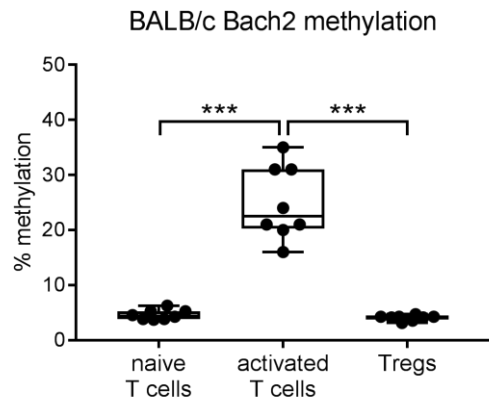
Figure 47. Methylation of a putative Bach2 regulatory region in T cell subsets. Methylation of the putative regulatory region upstream of the Bach2 TSS (mean of all sites) in T cell subsets isolated from lymph nodes of BALB/c mice. n = 8. One data point represents one subject. Experiments were performed in two technical replicates per subject. Data are presented as box-and-whisker plots with min and max values. Student's t-test. ***$P < 0.001$.

5 Discussion

During the last decades a multitude of studies has significantly improved our understanding of T1D development. Both genetic and environmental factors contribute to T1D risk and autoimmune activation. The destruction of the pancreatic beta cells is assumed to result from a defective immune tolerance and is mainly mediated by T cells. Therefore, a better understanding of the underlying mechanisms in T cells, modifying T1D risk and triggering activation of islet autoimmunity as well as the critical progression to symptomatic T1D are crucial for the development of novel intervention strategies. Since Tregs play a major role in immune regulation and their impaired function and stability can contribute critically to the onset of islet autoimmunity and T1D, the major aim of this thesis was the dissection of mechanisms underlying impaired Treg homeostasis in the setting of islet autoimmunity. Specifically, the focus was set on DNA methylation and miRNAs as potentially important regulators of Treg development, maintenance, function and stability.

Impaired Treg induction from naive CD4$^+$ T cells in children with recent onset of islet autoimmunity (Serr et al., 2016b, 2018) suggests *in vitro* Treg induction assays as an important tool to investigate the underlying molecular mechanisms of autoimmune activation. Therefore, I performed a first set of experiments aiming at optimizing murine and human Treg induction *in vitro* using subimmunogenic TCR stimulation, in the absence of exogenous TGFβ. The early withdrawal of the TCR stimulus, mimicking subimmunogenic conditions, resulted in a substantially improved Treg induction efficacy compared to continuous TCR stimulation. This further supports the concept of an ideal window regarding quality, quantity and duration of stimulation for efficient Treg induction *in vitro*, as indicated by previous studies (Daniel et al., 2011a; Gottschalk et al., 2010; Serr et al., 2016b). In addition, and linking these results to the regulation of Treg stability, the expression of Foxp3 and additional important Treg markers was more stable in Tregs induced using short-term TCR stimulation compared to their continuously induced counterparts.

Since maintained Foxp3 expression and consequently Treg stability are directly linked to the demethylated state of the Foxp3 CNS2, I established a HRM and pyrosequencing based methylation assay, covering the relevant CpG sites within the human and the murine CNS2, enabling a quantitative analysis of Treg stability on a molecular level. The assay could

reproduce the previously reported differential methylation of the Foxp3 CNS2 in five distinct ex vivo CD4$^+$ T cell subsets, linking the different expression levels of Foxp3 in the analyzed T cell populations to the DNA methylation state of the Foxp3 CNS2. Consequently, and as previously reported, the level of Foxp3 expression and its maintenance is directly linked to the methylation status of the Foxp3 CNS2 and the methylation assay represents a valuable tool to assess Treg stability in the context of this research project. This includes the transient low expression of Foxp3 in human activated CD4$^+$ T cells. Of note, although the short-term *in vitro* Treg induction assay resulted in significantly higher percentages of induced Tregs and this was accompanied by a higher stability of the Treg phenotype, this increase in stability was not reflected by a DNA demethylation of the Foxp3 CNS2 in induced Tregs.

However, the differences in Tregs stability after induction *in vitro* suggest a role for Foxp3 CNS2 DNA methylation at least at a certain point during Treg induction and especially activation and maintenance of Foxp3 expression. This hypothesis is further supported by previous findings showing the importance of methylation changes in the Foxp3 CNS2 during Treg development and Treg induction *in vitro* (Yang et al., 2015b; Yue et al., 2016). To capture potential methylation dynamics during the early phase of murine and human Treg induction from naive CD4$^+$ T cells, I analyzed Treg markers and Foxp3 CNS2 methylation as early as 12 hours of Treg induction. This analysis revealed cells expressing Treg markers, especially high levels of Foxp3, with an increase over time and importantly a rapid demethylation of the Foxp3 CNS2 in the early phase of the Treg induction. The observed methylation dynamic was restricted to cells with high levels of Foxp3, indicating that CNS2 demethylation is an active process and does not result from TCR stimulation or cell proliferation per se.

Importantly, the higher Treg induction efficacy following short-term stimulation, suggests that the termination of the stimulus during the short phase of DNA demethylation within the Foxp3 CNS2 might be a critical contributor to efficient Treg generation. Although these epigenetic changes are not maintained in the *in vitro* Treg induction assay, the temporary demethylation seems to be critically linked with an ideal window for the induction and maintenance of Foxp3 as previously suggested (Daniel et al., 2011b; Serr et al., 2016b).

Recent studies showed that the onset of islet autoimmunity and T1D in mice or humans is accompanied by a reduced capacity of naive CD4$^+$ T cells to be differentiated into Tregs *in vitro* (Serr et al., 2016b, 2018). These findings were validated by *in vitro* Treg induction assays

using naive CD4$^+$ T cells from NOD mice and human subjects with different stages of autoimmunity, revealing impaired Treg induction capacity upon onset of islet autoimmunity. This again highlights intrinsic defects in Tregs during islet autoimmunity which could contribute to autoimmune activation and raises the question of contributors to these impairments.

The molecular mechanisms underlying the impaired Treg induction during islet autoimmunity as well as promoting both onset of autoimmunity and the highly variable progression to symptomatic T1D remain poorly understood. Recent studies have highlighted miRNAs as critical contributors to immune regulation and suggested that their dysregulation can promote the onset of autoimmunity and/or the progression to clinically overt T1D. Potential target genes of miRNAs can be predicted in silico based on their nucleotide sequence. These approaches result in a multitude of potential targets, the relevance of which has remained unclear. Therefore, this thesis aimed at the identification of specific miRNAs that contribute to the onset of autoimmunity and the identification of their relevant targets and downstream pathways which could considerably advance our understanding of autoimmune activation. Here, I identified increased levels of miR142-3p, which is the most abundant active miRNA in the RISC of human CD4$^+$ T cells, during the onset of islet autoimmunity and T1D in CD4$^+$ T cells of mice and humans. Most previous studies analyzed the abundance of circulating miRNAs and T cell specific miRNAs without investigating their RISC association. In contrast, the high abundance of miR142-3p specifically in the RISC provides an additional layer of information pointing towards an important regulatory role of this miRNA.

The identification of differentially expressed miRNAs can enable their use as biomarkers, however, the differential expression does not necessarily imply a causative role of these miRNAs in the respective disease setting. To gain insight into the involvement in mechanisms underlying disease pathogenesis, the identification of direct targets of the miRNAs and their downstream pathways are crucial. The analysis of an existing mRNA sequencing dataset showed that the majority of in silico predicted miR142-3p targets was downregulated in CD4$^+$ T cells of individuals with ongoing islet autoimmunity compared to healthy controls. These findings provide additional evidence that the increased abundance of miR142-3p during islet autoimmunity might be associated with a regulatory function and support a potentially important role of this miRNA for the activation of T cell specific islet autoimmunity.

In the context of immune function and specifically Tregs, miR142-3p has been identified as a regulator of ATG16L1 and its role in regulating autophagy, proliferation and function in thymic-derived Tregs as well as the implication of these findings for graft-versus-host disease have been highlighted (Lu et al., 2018). Another study has shown that miR142-3p regulates GARP expression in Tregs and, as a result, their expansion in response to activation, which provides insight into mechanisms involved in Treg proliferation (Zhou et al., 2013). While the findings of both studies are important for the field, they do not address the impact of miR142-3p on de novo Treg induction from naive CD4$^+$ T cells and stability of induced Tregs during the onset of islet autoimmunity, which was the focus of this project.

To further investigate the role of miR142-3p for activation of autoimmunity I performed HITS CLIP analysis of human CD4$^+$ T cells. This method analyses miRNA and mRNA fragments present in the RISC and therefore offers a valuable tool to gain information about the specific contribution of individual miRNAs to mRNA regulation as well as the miRNA-mRNA target relationships in the specific setting. The analysis identified 271 unique RISC-associated miRNAs, of which miR142-3p was the most abundant miRNA, and 7,829 corresponding mRNA targets which showed a significant enrichment of biological processes involved in immune activation and regulation. These findings support the notion that miRNAs can critically contribute to immune regulation in CD4$^+$ T cells and suggest that miR142-3p might be of particular importance during onset of autoimmunity.

Bringing together the impaired Treg induction during the onset of islet autoimmunity and the crucial importance of Foxp3 CNS2 DNA methylation for Treg induction and stability, I identified the methylcytosine dioxygenase Tet2, which is a mediator of DNA demethylation, as a target of miRNA mediated regulation in CD4$^+$ T cells. By catalyzing DNA demethylation of regulatory regions and consequently altering the accessibility of the DNA to transcription factors, Tet enzymes are involved in the regulation of various cellular processes. They're involved in the differentiation of CD4$^+$ T cells in humans and mice, as well as Treg homeostasis and function by active demethylation of the Foxp3 CNS2 (Nair and Oh, 2014; Wang et al., 2013; Yang et al., 2015b; Yue et al., 2016). Furthermore, and supporting the important role of Tet enzymes for Tregs, overexpression of the Tet1 catalytic domain improves the stability of Foxp3 expression in induced Tregs (Someya et al., 2017).

To answer the question, whether miR142-3p mediated regulation of Tet2 expression contributes to the observed Treg induction impairments during the onset of islet autoimmunity, I analyzed Tet2 expression upon onset of murine and human autoimmunity/T1D. Indeed, the high levels of miR142-3p correlated with a reduced abundance of Tet2 protein in CD4$^+$ T cells isolated from lymph nodes and pancreata of IAA$^+$ NOD mice. Similarly, the abundance of Tet2$^+$ T cells was significantly reduced in the peripheral blood of subjects with recent onset of T1D. Providing the next aspect of a potentially causative downstream pathway of miR142-3p, which has not been reported previously, I furthermore demonstrate that these observations are directly linked to epigenetic remodeling of the Foxp3 CNS2. There was a significant increase in Foxp3 CNS2 DNA methylation of Tregs upon recent onset of islet autoimmunity in NOD mice and recent onset of T1D in humans. The expression of Helios, which is a marker of thymic-derived Tregs (Thornton et al., 2010), did not differ in Tregs from individuals with recent onset of T1D and healthy controls, showing that the observed differential DNA methylation does not result from differences in the composition of the Treg pool. These findings further support the hypothesis that dysregulated DNA methylation remodeling impairs Treg homeostasis and consequently contributes to the onset and progression of islet autoimmunity. Importantly, I identified increased Foxp3 CNS2 DNA methylation in Tregs from NOD mice below 30 days of age with a very early onset of autoimmunity, providing strong evidence for a potential causative role of miR142-3p/Tet2 signaling in promoting Treg impairments and autoimmunity. The novel findings provided here are crucial for the assessment of the applicability of a differentially expressed, disease associated miRNA for potential intervention strategies.

In line with a critical contribution of Tet2 to Treg function and Treg induction (Nair and Oh, 2014; Wang et al., 2013; Yang et al., 2015b; Yue et al., 2016), I showed increased levels of Tet2 mRNA and protein during the early phase of Treg induction. Furthermore, the reduced Treg induction efficacy in the presence of a Tet2 siRNA provides additional conceptual support for the relevance of Tet2 for murine and human Treg induction and its potential involvement in impaired Treg homeostasis during islet autoimmunity. The finding that reduced Tet2 expression alone was sufficient to interfere with Treg induction potential underscores the critical contribution of Tet2. This is partially in contrast to previous studies employing

combined Tet targeting and suggesting that reduced Tet2 function can be compensated by increased activity of Tet1 and Tet3 (Yue et al., 2016).

In order to understand whether the observed link between Tet2 and the onset of islet autoimmunity is indeed mediated by miR142-3p, I used miR142-3p inhibitors and mimics to modulate miRNA activity during Treg induction *in vitro*. The uptake of the inhibitor by CD4^{+} T cells, as well as its ability to inhibit miRNA activity, were shown in an extensive set of experiments. Importantly, and confirming Tet2 to be regulated by miR142-3p, the inhibition of miR142-3p resulted in increased levels of Tet2 mRNA and protein during the early phase of Treg induction while no comparable effect on Tet1 or Tet3 abundance were observed.

Since miRNAs target many genes which are likewise regulated by many different miRNAs, the clear verification of a direct miRNA-mRNA target relationship is crucial for the understanding of miRNA mediated pathways. Here, the first approaches are usually in silico target prediction tools like Targetscan (Agarwal et al., 2015) or miRNADA (Betel et al., 2010). The complementary pairing of miRNA seed sequences and mRNA is widely used for prediction of miRNA-mRNA pairs, often in combination with evolutionary conservation (Lewis et al., 2005), secondary structure (Long et al., 2007), or neighboring context information (Grimson et al., 2007). While these rules have been valuable to identify multitudes of potential miRNA targets, both false positive and false negative predictions cannot be excluded and some non-canonical target sites might not be identified (Chi et al., 2012; Mittal and Zavolan, 2014). The functional relevance of imperfectly matched miRNA seeds has been shown in various studies (Didiano and Hobert, 2006; Tay et al., 2008; Vella et al., 2004). This highlights the importance of methods like HITS-CLIP that can directly assess functional miRNA-mRNA interactions *in vivo*, regardless and despite of in silico predictions. The validity and robustness of HITS-CLIP and comparable methods, including the analysis of chimeric reads, has been shown in several studies (Chi et al., 2009; Kameswaran et al., 2014; Mittal and Zavolan, 2014; Schug et al., 2013). However, also HITS-CLIP data alone are not sufficient to define definite target relationships, they are a valuable source of information for miRNA-mRNA pairs *in vivo* and here provide important and sufficient experimental evidence to dissect the identified miR142-3p/Tet2 relationship and to follow up with additional molecular and cellular experimental approaches.

3'UTR luciferase reporter assays are the most common approach to confirm genes as direct targets of a particular miRNA. Here, the co-transfection of HEK-293 cells with a reporter construct containing the Tet2 3'UTR and a miR142-3p mimic resulted in reduced luciferase activity. In control experiments with mutated binding sites the HITS CLIP mut showed an effect comparable to the wildtype construct, but the effect of the miR142-3p mimic was fully abrogated using the predicted mut. This indicates that the binding sites in the Tet2 3´UTR at positions 4135-4141 and 5392-5398 are the ones targeted by miR142-3p. These findings therefore provide clear experimental evidence for the direct targeting of Tet2 by miR142-3p, which has not been reported previously.

In addition, I analyzed the role of miR142-3p signaling in non-hematopoietic 3T3 fibroblasts, which do not express miR142-3p endogenously. Here, the gain of function experiment using the application of a miR142-3p mimic caused a diminished Tet2 expression. In addition, increased Tet2 mRNA and protein levels of *in vitro* activated T cells isolated from miR142$^{-/-}$ compared to miR142 competent mice, provide compelling mechanistic evidence for direct targeting of Tet2 by miR142-3p.

Having established increased levels of miR142-3p and impaired Treg induction from naive CD4$^+$ T cells during the onset of islet autoimmunity, I next asked the question whether the upregulated miR142-3p interferes with Treg induction, thereby promoting autoimmune activation and progression. To integrate the role of miR142-3p activity with Treg induction and islet autoimmunity, I performed murine and human *in vitro* Treg induction experiments in presence of a miR142-3p mimic or inhibitor respectively. This is not only relevant for the identification of the underlying signaling pathways, but also to obtain information whether miRNA targeting could be a promising strategy to improve the impaired Treg induction in islet autoimmunity and thereby delay or even prevent the transition to symptomatic T1D in the context of future intervention strategies.

In both mice and humans, the onset of islet autoimmunity and T1D is accompanied by a reduced Treg induction capacity of naive CD4$^+$ T cells to be differentiated into Tregs *in vitro*. Critically, this effect was reproduced by *in vitro* Treg induction assays in the presence of a miR142-3p mimic, suggesting that the increased expression of miR142-3p indeed contributes to impaired Treg induction. Conversely, the inhibition of miR142-3p during *in vitro* Treg induction from naive CD4$^+$ T cells of individuals with and without islet autoimmunity or T1D

improved Treg induction efficacy. Importantly, in individuals or mice with ongoing islet autoimmunity or T1D, miR142-3p inhibition increased frequencies of induced Tregs to levels observed in healthy subjects, suggesting miR142-3p inhibition as a promising starting point for treatment approaches in settings of reduced Treg induction capacity.

Since miR142-3p targets the methylcytosine dioxygenase Tet2, which is involved in DNA demethylation of the Foxp3 CNS2 and consequently ensures stable expression of Foxp3 in Tregs, I wanted to investigate if the beneficial effect of miR142-3p inhibition on Treg induction *in vitro* was accompanied by increased Treg stability. Remarkably, the inhibition of miR142-3p during re-stimulation of induces Tregs resulted in a significantly higher maintenance of the Treg phenotype.

These findings provide compelling evidence for a miR142-3p/Tet2/Foxp3 axis as one possible mechanism to explain increased Treg induction efficacy and Treg stability *in vitro* upon miR142-3p inhibition. I showed rapid methylation dynamics during the early phase of Treg induction and a miR142-3p inhibition mediated increase in Tet2 in this time frame. This is in line with the crucial role of Tet2 for Treg induction (Nair and Oh, 2014; Wang et al., 2013; Yang et al., 2015b; Yue et al., 2016) and suggests that miR142-3p inhibition leads to improved epigenetic remodeling in this early phase of Treg induction. However, I could not show a direct effect of miR142-3p inhibition on Foxp3 CNS2 DNA methylation in the early phase of Treg induction. This is most likely a result of the *in vitro* Treg induction assay and specifically the very rapid molecular changes and the dynamics of more cells acquiring the Foxp3 phenotype while other cells already are becoming remethylated.

To address a potential pathological relevance by expanding these findings to *in vivo* models of T1D, I next analyzed the effect of miR142-3p *in vivo*.

For the inhibition of miR142-3p *in vivo* I used an LNA *in vivo* miRNA inhibitor which has been shown to accumulate in a broad range of tissues and to efficiently inhibit its targets in several independent studies. When delivered systemically LNA miRNA inhibitors distribute broadly into most tissues, including hematopoietic tissues such as lymph nodes, spleen and bone marrow (Cantafio et al., 2016; Straarup et al., 2010). In line with these studies, I provide clear experimental evidence for the delivery of functional miR142-3p inhibitors specifically to CD4^{+} T cells *in vivo* using a fluorescently-labeled miR142-3p inhibitor. Importantly, the successful delivery of the inhibitor to CD4^{+} T cells was confirmed in relevant draining lymph nodes

including liver-draining lymph nodes, mesenteric lymph nodes as well as pancreatic lymph nodes and directly in pancreas-residing CD4^{+} T cells. Moreover, I validated the efficiency of the delivered miR142-3p inhibitor in pancreatic tissue and local immune cells by showing increased expression of Tgfbr1, a well-established target of miR142-3p, in pancreatic T cells. These rigorous validation experiments clearly show that LNA miRNA inhibitors are an efficient tool for miRNA inhibition *in vivo* which does not result in any obvious side effects.

Importantly, the inhibition of miR142-3p in NOD mice with islet autoimmunity resembled the previously observations *in vitro* and in ex vivo T cell samples. In line with a miR142-3p/Tet2/Foxp3 axis, the inhibition of miR142-3p resulted in increased frequencies of Tet2^{+} T cells in pancreata of IAA[+] NOD mice as well as elevated Tet2 protein abundance in peripheral T cells and consequently decreased DNA methylation of the Foxp3 CNS2 in Tregs. In a next step I could show that these epigenetic alternations have a direct causative effect on Tregs in islet autoimmunity by demonstrating that inhibitor treated mice exhibit higher frequencies of Tregs in the pancreas. Intriguingly, these observed effects could be directly linked to the progression of islet autoimmunity in IAA[+] NOD mice *in vivo*. The *in vivo* inhibition of miR142-3p reduced murine islet autoimmunity and islet autoantibody levels while blood glucose and body mass were unaffected. These important findings show that miR142-3p modulation can directly reduce islet infiltration in a mouse model of T1D, suggesting miR142-3p as a promising target for intervention strategies aiming at delaying or preventing the onset of symptomatic T1D. Here, further experiments are required to investigate if miR142-3p inhibition can indeed interfere with autoimmune progression to symptomatic T1D. Additionally, potential treatment strategies necessitate the development of improved targeted application strategies. In particular, the optimization of both specificity and efficiency is crucial to facilitate the translation of mechanistic findings into therapeutic approaches to delay or even prevent the onset of autoimmunity.

Although mouse models, like the NOD mouse in the setting of T1D, are valuable tools for the investigation of mechanisms underlying disease development and the development of intervention strategies, the challenging translatability from these mouse models to the human disease remain a limiting factor. Therefore, humanized mouse models are a useful intermediate step to assess the translatability of findings gained in the mouse system. Especially the reconstitution of humanized mice with cells from subjects with different stages of islet autoimmunity makes it possible to study the effect of newly developed treatment strategies in a setting resembling human islet autoimmunity and T1D. Ideally humanized mice are reconstituted with human hematopoietic stem cells, but their availability is very limited in the peripheral blood. The reconstitution with PBMCs is not suitable for long term studies because of profound graft versus host disease but it is a useful alternative to hematopoietic stem cells in short term studies (King et al., 2008). Here, I reconstituted MHCII deficient HLA-DQ8 transgenic NSG mice with PBMCs from individuals with established T1D to expand the findings from the NOD model to a model of the human disease. Intriguingly, the inhibition of miR142-3p in this pilot experiment resulted in increased levels of Tet2 in pancreatic T cells and a trend towards elevated Treg frequencies, suggesting that miR142-3p inhibition might have a beneficial effect in improving Treg homeostasis even in the context of established human T1D. Future studies including dose-titration and variations in application duration will be necessary to validate these findings in Tregs in the experimental setting of established T1D.

Although I was able to show a direct link between miR142-3p, Tet2 and epigenetic remodeling of the Foxp3 CNS2 in Tregs and the inhibition of miR142-3p had a considerable impact on Tet2 expression, Treg function and even autoimmunity, it is important to note that miR142-3p targets a multitude of genes, potentially impacting their expression and various downstream pathways. Interestingly the analysis of the HITS CLIP dataset and in silico target prediction revealed multiple target genes of miR142-3p that might be involved in Treg development and function. Specifically, Stat5, Smad3 and TGFB receptors (TGFBR1, TGFBR2 and TGFBR3) were identified and as for Tet2, the direct targeting of these genes by miR142-3p was further validated by showing elevated mRNA expression levels after 6 hours of TCR stimulation in presence of a miR142-3p inhibitor compared to a control inhibitor. Stat5 has been shown as a downstream target of IL2 involved in Treg development (Mahmud et al., 2013). CD4^{+} T cells receiving a high affinity TCR signal express IL2Rα and IL2Rβ which makes them highly

responsive to IL2. In a second, TCR independent step these Treg progenitors receive IL2 signals which are transmitted via Stat5 to induce Foxp3 expression, resulting in Treg maturation. TGFβ has been shown to exhibit potent immunoregulatory properties, among others by inducing the expression of Foxp3 in Tregs (Konkel et al., 2017). TGFB binds to TGFBR which activates several transcriptions factors, including Smad proteins. These are phosphorylated and activated which results in their translocation to the nucleus where they regulate the transcription of their target genes like Foxp3. Both signaling pathways add to the identified mechanism of Tet2-mediated DNA demethylation to ensure Foxp3 expression and maintenance and consequently proper Treg function and stability. These findings suggest that a regulatory network of genes involved in the regulation of Treg function and stability is targeted by miR142-3p. This contributes to our understanding why the targeting of a single miRNA has a profound effect on Treg function and stability in a highly complex context like T1D autoimmunity. Furthermore, the discovery of a complex signaling network downstream of miR142-3p offers additional potential targets for therapeutic interventions.

In addition, Tet2, the validated target of miR142-3p, has been shown to be involved in the regulation of several cellular processes by catalyzing the demethylation of regulatory regions of various genes. In the present project I focused on the role of Tet2 mediated demethylation of the Foxp3 CNS2 for Treg function and stability in the context of autoimmunity. However, additional regulatory regions might be controlled by Tet2 and contribute to the regulation of Foxp3. Therefore, I performed Tet2 ChIP Sequencing in CD4^{+} T cells to identifying gene regions bound by Tet2. In addition to Foxp3, which has been described as a target of Tet protein mediated demethylation in several studies, the ChIP Sequencing revealed Tet2 binding of multiple genes in human and murine T cells. One interesting candidate was Bach2, where the analysis identified four Tet2 binding peaks upstream of the transcriptional start site. Bach2 is involved in the development of Tregs by inducing the expression of Foxp3. Specifically, by occupying enhancer regions of genes associated with effector T cell function, Bach2 represses the transcriptional program of this cell subset and consequently supports the maintenance of the Treg phenotype. Methylation analysis of the regions potentially targeted by Tet2 revealed differential methylation of the CpG sites in one of these regions in T cells subsets (32,422,750 – 32,422,924). This region is highly demethylated in naive CD4^{+} T cells (5.4%) as well as Foxp3^{+} Tregs (4.1%), whereas the methylation is considerably higher in activated T cells (18.7%).

These first results are in line with previously reported Bach2 expression levels in T cell subsets. Naive T cells as well Tregs express high levels of Bach2 (Tsukumo et al., 2013) to maintain their cell specific transcriptional program and prevent the expression of effector function genes (Kim et al., 2014; Roychoudhuri et al., 2013; Tsukumo et al., 2013). This suggests that a Tet2 mediated DNA demethylation in this region of the Bach2 gene is associated with high expression levels of the gene, and that the epigenetic regulation of this putative enhancer region could contribute to proper Treg induction and maintenance. This provides another line of evidence that miR142-3p/Tet2 signaling is involved in the regulation of Treg induction and stability which supports the important role of this pathway for immune homeostasis.

The importance of miRNAs for the precise regulation of immune homeostasis and how their dysregulation can contribute to various diseases including autoimmunity and T1D has been highlighted in numerous studies. Regarding the potential clinical application for novel prevention or treatment strategies the well-known and relatively simple structure of miRNAs makes them promising potential drug targets. Due to their structure miRNAs can be efficiently targeted using highly specific inhibitors or mimics. Therefore, the activity of miRNAs can be easily blocked or increased, enabling a precise interference in the regulation of the respective target genes. In this context it is important to keep in mind that miRNAs target a multitude of genes, hindering the direct and precise control of individual genes. However, it is most likely that these complex regulatory networks are involved in diseases pathogenesis, supporting the concept of miRNAs as promising drug targets. In the setting of autoimmunity and T1D miRNA-targeting strategies have been successfully used in various settings including *in vitro*, mouse models of T1D and humanized mice, resulting in an increased expression of the respective miRNA targets, improved Treg function and decreased immune infiltration in the pancreas (Serr et al., 2016a, 2018). Furthermore, a specific miRNA inhibitor has already been successfully tested in a clinical trial to treat hepatitis C virus infection (Janssen et al., 2013). To ensure both efficacy and safety of miRNA-targeting drugs, these approaches require the selective and targeted delivery of miRNA inhibitors to the desired cell population. This is of particular importance for the treatment of organ-specific autoimmune diseases such as T1D but also for other diseases setting which require a precise and local intervention in affected cell types, which remains a major challenge (Li and Rana, 2014). However, considerable advancements have been made to improve both, the uptake of miRNA inhibitors by immune

cells and the targeted delivery of these inhibitors. The use of nanoparticles and oligonucleotide encapsulation techniques improved uptake by lymphocytes and combinations of antibodies and nanoparticles or single chain fusion antibodies, which already have T cell specific delivery of miRNA inhibitors in mouse models, could improve the specific targeting of T cells or even T cell subsets (Kumar et al., 2008; Peer et al., 2008). However, the T cell specific targeting of miRNAs *in vivo* for therapeutic strategies remains challenging and additional hurdles have to be overcome. To overcome these limitations, the optimization of both delivery efficiency and specificity is of particular importance and will enable the translation of mechanistic insights into novel treatment and prevention strategies in the context of islet autoimmunity.

In line with the data presented in this thesis, several recent studies reported a direct link between the high abundance of two specific miRNAs in T cells and impairments in Treg induction during the onset of islet autoimmunity (Serr et al., 2016a, 2018). Importantly, even the targeting of individual miRNAs resulted in considerable changes in gene expression, effects on the downstream signaling pathways of these genes and improved islet autoimmunity in mouse models. Therefore, the targeting of individual miRNAs or a combination of several miRNAs with improved, highly specific and efficient delivery techniques, could contribute to the reestablishment of immune homeostasis and ultimately interfere with the onset of islet autoimmunity. The development and validation of future treatment approaches will require optimized humanized mouse models to mimic the mechanisms underlying human autoimmune diseases in a preclinical model. These models are valuable tools to underpin findings based on both murine and human studies and to considerably advance the field towards novel translational treatment strategies based on specific miRNA targeting.

In conclusion, I identified a miR142-3p/Tet2/Foxp3 axis in murine and human CD4$^+$ T cells that during islet autoimmunity leads to impaired epigenetic remodeling and consequently interferes with the efficient induction of Tregs and impaired Treg stability. These results offer a new mechanistic model where during islet-autoimmunity miR142-3p/Tet2-mediated Treg instability can contribute to autoimmune activation and progression and suggest that targeting miR142-3p could contribute to the development of novel intervention strategies, aiming at improved Treg induction and stability to interfere with islet autoimmunity.

6 References

Achenbach, P., Lampasona, V., Landherr, U., Koczwara, K., Krause, S., Grallert, H., Winkler, C., Pflüger, M., Illig, T., Bonifacio, E., et al. (2009). Autoantibodies to zinc transporter 8 and SLC30A8 genotype stratify type 1 diabetes risk. Diabetologia *52*, 1881–1888.

Agarwal, V., Bell, G.W., Nam, J., and Bartel, D.P. (2015). Predicting effective microRNA target sites in mammalian mRNAs. 1–38.

Åkerman, L., Casas, R., Ludvigsson, J., Tavira, B., and Skoglund, C. (2018). Serum miRNA levels are related to glucose homeostasis and islet autoantibodies in children with high risk for type 1 diabetes. PLoS One *13*.

Alleva, D.G., Crowe, P.D., Jin, L., Kwok, W.W., Ling, N., Gottschalk, M., Conlon, P.J., Gottlieb, P.A., Putnam, A.L., and Gaur, A. (2001). A disease-associated cellular immune response in type 1 diabetics to an immunodominant epitope of insulin. J. Clin. Invest. *107*, 173–180.

Anders, S., Pyl, P.T., and Huber, W. (2015). HTSeq-A Python framework to work with high-throughput sequencing data. Bioinformatics *31*, 166–169.

Arif, S., Moore, F., Marks, K., Bouckenooghe, T., Dayan, C.M., Planas, R., Vives-Pi, M., Powrie, J., Tree, T., Marchetti, P., et al. (2011). Peripheral and islet interleukin-17 pathway activation characterizes human autoimmune diabetes and promotes cytokine-mediated β-cell death. Diabetes *60*, 2112–2119.

Asseman, C., Mauze, S., Leach, M.W., Coffman, R.L., and Powrie, F. (1999). An essential role for interleukin 10 in the function of regulatory T cells that inhibit intestinal inflammation. J. Exp. Med. *190*, 995–1003.

Assmann, T.S., Recamonde-Mendoza, M., De Souza, B.M., and Crispim, D. (2017). MicroRNA expression profiles and type 1 diabetes mellitus: systematic review and bioinformatic analysis. Endocr. Connect. *6*, 773–790.

Baekkeskov, S., Aanstoot, H.J., Christgai, S., Reetz, A., Solimena, M., Cascalho, M., Folli, F., Richter-Olesen, H., and Camilli, P. De (1990). Identification of the 64K autoantigen in insulin-dependent diabetes as the GABA-synthesizing enzyme glutamic acid decarboxylase. Nature *347*, 151–156.

Bandukwala, H.S., Wu, Y., Feuerer, M., Chen, Y., Barboza, B., Ghosh, S., Stroud, J.C., Benoist, C., Mathis, D., Rao, A., et al. (2011). Article Structure of a Domain-Swapped FOXP3 Dimer on DNA and Its Function in Regulatory T Cells. *3*, 479–491.

Baron, U., Floess, S., Wieczorek, G., Baumann, K., Grützkau, A., Dong, J., Thiel, A., Boeld, T.J., Hoffmann, P., Edinger, M., et al. (2007). DNA demethylation in the human FOXP3 locus discriminates regulatory T cells from activated FOXP3 + conventional T cells. 2378–2389.

Bartel, D.P. (2004). MicroRNAs: Genomics, Biogenesis, Mechanism, and Function. Cell *116*, 281–297.

Bennett, C.L., Christie, J., Ramsdell, F., Brunkow, M.E., Ferguson, P.J., Whitesell, L., Kelly, T.E., Saulsbury, F.T., Chance, P.F., and Ochs, H.D. (2001). The immune dysregulation, polyendocrinopathy, enteropathy, X-linked syndrome (IPEX) is caused by mutations of FOXP3. Nat. Genet. *27*, 20–21.

Berezikov, E. (2011). Evolution of microRNA diversity and regulation in animals. Nat. Rev. Genet. *12*, 846–860.

Betel, D., Koppal, A., Agius, P., Sander, C., and Leslie, C. (2010). Comprehensive modeling of microRNA targets predicts functional non-conserved and non-canonical sites.

Bluestone, J.A., and Tang, Q. (2005). How do CD4+CD25+ regulatory T cells control autoimmunity? Curr. Opin. Immunol. *17*, 638–642.

Bluestone, J.A., Herold, K., and Eisenbarth, G. (2010). Genetics, pathogenesis and clinical interventions in type 1 diabetes. Nature *464*, 1293–1300.

von Boehmer, H., and Daniel, C. (2013). Therapeutic opportunities for manipulating T(Reg) cells in autoimmunity and cancer. Nat. Rev. Drug Discov. *12*, 51–63.

Bonifacio, E., Hummel, M., Walter, M., Schmid, S., and Ziegler, A.G. (2004). IDDM1 and multiple family history of type 1 diabetes combine to identify neonates at high risk for type 1 diabetes. Diabetes Care *27*, 2695–2700.

Breitfeld, D., Ohl, L., Kremmer, E., Ellwart, J., Sallusto, F., Lipp, M., and Förster, R. (2000). Follicular B helper T cells express CXC chemokine receptor 5, localize to B cell follicles, and support immunoglobulin production. J. Exp. Med. *192*, 1545–1552.

Briggs, S.F., and Reijo Pera, R.A. (2014). X chromosome inactivation: Recent advances and a look forward. Curr. Opin. Genet. Dev. *28*, 78–82.

Burchill, M.A., Yang, J., Vogtenhuber, C., Blazar, B.R., Farrar, M.A., Burchill, M.A., Yang, J., Vogtenhuber, C., Blazar, B.R., and Farrar, M.A. (2007). IL‑2 receptor β-dependent STAT5 activation is required for the development of Foxp3+ regulatory T cells. J. Immunol. *178*, 280–290.

Burnet, F.M. (1959). The clonal selection theory of acquired immunity. (Nashville: Vanderbilt University Press).

Cantafio, M.E.G., Nielsen, B.S., Mignogna, C., Arbitrio, M., Botta, C., Frandsen, N.M., Rolfo, C., Tagliaferri, P., Tassone, P., and Di Martino, M.T. (2016). Pharmacokinetics and pharmacodynamics of a 13-mer LNA-inhibitor-miR-221 in mice and non-human primates. Mol. Ther. - Nucleic Acids *5*.

Chao, K., Zhang, S., Yao, J., He, Y., Chen, B., Zeng, Z., Zhong, B., and Chen, M. (2014). Imbalances of CD4+ T-cell subgroups in Crohn's disease and their relationship with disease activity and prognosis. J. Gastroenterol. Hepatol. *29*, 1808–1814.

Chapnik, E., Rivkin, N., Mildner, A., Beck, G., Pasvolsky, R., Metzl-Raz, E., Birger, Y., Amir, G., Tirosh, I., Porat, Z., et al. (2014). MiR-142 orchestrates a network of actin cytoskeleton regulators during megakaryopoiesis. Elife *2014*.

Chen, C.Z., Li, L., Lodish, H.F., and Bartel, D.P. (2004). MicroRNAs Modulate Hematopoietic Lineage Differentiation. Science (80-.). *303*, 83–86.

Chi, S.W., Zang, J.B., Mele, A., and Darnell, R.B. (2009). Argonaute HITS-CLIP decodes microRNA–mRNA interaction maps. Nature *460*, 479–486.

Chi, S.W., Hannon, G.J., and Darnell, R.B. (2012). An alternative mode of microRNA target recognition. Nat. Struct. Mol. Biol. *19*, 321–327.

Cho, S., Wu, C.-J., Yasuda, T., Cruz, L.O., Khan, A.A., Lin, L.-L., Nguyen, D.T., Miller, M., Lee, H.-M., Kuo, M.-L., et al. (2016). miR-23 approximately 27 approximately 24 clusters control effector T cell differentiation and function. J. Exp. Med. *213*, 235–249.

Chong, M.M.W., Rasmussen, J.P., Rudensky, A.Y., and Littman, D.R. (2008). The RNAseIII enzyme Drosha is critical in T cells for preventing lethal inflammatory disease. J. Exp. Med. *205*, 2449–2449.

Cobb, B., Hertweck, A., Smith, J., O'Connor, E., Graf, D., Cook, T., Smale, S., Sakaguchi, S., Livesey, F., Fisher, A., et al. (2006). A role for Dicer in immune regulation. J. Exp. Med. *203*, 2519–2527.

Cope, A.P., Schulze-Koops, H., and Aringer, M. (2007). The central role of T cells in rheumatoid arthritis. Clin. Exp. Rheumatol. *25*.

Covassin, L., Jangalwe, S., Jouvet, N., Laning, J., Burzenski, L., Shultz, L.D., and Brehm, M.A. (2013). Human immune system development and survival of non-obese diabetic (NOD)-scid IL2rγ null (NSG) mice engrafted with human thymus and autologous haematopoietic stem cells. Clin. Exp. Immunol. *174*, 372–388.

Crawford, F., Stadinski, B., Jin, N., Michels, A., Nakayama, M., Pratt, P., Marrack, P., Eisenbarth, G., and Kappler, J.W. (2011). Specificity and detection of insulin-reactive CD4 +T cells in type 1 diabetes in the nonobese diabetic (NOD) mouse. Proc. Natl. Acad. Sci. U. S. A. *108*, 16729–16734.

Dang, M.N., Buzzetti, R., and Pozzilli, P. (2013). Epigenetics in autoimmune diseases with focus on type 1 diabetes. Diabetes. Metab. Res. Rev. *29*, 8–18.

Daniel, C., and von Boehmer, H. (2011). Extrathymic Generation of Regulatory T Cells-Chances and Challenges for Prevention of Autoimmune Disease (Elsevier Inc.).

Daniel, C., Wennhold, K., Kim, H.-J., and von Boehmer, H. (2010). Enhancement of antigen-specific Treg vaccination *in vivo*. Proc. Natl. Acad. Sci. U. S. A. *107*, 16246–16251.

Daniel, C., Weigmann, B., Bronson, R., and von Boehmer, H. (2011a). Prevention of type 1 diabetes in mice by tolerogenic vaccination with a strong agonist insulin mimetope. J. Exp. Med. *208*, 1501–1510.

Daniel, C., Weigmann, B., Bronson, R., and von Boehmer, H. (2011b). Prevention of type 1 diabetes in mice by tolerogenic vaccination with a strong agonist insulin mimetope. J. Exp. Med. *208*, 1501–1510.

Daniel, D., Gill, R.G., Schloot, N., and Wegmann, D. (1995). Epitope specificity, cytokine production profile and diabetogenic activity of insulin-specific T cell clones isolated from NOD mice. Eur. J. Immunol. *25*, 1056–1062.

Deaglio, S., Dwyer, K.M., Gao, W., Friedman, D., Usheva, A., Erat, A., Chen, J.F., Enjyoji, K., Linden, J., Oukka, M., et al. (2007). Adenosine generation catalyzed by CD39 and CD73 expressed on regulatory T cells mediates immune suppression. J. Exp. Med. *204*, 1257–1265.

Delgoffe, G.M., Woo, S.R., Turnis, M.E., Gravano, D.M., Guy, C., Overacre, A.E., Bettini, M.L., Vogel, P., Finkelstein, D., Bonnevier, J., et al. (2013). Stability and function of regulatory T cells is maintained by a neuropilin-1-semaphorin-4a axis. Nature *501*, 252–256.

Denli, A.M., Tops, B.B.J., Plasterk, R.H.A., Ketting, R.F., and Hannon, G.J. (2004). Processing of primary microRNAs by the Microprocessor complex. Nature *432*, 231–235.

Didiano, D., and Hobert, O. (2006). Perfect seed pairing is not a generally reliable predictor for miRNA-target interactions. Nat. Struct. Mol. Biol. *13*, 849–851.

Dittel, B.N. (2008). CD4 T cells: Balancing the coming and going of autoimmune-mediated inflammation in the CNS. Brain. Behav. Immun. *22*, 421–430.

Doi, A., Park, I.H., Wen, B., Murakami, P., Aryee, M.J., Irizarry, R., Herb, B., Ladd-Acosta, C., Rho, J., Loewer, S., et al. (2009). Differential methylation of tissue-and cancer-specific CpG island shores distinguishes human induced pluripotent stem cells, embryonic stem cells and fibroblasts. Nat. Genet. *41*, 1350–1353.

Egger, G., Jeong, S., Escobar, S.G., Cortez, C.C., Li, T.W.H., Saito, Y., Yoo, C.B., Jones, P.A., and Liang, G. (2006). Identification of DNMT1 (DNA methyltransferase 1) hypomorphs in somatic knockouts suggests an essential role for DNMT1 in cell survival. Proc. Natl. Acad. Sci. U. S. A. *103*, 14080–14085.

Ehrlich, P., Bolduan, C., and Howard (1907). Collected Studies on Immunity. J. Nerv. Ment. Dis. *34*, 549.

Emery, L.M., Babu, S., Bugawan, T.L., Norris, J.M., Erlich, H.A., Eisenbarth, G.S., and Rewers, M. (2005). Newborn HLA-DR,DQ genotype screening: Age- and ethnicity-specific type 1 diabetes risk estimates. Pediatr. Diabetes *6*, 136–144.

Espada, J., Ballestar, E., Santoro, R., Fraga, M.F., Villar-Garea, A., Németh, A., Lopez-Serra, L., Ropero, S., Aranda, A., Orozco, H., et al. (2007). Epigenetic disruption of ribosomal RNA genes and nucleolar architecture in DNA methyltransferase 1 (Dnmt1) deficient cells. Nucleic Acids Res. *35*, 2191–2198.

Esteller, M. (2007). Epigenetic gene silencing in cancer: The DNA hypermethylome. Hum. Mol. Genet. *16*.

Esteller, M. (2008). Epigenetics in evolution and disease. Lancet *372*, S90–S96.

Fahlén, L., Read, S., Gorelik, L., Hurst, S.D., Coffman, R.L., Flavell, R.A., and Powrie, F. (2005). T cells that cannot respond to TGF-β escape control by CD4+ CD25+ regulatory T cells. J. Exp. Med. *201*, 737–746.

Feng, S., Jacobsen, S.E., and Reik, W. (2010). Epigenetic reprogramming in plant and animal development. Science (80-.). *330*, 622–627.

Feng, Y., Arvey, A., Chinen, T., van der Veeken, J., Gasteiger, G., and Rudensky, A.Y. (2014). Control of the inheritance of regulatory T cell identity by a cis element in the Foxp3 locus. Cell *158*, 749–763.

Ferraro, A., Socci, C., Stabilini, A., Valle, A., Monti, P., Piemonti, L., Nano, R., Olek, S., Maffi, P., Scavini, M., et al. (2011). Expansion of Th17 cells and functional defects in T regulatory cells are key features of the pancreatic lymph nodes in patients with type 1 diabetes. Diabetes *60*, 2903–2913.

Ferreira, R.C., Simons, H.Z., Thompson, W.S., Cutler, A.J., Dopico, X.C., Smyth, D.J., Mashar, M., Schuilenburg, H., Walker, N.M., Dunger, D.B., et al. (2015). IL-21 production by CD4+ effector T cells and frequency of circulating follicular helper T cells are increased in type 1 diabetes patients. Diabetologia *58*, 781–790.

Floess, S., Freyer, J., Siewert, C., Baron, U., Olek, S., Polansky, J., Schlawe, K., Chang, H.-D., Bopp, T., Schmitt, E., et al. (2007). Epigenetic control of the foxp3 locus in regulatory T cells. PLoS Biol. *5*, e38.

Fontenot, J.D., Gavin, M.A., and Rudensky, A.Y. (2003). Foxp3 programs the development and function of CD4+CD25+ regulatory T cells. Nat.Immunol. *4*, 330–336.

Foulis, A.K., Liddle, C.N., Farquharson, M.A., Richmond, J.A., and Weir, R.S. (1986). The histopathology of the pancreas in Type I (insulin-dependent) diabetes mellitus: a 25-year review of deaths in patients under 20 years of age in the United Kingdom. Diabetologia *29*, 267–274.

Friedman, R.C., Farh, K.K.H., Burge, C.B., and Bartel, D.P. (2009). Most mammalian mRNAs are conserved targets of microRNAs. Genome Res. *19*, 92–105.

Garçon, F., Patton, D.T., Emery, J.L., Hirsch, E., Rottapel, R., Sasaki, T., and Okkenhaug, K. (2008). CD28 provides T-cell costimulation and enhances PI3K activity at the immune synapse independently of its capacity to interact with the p85/p110 heterodimer. Blood *111*, 1464–1471.

Generali, E., Ceribelli, A., Stazi, M.A., and Selmi, C. (2017). Lessons learned from twins in autoimmune and chronic inflammatory diseases. J. Autoimmun. *83*, 51–61.

Gershon, R.K., and Kondo, K. (1970). Cell interactions in the induction of tolerance: the role of thymic lymphocytes. Immunology *18*, 723–737.

Girardot, M., Feil, R., and Llères, D. (2013). Epigenetic deregulation of genomic imprinting in humans: Causal mechanisms and clinical implications. Epigenomics *5*, 715–728.

Gottschalk, R.A., Corse, E., and Allison, J.P. (2010). TCR ligand density and affinity determine peripheral induction of Foxp3 *in vivo*. J. Exp. Med. *207*, 1701–1711.

Green, D.R., Flood, P.M., and Gershon, R.K. (1983). Immunoregulatory T-Cell Pathways. Annu. Rev. Immunol. *1*, 439–461.

Green, E.A., Gorelik, L., McGregor, C.M., Tran, E.H., and Flavell, R.A. (2003). CD4+CD25+ T regulatory cells control anti-islet CD8+ T cells through TGF-β-TGF-β receptor interactions in type 1 diabetes. Proc. Natl. Acad. Sci. U. S. A. *100*, 10878–10883.

Gregory, R.I., Yan, K.P., Amuthan, G., Chendrimada, T., Doratotaj, B., Cooch, N., and Shiekhattar, R. (2004). The Microprocessor complex mediates the genesis of microRNAs. Nature *432*, 235–240.

Grimson, A., Farh, K.K.H., Johnston, W.K., Garrett-Engele, P., Lim, L.P., and Bartel, D.P. (2007). MicroRNA Targeting Specificity in Mammals: Determinants beyond Seed Pairing. Mol. Cell *27*, 91–105.

Grossman, W.J., Verbsky, J.W., Tollefsen, B.L., Kemper, C., Atkinson, J.P., and Ley, T.J. (2004). Differential expression of granzymes A and B in human cytotoxic lymphocyte subsets and T regulatory cells. Blood *104*, 2840–2848.

Ha, M., and Kim, V.N. (2014). Regulation of microRNA biogenesis. Nat. Rev. Mol. Cell Biol. *15*, 509–524.

Hattori, M., Buse, J.B., Jackson, R.A., Glimcher, L., Dorf, M.E., Minami, M., Makino, S., Moriwaki, K., Kuzuya, H., Imura, H., et al. (1986). The NOD mouse: Recessive diabetogenic gene in the major histocompatibility complex. Science (80-.). *231*, 733–735.

He, Y.-F., Li, B.-Z., Li, Z., Liu, P., Wang, Y., Tang, Q., Ding, J., Jia, Y., Chen, Z., Li, L., et al. (2011). Tet-mediated formation of 5-carboxylcytosine and its excision by TDG in mammalian DNA. Science *333*, 1303–1307.

Hemminki, K., Li, X., Sundquist, J., and Sundquist, K. (2009). Familial association between type 1 diabetes and other autoimmune and related diseases. Diabetologia *52*, 1820–1828.

Heninger, A.K., Eugster, A., Kuehn, D., Buettner, F., Kuhn, M., Lindner, A., Dietz, S., Jergens, S., Wilhelm, C., Beyerlein, A., et al. (2017). A divergent population of autoantigen-responsive CD4+ T cells in infants prior to b cell autoimmunity. Sci. Transl. Med. *9*.

Hill, J.A., Feuerer, M., Tash, K., Haxhinasto, S., Perez, J., Melamed, R., Mathis, D., and Benoist, C. (2007). Foxp3 transcription-factor-dependent and -independent regulation of the regulatory T cell transcriptional signature. Immunity *27*, 786–800.

Horike, S.I., Cai, S., Miyano, M., Cheng, J.F., and Kohwi-Shigematsu, T. (2005). Loss of silent-chromatin looping and impaired imprinting of DLX5 in Rett syndrome. Nat. Genet. *37*, 31–40.

Huehn, J., and Beyer, M. (2015). Epigenetic and transcriptional control of Foxp3(+) regulatory T cells. Semin. Immunol. *27*, 10–18.

Huehn, J., Polansky, J.K., and Hamann, A. (2009). Epigenetic control of FOXP3 expression: the key to a stable regulatory T-cell lineage? Nat. Rev. Immunol. *9*, 83–89.

Hutvágner, G., McLachlan, J., Pasquinelli, A.E., Bálint, É., Tuschl, T., and Zamore, P.D. (2001). A cellular function for the RNA-interference enzyme dicer in the maturation of the let-7 small temporal RNA. Science (80-.). *293*, 834–838.

Ichikawa, S., Fukuhara, N., Katsushima, H., Takahashi, T., Yamamoto, J., Yokoyama, H., Sasaki, O., Fukuhara, O., Nomura, J., Ishizawa, K., et al. (2014). Association between BACH2 expression and clinical prognosis in diffuse large B-cell lymphoma. Cancer Sci. *105*, 437–444.

Im, H.I., and Kenny, P.J. (2012). MicroRNAs in neuronal function and dysfunction. Trends Neurosci. *35*, 325–334.

Insel, R.A., Dunne, J.L., Atkinson, M.A., Chiang, J.L., Dabelea, D., Gottlieb, P.A., Greenbaum, C.J., Herold, K.C., Krischer, J.P., Lernmark, A., et al. (2015). Staging presymptomatic type 1 diabetes: A scientific statement of jdrf, the endocrine society, and the American diabetes association. Diabetes Care *38*, 1964–1974.

Irizarry, R.A., Ladd-Acosta, C., Wen, B., Wu, Z., Montano, C., Onyango, P., Cui, H., Gabo, K., Rongione, M., Webster, M., et al. (2009). The human colon cancer methylome shows similar hypo- and hypermethylation at conserved tissue-specific CpG island shores. Nat. Genet. *41*, 178–186.

Ito, S., Shen, L., Dai, Q., Wu, S.C., Collins, L.B., Swenberg, J.A., He, C., and Zhang, Y. (2011). Tet Proteins Can Convert 5-Methylcytosine to 5-Formylcytosine and 5-Carboxylcytosine. Science (80-.). *333*, 1300–1303.

Iyer, L.M., Tahiliani, M., Rao, A., and Aravind, L. (2009). Prediction of novel families of enzymes involved in oxidative and other complex modifications of bases in nucleic acids. Cell Cycle *8*, 1698–1710.

Jaeckel, E., Lipes, M.A., and Von Boehmer, H. (2004). Recessive tolerance to preproinsulin 2 reduces but does not abolish type 1 diabetes. Nat. Immunol. *5*, 1028–1035.

Janssen, H.L.A., Reesink, H.W., Lawitz, E.J., Zeuzem, S., Rodriguez-Torres, M., Patel, K., Van Der Meer, A.J., Patick, A.K., Chen, A., Zhou, Y., et al. (2013). Treatment of HCV infection by targeting microRNA. N. Engl. J. Med. *368*, 1685–1694.

Javierre, B.M., Esteller, M., and Ballestar, E. (2008). Epigenetic connections between autoimmune disorders and haematological malignancies. Trends Immunol. *29*, 616–623.

Javierre, B.M., Fernandez, A.F., Richter, J., Al-Shahrour, F., Ignacio Martin-Subero, J., Rodriguez-Ubreva, J., Berdasco, M., Fraga, M.F., O'Hanlon, T.P., Rider, L.G., et al. (2010). Changes in the pattern of DNA methylation associate with twin discordance in systemic lupus erythematosus. Genome Res. *20*, 170–179.

Jeker, L.T., Zhou, X., Gershberg, K., de Kouchkovsky, D., Morar, M.M., Stadthagen, G., Lund, A.H., and Bluestone, J.A. (2012). MicroRNA 10a marks regulatory T cells. PLoS One *7*, 1–8.

Jerram, S.T., Dang, M.N., and Leslie, R.D. (2017). The Role of Epigenetics in Type 1 Diabetes. Curr. Diab. Rep. *17*.

Jiang, S., Li, C., Olive, V., Lykken, E., Feng, F., Sevilla, J., Wan, Y., He, L., and Li, Q.J. (2011). Molecular dissection of the miR-17-92 cluster's critical dual roles in promoting Th1 responses and preventing inducible Treg differentiation. Blood *118*, 5487–5497.

Josefowicz, S.Z., Wilson, C.B., and Rudensky, A.Y. (2009). Cutting edge: TCR stimulation is sufficient for induction of Foxp3 expression in the absence of DNA methyltransferase 1. J. Immunol. *182*, 6648–6652.

Josefowicz, S.Z., Lu, L.-F., and Rudensky, A.Y. (2012). Regulatory T cells: mechanisms of differentiation and function. Annu. Rev. Immunol. *30*, 531–564.

Kameswaran, V., Bramswig, N.C., McKenna, L.B., Penn, M., Schug, J., Hand, N.J., Chen, Y., Choi, I., Vourekas, A., Won, K.J., et al. (2014). Epigenetic regulation of the DLK1-MEG3 MicroRNA cluster in human type 2 diabetic islets. Cell Metab. *19*, 135–145.

Kenefeck, R., Wang, C.J., Kapadi, T., Wardzinski, L., Attridge, K., Clough, L.E., Heuts, F., Kogimtzis, A., Patel, S., Rosenthal, M., et al. (2015). Follicular helper T cell signature in type 1 diabetes. J. Clin. Invest. *125*, 292–303.

Khattri, R., Cox, T., Yasayko, S.A., and Ramsdell, F. (2003). An essential role for Scurfin in CD4+CD25+ T regulatory cells. Nat.Immunol. *4*, 337–342.

Kim, H.-P., and Leonard, W.J. (2007). CREB/ATF-dependent T cell receptor-induced FoxP3 gene expression: a role for DNA methylation. J. Exp. Med. *204*, 1543–1551.

Kim, E.H., Gasper, D.J., Lee, S.H., Plisch, E.H., Svaren, J., and Suresh, M. (2014). Bach2 Regulates Homeostasis of Foxp3+ Regulatory T Cells and Protects against Fatal Lung Disease in Mice. J. Immunol. *192*, 985–995.

Kim, J.M., Rasmussen, J.P., and Rudensky, A.Y. (2007). Regulatory T cells prevent catastrophic autoimmunity throughout the lifespan of mice. *8*, 191–197.

King, M., Pearson, T., Shultz, L.D., Leif, J., Bottino, R., Trucco, M., Atkinson, M.A., Wasserfall, C., Herold, K.C., Woodland, R.T., et al. (2008). A new Hu-PBL model for the study of human islet alloreactivity based on NOD-scid mice bearing a targeted mutation in the IL-2 receptor gamma chain gene. Clin. Immunol. *126*, 303–314.

Ko, M., Bandukwala, H.S., An, J., Lamperti, E.D., Thompson, E.C., and Hastie, R. (2011). Homeostasis and Differentiation of Hematopoietic Stem Cells in Mice. Pnas *2*.

Kohlhaas, S., Garden, O.A., Okkenhaug, K., Vigorito, E., Turner, M., and Scudamore, C. (2009). Cutting Edge: The Foxp3 Target miR-155 Contributes to the Development of Regulatory T Cells. J. Immunol. *182*, 2578–2582.

Kong, Y. (2011). Btrim: A fast, lightweight adapter and quality trimming program for next-generation sequencing technologies. Genomics *98*, 152–153.

Konkel, J.E., Zhang, D., Zanvit, P., Chia, C., Zangarle-Murray, T., Jin, W., Wang, S., and Chen, W.J. (2017). Transforming Growth Factor-β Signaling in Regulatory T Cells Controls T Helper-17 Cells and Tissue-Specific Immune Responses. Immunity *46*, 660–674.

Kozomara, A., and Griffiths-Jones, S. (2014). MiRBase: Annotating high confidence microRNAs using deep sequencing data. Nucleic Acids Res. *42*, 68–73.

Kretschmer, K., Apostolou, I., Hawiger, D., Khazaie, K., Nussenzweig, M.C., and von Boehmer, H. (2005). Inducing and expanding regulatory T cell populations by foreign antigen. Nat.Immunol. *6*, 1219–1227.

Kronenberg, M., Steinmetz, M., Kobori, J., Kraig, E., Kapp, J.A., Pierce, C.W., Sorensen, C.M., Suzuki, G., Tada, T., and Hood, L. (1983). RNA transcripts for I-J polypeptides are apparently not encoded between the I-A and I-E subregions of the murine major histocompatibility complex. Proc. Natl. Acad. Sci. U. S. A. *80*, 5704–5708.

Kumar, M.N.V.R., Muzzarelli, R.A.A., Muzzarelli, C., Sashiwa, H., and Domb, A.J. (2004). Chitosan chemistry and pharmaceutical perspectives. Chem. Rev. *104*, 6017–6084.

Kumar, P., Ban, H.S., Kim, S.S., Wu, H., Pearson, T., Greiner, D.L., Laouar, A., Yao, J., Haridas, V., Habiro, K., et al. (2008). T Cell-Specific siRNA Delivery Suppresses HIV-1 Infection in Humanized Mice. Cell *134*, 577–586.

Kuroda, A., Rauch, T.A., Todorov, I., Ku, H.T., Al-Abdullah, I.H., Kandeel, F., Mullen, Y., Pfeifer, G.P., and Ferreri, K. (2009). Insulin gene expression is regulated by DNA methylation. PLoS One *4*.

Lahl, K., Loddenkemper, C., Drouin, C., Freyer, J., Arnason, J., Eberl, G., Hamann, A., Wagner, H., Huehn, J., and Sparwasser, T. (2007). Selective depletion of Foxp3 + regulatory T cells induces a scurfy-like disease. *204*, 57–63.

Lan, M.S., Lu, J., Goto, Y., and Notkins, A.L. (2009). Molecular Cloning and Identification of a Receptor-Type Protein Tyrosine Phosphatase, IA-2, from Human Insulinoma. DNA Cell Biol. *13*, 505–514.

Landgraf, P., Rusu, M., Sheridan, R., Sewer, A., Iovino, N., Aravin, A., Pfeffer, S., Rice, A., Kamphorst, A.O., Landthaler, M., et al. (2007). A Mammalian microRNA Expression Atlas Based on Small RNA Library Sequencing. Cell *129*, 1401–1414.

Langmead, B., and Salzberg, S.L. (2012). Fast gapped-read alignment with Bowtie 2. Nat. Methods *9*, 357–359.

Langmead, B., Trapnell, C., Pop, M., and Salzberg, S.L. (2009). Ultrafast and memory-efficient alignment of short DNA sequences to the human genome. Genome Biol. *10*, R25.

Lederberg, J. (1959). Genes and antibodies. Science (80-.). *129*, 1649–1653.

Lee, J.Y., Skon, C.N., Lee, Y.J., Oh, S., Taylor, J.J., Malhotra, D., Jenkins, M.K., Rosenfeld, M.G., Hogquist, K.A., and Jameson, S.C. (2015). The Transcription Factor KLF2 Restrains CD4+ T Follicular Helper Cell Differentiation. Immunity *42*, 252–264.

Lee, Y., Ahn, C., Han, J., Choi, H., Kim, J., Yim, J., Lee, J., Provost, P., Rådmark, O., Kim, S., et al. (2003). The nuclear RNase III Drosha initiates microRNA processing. Nature *425*, 415–419.

Lee, Y., Kim, M., Han, J., Yeom, K.H., Lee, S., Baek, S.H., and Kim, V.N. (2004). MicroRNA genes are transcribed by RNA polymerase II. EMBO J. *23*, 4051–4060.

Leete, P., Willcox, A., Krogvold, L., Dahl-Jørgensen, K., Foulis, A.K., Richardson, S.J., and Morgan, N.G. (2016). Differential insulitic profiles determine the extent of β-cell destruction and the age at onset of type 1 diabetes. Diabetes *65*, 1362–1369.

Lewis, B.P., Burge, C.B., and Bartel, D.P. (2005). Conserved seed pairing, often flanked by adenosines, indicates that thousands of human genes are microRNA targets. Cell *120*, 15–20.

Li, E. (2002). Chromatin modification and epigenetic reprogramming in mammalian development. Nat. Rev. Genet. *3*, 662–673.

Li, Z., and Rana, T.M. (2014). Therapeutic targeting of microRNAs: Current status and future challenges. Nat. Rev. Drug Discov. *13*, 622–638.

Li, B., Samanta, A., Song, X., Iacono, K.T., Bembas, K., Tao, R., Basu, S., Riley, J.L., Hancock, W.W., Shen, Y., et al. (2007a). FOXP3 interactions with histone acetyltransferase and class II histone deacetylases are required for repression. *104*, 4571–4576.

Li, Q.J., Chau, J., Ebert, P.J.R., Sylvester, G., Min, H., Liu, G., Braich, R., Manoharan, M., Soutschek, J., Skare, P., et al. (2007b). miR-181a Is an Intrinsic Modulator of T Cell Sensitivity and Selection. Cell *129*, 147–161.

Li, X., Liang, Y., Leblanc, M., Benner, C., and Zheng, Y. (2014). Function of a foxp3 cis-element in protecting regulatory T cell identity. Cell *158*, 734–748.

Lister, R., Pelizzola, M., Dowen, R.H., Hawkins, R.D., Hon, G., Tonti-Filippini, J., Nery, J.R., Lee, L., Ye, Z., Ngo, Q.M., et al. (2009). Human DNA methylomes at base resolution show widespread epigenomic differences. Nature *462*, 315–322.

Liston, A., Rudensky, A.Y., Lu, L.-F., O'Carroll, D., and Tarakhovsky, A. (2008). Dicer-dependent microRNA pathway safeguards regulatory T cell function. J. Exp. Med. *205*, 1993–2004.

Long, D., Lee, R., Williams, P., Chan, C.Y., Ambros, V., and Ding, Y. (2007). Potent effect of target structure on microRNA function. Nat. Struct. Mol. Biol. *14*, 287–294.

Long, H., Yin, H., Wang, L., Gershwin, M.E., and Lu, Q. (2016). The critical role of epigenetics in systemic lupus erythematosus and autoimmunity. J. Autoimmun. *74*, 118–138.

Lopes, J.E., Torgerson, T.R., Schubert, L.A., Anover, S.D., Ocheltree, E.L., Ochs, H.D., Ziegler, S.F., Lopes, J.E., Torgerson, T.R., Schubert, L.A., et al. (2006). Analysis of FOXP3 Reveals Multiple Domains Required for Its Function as a Transcriptional Repressor. J. Immunol. *177*, 3133–3142.

Lopez-Serra, L., and Esteller, M. (2008). Proteins that bind methylated DNA and human cancer: Reading the wrong words. Br. J. Cancer *98*, 1881–1885.

Love, M.I., Huber, W., and Anders, S. (2014). Moderated estimation of fold change and dispersion for RNA-seq data with DESeq2. Genome Biol. *15*, 1–21.

Lu, Q. (2013). The critical importance of epigenetics in autoimmunity. J. Autoimmun. *41*, 1–5.

Lu, L.F., Thai, T.H., Calado, D.P., Chaudhry, A., Kubo, M., Tanaka, K., Loeb, G.B., Lee, H., Yoshimura, A., Rajewsky, K., et al. (2009). Foxp3-Dependent MicroRNA155 Confers Competitive Fitness to Regulatory T Cells by Targeting SOCS1 Protein. Immunity *30*, 80–91.

Lu, Y., Gao, J., Zhang, S., Gu, J., Lu, H., Xia, Y., Zhu, Q., Qian, X., Zhang, F., Zhang, C., et al. (2018). miR-142-3p regulates autophagy by targeting ATG16L1 in thymic-derived regulatory T cell (tTreg). Cell Death Dis.

Lujambio, A., and Lowe, S.W. (2012). The microcosmos of cancer. Nature *482*, 347–355.

Mahmud, S.A., Manlove, L.S., and Farrar, M.A. (2013). Interleukin-2 and STAT5 in regulatory T cell development and function. JAK-STAT *2*, e23154.

Mantel, P.-Y., Ouaked, N., Rückert, B., Karagiannidis, C., Welz, R., Blaser, K., and Schmidt-Weber, C.B. (2006). Molecular Mechanisms Underlying FOXP3 Induction in Human T Cells. J. Immunol. *176*, 3593–3602.

Marson, A., Kretschmer, K., Frampton, G.M., Jacobsen, E.S., Polansky, J.K., Macisaac, K.D., Levine, S.S., Fraenkel, E., Boehmer, H. Von, and Young, R.A. (2007). Foxp3 occupancy and regulation of key target genes during T-cell stimulation. *445*, 931–935.

Martin, M. (2011). Cutadapt removes adapter sequences from high-throughput sequencing reads. EMBnet.journal *17*, 10.

Mildner, A., Chapnik, E., Manor, O., Yona, S., Kim, K.W., Aychek, T., Varol, D., Beck, G., Itzhaki, Z.B., Feldmesser, E., et al. (2013). Mononuclear phagocyte miRNome analysis identifies miR-142 as critical regulator of murine dendritic cell homeostasis. Blood *121*, 1016–1027.

Miller, A., Lider, O., and Weiner, H.L. (1991). Antigen-driven bystander suppression after oral administration of antigens. J. Exp. Med. *174*, 791–798.

Mittal, N., and Zavolan, M. (2014). Seq and CLIP through the miRNA world. Genome Biol. *15*.

Morgan, N.G., and Richardson, S.J. (2018). Fifty years of pancreatic islet pathology in human type 1 diabetes: insights gained and progress made. Diabetologia *61*, 2499–2506.

Murugaiyan, G., Weiner, H.L., Beynon, V., Mittal, A., and Joller, N. (2011). Silencing MicroRNA-155 Ameliorates Experimental Autoimmune Encephalomyelitis. J. Immunol. *187*, 2213–2221.

Muto, A., Hoshino, H., Madisen, L., Yanai, N., Obinata, M., Karasuyama, H., Hayashi, N., Nakauchi, H., Yamamoto, M., Groudine, M., et al. (1998). Identification of Bach2 as a B-cell-specific partner for small Maf proteins that negatively regulate the immunoglobulin heavy chain gene 3' enhancer. EMBO J. *17*, 5734–5743.

Nabozny, G.H., Baisch, J.M., Cheng, S., Cosgrove, D., Griffiths, M.M., Luthra, H.S., and David, C.S. (1996). HLA-DQ8 transgenic mice are highly susceptible to collagen-induced arthritis: A novel model for human polyarthritis. J. Exp. Med. *183*, 27–37.

Nair, V.S., and Oh, K.I. (2014). Down-regulation of Tet2 prevents TSDR demethylation in IL2 deficient regulatory T cells. Biochem. Biophys. Res. Commun. *450*, 918–924.

Nakayama, M., Abiru, N., Moriyama, H., Babaya, N., Liu, E., Miao, D., Yu, L., Wegmann, D.R., Hutton, J.C., Elliott, J.F., et al. (2005). Prime role for an insulin epitope in the development of type 1 diabetes in NOD mice. Nature *435*, 220–223.

Nestor, C.E., Lentini, A., Hägg Nilsson, C., Gawel, D.R., Gustafsson, M., Mattson, L., Wang, H., Rundquist, O., Meehan, R.R., Klocke, B., et al. (2016). 5-Hydroxymethylcytosine Remodeling Precedes Lineage Specification during Differentiation of Human CD4(+) T Cells. Cell Rep. *16*, 559–570.

Nielsen, L.B., Wang, C., Sørensen, K., Bang-Berthelsen, C.H., Hansen, L., Andersen, M.L.M., Hougaard, P., Juul, A., Zhang, C.Y., Pociot, F., et al. (2012). Circulating levels of MicroRNA from children with newly diagnosed type 1 diabetes and healthy controls: Evidence that miR-25 associates to residual beta-cell function and glycaemic control during disease progression. Exp. Diabetes Res. *2012*.

Oderup, C., Cederbom, L., Makowska, A., Cilio, C.M., and Ivars, F. (2006). Cytotoxic T lymphocyte antigen-4-dependent down-modulation of costimulatory molecules on dendritic cells in CD4+ CD25+ regulatory T-cell-mediated suppression. Immunology *118*, 240–249.

Okano, M., Xie, S., and Li, E. (1998). Cloning and characterization of a family of novel mammalian DNA (cytosine-5) methyltransferases [1]. Nat. Genet. *19*, 219–220.

Okano, M., Bell, D.W., Haber, D.A., and Li, E. (1999). DNA methyltransferases Dnmt3a and Dnmt3b are essential for de novo methylation and mammalian development. Cell *99*, 247–257.

Ono, M., Yaguchi, H., Ohkura, N., Kitabayashi, I., Nagamura, Y., Nomura, T., Miyachi, Y., Tsukada, T., and Sakaguchi, S. (2007). Foxp3 controls regulatory T-cell function by interacting with AML1 / Runx1. *446*, 685–689.

Ouyang, W., Beckett, O., Ma, Q., Paik, J.H., Depinho, R.A., and Li, M.O. (2010). Foxo proteins cooperatively control the differentiation of Foxp3+regulatory T cells. Nat. Immunol. *11*, 618–627.

Palmer, J.P., Asplin, C.M., Clemons, P., Lyen, K., Tatpati, O., Raghu, P.K., and Paquette, T.L. (1983). Insulin antibodies in insulin-dependent diabetics before insulin treatment. Science (80-.). *222*, 1337–1339.

Pandiyan, P., Zheng, L., Ishihara, S., Reed, J., and Lenardo, M.J. (2007). CD4+CD25+Foxp3+ regulatory T cells induce cytokine deprivation-mediated apoptosis of effector CD4+ T cells. Nat. Immunol. *8*, 1353–1362.

Pastor, W.A., Aravind, L., and Rao, A. (2013). TETonic shift: biological roles of TET proteins in DNA demethylation and transcription. Nat. Rev. Mol. Cell Biol. *14*, 341–356.

Patterson, C.C., Dahlquist, G.G., Gyürüs, E., Green, A., and Soltész, G. (2009). Incidence trends for childhood type 1 diabetes in Europe during 1989-2003 and predicted new cases 2005-20: a multicentre prospective registration study. Lancet *373*, 2027–2033.

Paul, D.S., Teschendorff, A.E., Dang, M.A.N., Lowe, R., Hawa, M.I., Ecker, S., Beyan, H., Cunningham, S., Fouts, A.R., Ramelius, A., et al. (2016). Increased DNA methylation variability in type 1 diabetes across three immune effector cell types. Nat. Commun. *7*, 13555.

Peer, D., Eun, J.P., Morishita, Y., Carman, C. V., and Shimaoka, M. (2008). Systemic leukocyte-directed siRNA delivery revealing cyclin D1 as an anti-inflammatory target. Science (80-.). *319*, 627–630.

Polansky, J.K., Kretschmer, K., Freyer, J., Floess, S., Garbe, A., Baron, U., Olek, S., Hamann, A., von Boehmer, H., and Huehn, J. (2008). DNA methylation controls Foxp3 gene expression. Eur. J. Immunol. *38*, 1654–1663.

Portela, A., and Esteller, M. (2010). Epigenetic modifications and human disease. Nat. Biotechnol. *28*, 1057–1068.

Probst, A. V., Dunleavy, E., and Almouzni, G. (2009). Epigenetic inheritance during the cell cycle. Nat. Rev. Mol. Cell Biol. *10*, 192–206.

Prochazka, M., Leiter, E.H., Serreze, D. V., and Coleman, D.L. (1987). Three recessive loci required for insulin-dependent diabetes in nonobese diabetic mice. Science (80-.). *237*, 286–289.

Qin, A., Wen, Z., Zhou, Y., Li, Y., Li, Y., Luo, J., Ren, T., and Xu, L. (2013). MicroRNA-126 regulates the induction and function of CD4+ Foxp3+ regulatory T cells through PI3K/AKT pathway. J. Cell. Mol. Med. *17*, 252–264.

Rabin, D.U., Pleasic, S.M., Shapiro, J.A., Yoo-Warren, H., Oles, J., Hicks, J.M., Goldstein, D.E., and Rae, P.M. (1994). Islet cell antigen 512 is a diabetes-specific islet autoantigen related to protein tyrosine phosphatases. J. Immunol. *152*, 3183–3188.

Rand, T.A., Petersen, S., Du, F., and Wang, X. (2005). Argonaute2 cleaves the anti-guide strand of siRNA during RISC activation. Cell *123*, 621–629.

Reik, W., and Walter, J. (2001). Genomic imprinting: Parental influence on the genome. Nat. Rev. Genet. *2*, 21–32.

Richardson, S.J., Rodriguez-Calvo, T., Gerling, I.C., Mathews, C.E., Kaddis, J.S., Russell, M.A., Zeissler, M., Leete, P., Krogvold, L., Dahl-Jørgensen, K., et al. (2016). Islet cell hyperexpression of HLA class I antigens: a defining feature in type 1 diabetes. Diabetologia *59*, 2448–2458.

Richer, M.J., Lang, M.L., and Butler, N.S. (2016). T Cell Fates Zipped Up: How the Bach2 Basic Leucine Zipper Transcriptional Repressor Directs T Cell Differentiation and Function. J. Immunol. *197*, 1009–1015.

Riddihough, G., and Zahn, L.M. (2010). Epigenetics. What is epigenetics? Introduction. Science *330*, 611.

Riggs, A.D., and Xiong, Z. (2004). Methylation and epigenetic fidelity. Proc. Natl. Acad. Sci. U. S. A. *101*, 4–5.

Robert Finestra, T., and Gribnau, J. (2017). X chromosome inactivation: silencing, topology and reactivation. Curr. Opin. Cell Biol. *46*, 54–61.

Robertson, K.D. (2005). DNA methylation and human disease. Nat. Rev. Genet. *6*, 597–610.

Rodríguez-Galán, A., Fernández-Messina, L., and Sánchez-Madrid, F. (2018). Control of immunoregulatory molecules by miRNAs in T cell activation. Front. Immunol. *9*, 1–10.

Roncador, G., Brown, P.J., Maestre, L., Hue, S., Martínez-Torrecuadrada, J.L., Ling, K.L., Pratap, S., Toms, C., Fox, B.C., Cerundolo, V., et al. (2005). Analysis of FOXP3 protein expression in human CD4+CD25+ regulatory T cells at the single-cell level. Eur. J. Immunol. *35*, 1681–1691.

Roychoudhuri, R., Hirahara, K., Mousavi, K., Clever, D., Dema, B., Yu, Z., Liu, H., Takahashi, H., Rao, M., Crompton, J.G., et al. (2013). Bach2 Represses Effector Programmes to Stabillize Treg-mediated immune homeostasis. Nature *498*, 506–510.

Rudra, D., Chaudhry, A., Niec, R.E., Arvey, A., Samstein, R.M., Leslie, C., Shaffer, S.A., Goodlett, D.R., and Rudensky, A.Y. (2012). Transcription factor Foxp3 and its protein partners form a complex regulatory network. *13*.

Ryba-Stanisławowska, M., Werner, P., Brandt, A., Myśliwiec, M., and Myśliwska, J. (2016). Th9 and Th22 immune response in young patients with type 1 diabetes. Immunol. Res. *64*, 730–735.

Sakaguchi, S., Sakaguchi, N., Asano, M., Itoh, M., and Toda, M. (1995). Immunologic Self-Tolerance Maintained by Activated T cells expressing IL-2 Receptor Alpha-Chains (CD25). J. Immunol. *155*, 1151–1164.

Sakaguchi, S., Yamaguchi, T., Nomura, T., and Ono, M. (2008). Regulatory T cells and immune tolerance. Cell *133*, 775–787.

Salas-Pérez, F., Codner, E., Valencia, E., Pizarro, C., Carrasco, E., and Pérez-Bravo, F. (2013). MicroRNAs miR-21a and miR-93 are down regulated in peripheral blood mononuclear cells (PBMCs) from patients with type 1 diabetes. Immunobiology *218*, 733–737.

Sauer, S., Bruno, L., Hertweck, A., Finlay, D., Leleu, M., Spivakov, M., Knight, Z.A., Cobb, B.S., Cantrell, D., O'Connor, E., et al. (2008). T cell receptor signaling controls Foxp3 expression via PI3K, Akt, and mTOR. Proc. Natl. Acad. Sci. U. S. A. *105*, 7797–7802.

Scherm, M.G., Ott, V.B., and Daniel, C. (2016). Follicular Helper T Cells in Autoimmunity. Curr. Diab. Rep. *16*.

Schuettengruber, B., Martinez, A.M., Iovino, N., and Cavalli, G. (2011). Trithorax group proteins: Switching genes on and keeping them active. Nat. Rev. Mol. Cell Biol. *12*, 799–814.

Schug, J., McKenna, L.B., Walton, G., Hand, N., Mukherjee, S., Essuman, K., Shi, Z., Gao, Y., Markley, K., Nakagawa, M., et al. (2013). Dynamic recruitment of microRNAs to their mRNA targets in the regenerating liver. BMC Genomics *14*.

Sebastiani, G., Spagnuolo, I., Patti, A., Grieco, F.A., Cataldo, D., Ferretti, E., Tibert, C., and Dotta, F. (2012). MicroRNA expression fingerprint in serum of type 1 diabetic patients. Diabetologia *55*, S48.

Serr, I., and Daniel, C. (2018). Regulation of T follicular helper cells in islet autoimmunity. Front. Immunol. *9*.

Serr, I., Fürst, R.W., Ott, V.B., Scherm, M.G., Nikolaev, A., Gökmen, F., Kälin, S., Zillmer, S., Bunk, M., Weigmann, B., et al. (2016a). MiRNA92a targets KLF2 and the phosphatase PTEN signaling to promote human T follicular helper precursors in T1D islet autoimmunity. Proc. Natl. Acad. Sci. U. S. A. *113*.

Serr, I., Fürst, R.W., Achenbach, P., Scherm, M.G., Gökmen, F., Haupt, F., Sedlmeier, E., Knopff, A., Shultz, L., Willis, R.A., et al. (2016b). Type 1 diabetes vaccine candidates promote human Foxp3(+)Treg induction in humanized mice. Nat. Commun. *7*, 10991.

Serr, I., Scherm, M.G., Zahm, A.M., Schug, J., Flynn, V.K., Hippich, M., Kälin, S., Becker, M., Achenbach, P., Nikolaev, A., et al. (2018). A miRNA181a/NFAT5 axis links impaired T cell tolerance induction with autoimmune type 1 diabetes. Sci. Transl. Med. *10*.

Shrestha, A., Carraro, G., Agha, E. El, Mukhametshina, R., and Chao, C. (2015). Generation and Validation of miR-142 Knock Out Mice. 1–14.

Simpson, L.J., and Ansel, K.M. (2015). MicroRNA regulation of lymphocyte tolerance and autoimmunity. J. Clin. Invest. *125*, 2242–2249.

Snowhite, I. V., Allende, G., Sosenko, J., Pastori, R.L., Messinger Cayetano, S., and Pugliese, A. (2017). Association of serum microRNAs with islet autoimmunity, disease progression and metabolic impairment in relatives at risk of type 1 diabetes. Diabetologia *60*, 1409–1422.

Someya, K., Nakatsukasa, H., Ito, M., Kondo, T., Tateda, K., Akanuma, T., Koya, I., Sanosaka, T., Kohyama, J., Tsukada, Y., et al. (2017). Improvement of Foxp3 stability through CNS2 demethylation by TET enzyme induction and activation. Int. Immunol. *29*, 365–375.

Sonda, N., Simonato, F., Peranzoni, E., Calì, B., Bortoluzzi, S., Bisognin, A., Wang, E., Marincola, F.M., Naldini, L., Gentner, B., et al. (2013). MiR-142-3p Prevents Macrophage Differentiation during Cancer-Induced Myelopoiesis. Immunity *38*, 1236–1249.

Stadinski, B.D., Zhang, L., Crawford, F., Marrack, P., Eisenbarth, G.S., and Kappler, J.W. (2010). Diabetogenic T cells recognize insulin bound to IAg7 in an unexpected, weakly binding register. Proc. Natl. Acad. Sci. U. S. A. *107*, 10978–10983.

Steffes, M.W., Sibley, S., Jackson, M., and Thomas, W. (2003). Beta-Cell Function and the Development of Diabetes-Related Complications in the Diabetes Control and Complications Trial. Diabetes Care *26*, 832–836.

Straarup, E.M., Lindholm, M.W., Fisker, N., Hedtja, M., Rosenbohm, C., Aarup, V., Hansen, H.F., Ørum, H., Hansen, J.B.R., and Koch, T. (2010). Short locked nucleic acid antisense oligonucleotides potently reduce apolipoprotein B mRNA and serum cholesterol in mice and non-human primates. *38*, 7100–7111.

Straussman, R., Nejman, D., Roberts, D., Steinfeld, I., Blum, B., Benvenisty, N., Simon, I., Yakhini, Z., and Cedar, H. (2009). Developmental programming of CpG island methylation profiles in the human genome. Nat. Struct. Mol. Biol. *16*, 564–571.

Strickland, F., and Richardson, B. (2008). Epigenetics in human autoimmunity. Autoimmunity *41*, 278–286.

Sun, Y., Varambally, S., Maher, C.A., Cao, Q., Chockley, P., Toubai, T., Malter, C., Nieves, E., Tawara, I., Wang, Y., et al. (2011). Targeting of microRNA-142-3p in dendritic cells regulates endotoxin-induced mortality. Blood *117*, 6172–6183.

Szebeni, A., Schloot, N., Kecskeméti, V., Hosszúfalusi, N., Pánczél, P., Prohászka, Z., Füst, G., Uray, K., Hudecz, F., and Meierhoff, G. (2005). Th1 and Th2 cell responses of type 1 diabetes patients and healthy controls to human heat-shock protein 60 peptides AA437-460 and AA394-408. Inflamm. Res. *54*, 415–419.

Tahiliani, M., Koh, K.P., Shen, Y., Pastor, W.A., Bandukwala, H., Brudno, Y., Agarwal, S., Iyer, L.M., Liu, D.R., Aravind, L., et al. (2009). Conversion of 5-Methylcytosine to 5-Hydroxymethylcytosine in Mammalian DNA by MLL Partner TET1. Science (80-.). *324*, 930–935.

Takahashi, H., Kanno, T., Nakayamada, S., Hirahara, K., Sciumè, G., Muljo, S.A., Kuchen, S., Casellas, R., Wei, L., Kanno, Y., et al. (2012). TGF-β and retinoic acid induce the microRNA miR-10a, which targets Bcl-6 and constrains the plasticity of helper T cells. Nat. Immunol. *13*, 587–595.

Talebi, F., Ghorbani, S., Chan, W.F., Boghozian, R., Masoumi, F., Ghasemi, S., Vojgani, M., Power, C., and Noorbakhsh, F. (2017). MicroRNA-142 regulates inflammation and T cell differentiation in an animal model of multiple sclerosis. 1–14.

Tay, Y., Zhang, J., Thomson, A.M., Lim, B., and Rigoutsos, I. (2008). MicroRNAs to Nanog, Oct4 and Sox2 coding regions modulate embryonic stem cell differentiation. Nature *455*, 1124–1128.

Thomson, J.P., Skene, P.J., Selfridge, J., Clouaire, T., Guy, J., Webb, S., Kerr, A.R.W., Deaton, A., Andrews, R., James, K.D., et al. (2010). CpG islands influence chromatin structure via the CpG-binding protein Cfp1. Nature *464*, 1082–1086.

Thornton, A.M., Korty, P.E., Tran, D.Q., Wohlfert, E.A., Murray, P.E., Belkaid, Y., and Shevach, E.M. (2010). Expression of Helios, an Ikaros Transcription Factor Family Member, Differentiates Thymic-Derived from Peripherally Induced Foxp3 + T Regulatory Cells.

Toker, A., Engelbert, D., Garg, G., Polansky, J.K., Floess, S., Miyao, T., Baron, U., Düber, S., Geffers, R., Giehr, P., et al. (2013). Active demethylation of the Foxp3 locus leads to the generation of stable regulatory T cells within the thymus. J. Immunol. *190*, 3180–3188.

Tone, Y., Furuuchi, K., Kojima, Y., Tykocinski, M.L., Greene, M.I., and Tone, M. (2008). Smad3 and NFAT cooperate to induce Foxp3 expression through its enhancer. *9*.

Trim, C.K.A.P., Huang, C., Martin, S., Pfleger, C., Buckner, J.H., Bluestone, J.A., Riley, J.L., Ziegler, S.F., Huang, C., Martin, S., et al. (2013). Cutting Edge: A Novel, Human-Specific

Interacting Protein Couples FOXP3 to a Chromatin-Remodeling Complex That Contains KAP1/TRIM28. J. Immunol. *190*, 4470–4473.

Tsagaratou, A., Äijö, T., Lio, C.-W.J., Yue, X., Huang, Y., Jacobsen, S.E., Lähdesmäki, H., and Rao, A. (2014). Dissecting the dynamic changes of 5-hydroxymethylcytosine in T-cell development and differentiation. Proc. Natl. Acad. Sci. U. S. A. *111*, E3306-15.

Tsukumo, S. -i., Unno, M., Muto, A., Takeuchi, A., Kometani, K., Kurosaki, T., Igarashi, K., and Saito, T. (2013). Bach2 maintains T cells in a naive state by suppressing effector memory-related genes. Proc. Natl. Acad. Sci. *110*, 10735–10740.

Turan, N., Katari, S., Coutifaris, C., and Sapienza, C. (2010). Explaining inter-individual variability in phenotype: Is epigenetics up to the challenge? Epigenetics *5*, 16–19.

Vaeth, M., Serfling, E., Berberich-Siebelt, F., Reissig, S., Sawitzki, B.S., Muller, G., Jonuleit, H., Tuettenberg, A., Waisman, A., Schliesser, U., et al. (2012). Dependence on nuclear factor of activated T-cells (NFAT) levels discriminates conventional T cells from Foxp3+ regulatory T cells. Proc. Natl. Acad. Sci. *109*, 16258–16263.

Vella, M.C., Choi, E.Y., Lin, S.Y., Reinert, K., and Slack, F.J. (2004). The C. elegans microRNA let-7 binds to imperfect let-7 complementary sites from the lin-41 3'UTR. Genes Dev. *18*, 132–137.

Vignali, D.A.A., Collison, L.W., and Workman, C.J. (2008). How regulatory T cells work. Nat. Rev. Immunol. *8*, 523–532.

Waddington, C.H. (1939). An introduction to modern genetics. (London: George Alien & Unwin Ltd.).

Walker, M.R., Kasprowicz, D.J., Gersuk, V.H., Bènard, A., Landeghen, M. Van, Buckner, J.H., and Ziegler, S.F. (2003). Induction of FoxP3 and acquisition of T regulatory activity by stimulated human CD4 + CD25 − T cells. *112*, 1437–1443.

Wang, L., Liu, Y., Han, R., Beier, U.H., Thomas, R.M., Wells, A.D., and Hancock, W.W. (2013). Mbd2 Promotes Foxp3 Demethylation and T-Regulatory-Cell Function. Mol. Cell. Biol. *33*, 4106–4115.

Wang, X.S., Gong, J.N., Yu, J., Wang, F., Zhang, X.H., Yin, X.L., Tan, Z.Q., Luo, Z.M., Yang, G.H., Shen, C., et al. (2012). MicroRNA-29a and microRNA-142-3p are regulators of myeloid differentiation and acute myeloid leukemia. Blood *119*, 4992–5004.

Warth, S.C., Hoefig, K.P., Ansel, K.M., Schallenberg, S., Klein, L., Heissmeyer, V., Jovanovic, K., Hiekel, A., and Kretschmer, K. (2015). Induced miR-99a expression represses Mtor cooperatively with miR-150 to promote regulatory T-cell differentiation. EMBO J. *34*, 1195–1213.

Wenzlau, J.M., Juhl, K., Yu, L., Moua, O., Sarkar, S.A., Gottlieb, P., Rewers, M., Eisenbarth, G.S., Jensen, J., Davidson, H.W., et al. (2007). The cation efflux transporter ZnT8 (Slc30A8) is a major autoantigen in human type 1 diabetes. Proc. Natl. Acad. Sci. *104*, 17040–17045.

Winkler, C., Jolink, M., Knopff, A., Kwarteng, N.A., Achenbach, P., Bonifacio, E., and Ziegler,

A.G. (2019). Age, HLA, and sex define a marked risk of organ-specific autoimmunity in first-degree relatives of patients with type 1 diabetes. Diabetes Care *42*, 1684–1691.

Wu, H., and Zhang, Y. (2014). Reversing DNA methylation: Mechanisms, genomics, and biological functions. Cell *156*, 45–68.

Wu, H., Neilson, J.R., Kumar, P., Manocha, M., Shankar, P., Sharp, P.A., and Manjunath, N. (2007). miRNA profiling of naïve, effector and memory CD8 T cells. PLoS One *2*.

Wu, Y., Borde, M., Heissmeyer, V., Feuerer, M., Lapan, A.D., Stroud, J.C., Bates, D.L., Guo, L., Han, A., Ziegler, S.F., et al. (2006). FOXP3 Controls Regulatory T Cell Function through Cooperation with NFAT. 375–387.

Wucherpfennig, K.W., and Sethi, D. (2011). T cell receptor recognition of self and foreign antigens in the induction of autoimmunity. Semin. Immunol. *23*, 84–91.

Xiang, Z., Yang, Y., Chang, C., and Lu, Q. (2017). The epigenetic mechanism for discordance of autoimmunity in monozygotic twins. J. Autoimmun. *83*, 43–50.

Xiao, C., Srinivasan, L., Calado, D.P., Patterson, H.C., Zhang, B., Wang, J., Henderson, J.M., Kutok, J.L., and Rajewsky, K. (2008). Lymphoproliferative disease and autoimmunity in mice with increased miR-17-92 expression in lymphocytes. Nat. Immunol. *9*, 405–414.

Yang, M., Ye, L., Wang, B., Gao, J., Liu, R., Hong, J., Wang, W., Gu, W., and Ning, G. (2015a). Decreased miR-146 expression in peripheral blood mononuclear cells is correlated with ongoing islet autoimmunity in type 1 diabetes patients. J. Diabetes *7*, 158–165.

Yang, R., Qu, C., Zhou, Y., Konkel, J.E., Shi, S., Liu, Y., Chen, C., Liu, S., Liu, D., Chen, Y., et al. (2015b). Hydrogen Sulfide Promotes Tet1- and Tet2-Mediated Foxp3 Demethylation to Drive Regulatory T Cell Differentiation and Maintain Immune Homeostasis. Immunity *43*, 251–263.

Yao, R., Ma, Y.L., Liang, W., Li, H.H., Ma, Z.J., Yu, X., and Liao, Y.H. (2012). MicroRNA-155 Modulates Treg and Th17 Cells Differentiation and Th17 Cell Function by Targeting SOCS1. PLoS One *7*.

Yue, X., Trifari, S., Äijö, T., Tsagaratou, A., Pastor, W.A., Zepeda-Martínez, J.A., Lio, C.-W.J., Li, X., Huang, Y., Vijayanand, P., et al. (2016). Control of Foxp3 stability through modulation of TET activity. J. Exp. Med. *213*, 377–397.

Zhang, F., Meng, G., and Strober, W. (2008). Interactions among the transcription factors Runx1 , ROR c t and Foxp3 regulate the differentiation of interleukin 17 – producing T cells. *9*.

Zhao, Z., Tavoosidana, G., Sjölinder, M., Göndör, A., Mariano, P., Wang, S., Kanduri, C., Lezcano, M., Sandhu, K.S., Singh, U., et al. (2006). Circular chromosome conformation capture (4C) uncovers extensive networks of epigenetically regulated intra- and interchromosomal interactions. Nat. Genet. *38*, 1341–1347.

Zheng, Y., Josefowicz, S., Chaudhry, A., Peng, X.P., Forbush, K., and Rudensky, A.Y. (2010). Role of conserved non-coding DNA elements in the Foxp3 gene in regulatory T-cell fate. Nature *463*, 808–812.

Zhou, L., Lopes, J.E., Chong, M.M.W., Ivanov, I.I., Min, R., Gabriel, D., Shen, Y., Du, J., Rubtsov, Y.P., Rudensky, A.Y., et al. (2008a). TGF- β -induced Foxp3 inhibits Th17 cell differentiation by antagonizing ROR γ t function. *453*, 236–240.

Zhou, Q., Haupt, S., Prots, I., Thümmler, K., Kremmer, E., Lipsky, P.E., Schulze-Koops, H., and Skapenko, A. (2013). miR-142-3p Is Involved in CD25 + CD4 T Cell Proliferation by Targeting the Expression of Glycoprotein A Repetitions Predominant . J. Immunol. *190*, 6579–6588.

Zhou, X., Jeker, L.T., Fife, B.T., Zhu, S., Anderson, M.S., McManus, M.T., and Bluestone, J.A. (2008b). Selective miRNA disruption in T reg cells leads to uncontrolled autoimmunity. J. Exp. Med. *205*, 1983–1991.

Ziegler, A.G., and Nepom, G.T. (2010). Prediction and Pathogenesis in Type 1 Diabetes. Immunity *32*, 468–478.

Ziegler, A.G., Rewers, M., Simell, O., Simell, T., Lempainen, J., Steck, A., Winkler, C., Ilonen, J., Veijola, R., Knip, M., et al. (2013). Seroconversion to multiple islet autoantibodies and risk of progression to diabetes in children. Jama *309*, 2473–2479.

Reinert-Hartwall, L., Honkanen, J., Salo, H.M., Nieminen, J.K., Luopajärvi, K., Härkönen, T., Veijola, R., Simell, O., Ilonen, J., et al. (2015). Th1/Th17 Plasticity Is a Marker of Advanced β Cell Autoimmunity and Impaired Glucose Tolerance in Humans. J. Immunol. *194*, 68–75.

Danksagung

Ein besonderer Dank gebührt Prof. Carolin Daniel für die außergewöhnliche Betreuung und Förderung. Vielen Dank für die unzähligen wissenschaftlichen Diskussionen, die Motivation in allen Phasen dieser Arbeit und nicht zuletzt dein Verständnis und dein Vertrauen.

Ich bedanke mich außerdem herzlich bei Prof. Anette-Gabriele Ziegler für die Möglichkeit meine Doktorarbeit an ihrem Institut durchzuführen. Vielen Dank für die Unterstützung während der letzten Jahre, für die hilfreichen Diskussionen und für das Patientenmaterial.

Vielen Dank auch an Prof. Martin Hrabě de Angelis für die Betreuung meiner Doktorarbeit als Zweitbetreuer, für das hilfreiche Feedback und für die interessanten Diskussionen in den Thesis Committee Meetings.

Ich bedanke mich auch bei allen Kollaborationspartnern, die mit ihrem Fachwissen und der Bereitstellung von Materialien, Reagenzien oder Mäusen ganz wesentlich zur erfolgreichen Durchführung wichtiger Experimente beigetragen haben. Insbesondere bedanke ich mich ganz herzlich bei Prof. Klaus Kaestner und dem gesamten Kaestner Lab für die vielfältige Unterstützung, die zahlreichen Diskussionen sowie die Möglichkeit wichtige Experimente an der University of Pennsylvania in Philadelphia durchführen zu können. Ebenfalls zu nennen sind hier Benno Weigmann und seine Arbeitsgruppe.

Vielen Dank auch an das ganze IDF1 für die vielfältige Unterstützung und die gute Zusammenarbeit. Insbesondere bedanke ich mich bei allen Studienbetreuern, Ärzten und Technischen Assistenten und natürlich bei allen Studienteilnehmern für das Bereitstellen des Probenmaterials. Ohne sie wären wichtige Experimente dieser Arbeit nicht durchführbar gewesen. Ein großes Dankeschön geht auch an das TEDDY Team für eure immer offene und freundliche Art.

Ein herzliches Dankeschön geht an alle derzeitigen und ehemaligen Mitglieder der AG Daniel. Vielen Dank für die angenehme Arbeitsatmosphäre, die zahlreichen hilfreichen Diskussionen und die Unterstützung in allen Bereichen. Euer Interesse und eure Hilfsbereitschaft haben nicht unerheblich zum Gelingen wichtiger Experimente und damit dieser Arbeit beigetragen.

Ein ganz besonderes Dankschön gilt außerdem meinen Teilzeit-Büronachbarn und Freunden Lisa, Markus und Jan. Vielen Dank für eure Unterstützung in unterschiedlichsten Bereichen und die tolle gemeinsame Zeit.

Zuletzt möchte ich mich bei meiner Familie und meinen Freunden für die bedingungslose Unterstützung während der letzten Jahre bedanken. Vielen Dank, dass ihr immer für mich da seid, ich weiß das sehr zu schätzen.